

# FOAMS, ITERATED WREATH PRODUCTS, FIELD EXTENSIONS AND SYLVESTER SUMS

MEE SEONG IM AND MIKHAIL KHOVANOV  
(WITH AN APPENDIX JOINT WITH LEV ROZANSKY)

**ABSTRACT.** Certain foams and relations on them are introduced to interpret functors and natural transformations in categories of representations of iterated wreath products of cyclic groups of order two. We also explain how patched surfaces with defect circles and foams relate to separable field extensions and Galois theory and explore a relation between overlapping foams and Sylvester double sums. In the appendix, joint with Lev Rozansky, we compare traces in two-dimensional TQFTs coming from matrix factorizations with those in field extensions.

## CONTENTS

1. Introduction	2
Acknowledgments	3
2. Foams and functors between representation categories of direct products of groups	3
2.1. Diagrammatics of induction and restriction	3
2.2. Extending to foams	4
3. Foams for the iterated wreath products of $S_2$ 's	7
3.1. Iterated wreath products of $S_2$ 's	7
3.2. A description of the center of $G_n$	8
3.3. Induction and restriction bimodules	9
3.4. Mackey induction-restriction formula and decomposition of Ind-Res functor	10
3.5. Central elements and bubbles	15
4. Defect lines and networks	16
4.1. Tensoring with induced representations	16
4.2. Foams for idempotents and basic relations on them	18
4.3. Simplified (planar) notation	20
4.4. Dihedral groups	22
4.5. Rooted trees and higher depth representations	29
5. Patched surfaces, separable extensions, and foams	32
5.1. Defect circles and Frobenius algebra automorphisms	32
5.2. Field extensions and patched surfaces	46
6. Foams, Galois extensions, and Sylvester sums	55
6.1. Base change for $\mathrm{GL}(N)$ foams and field extensions	55

---

*Date:* July 16, 2021.

*2020 Mathematics Subject Classification.* Primary: 57K16, 18M30, 20E22. Secondary: 18N25, 13P15, 57K99, 20C99.

*Key words and phrases.* Iterated wreath products, categorification, Frobenius algebras, field extensions, separable extensions, matrix factorizations, Sylvester sums, foam evaluation, defect TQFTs.

6.2. Overlapping foams and Sylvester double sums	62
7. Appendix (joint with Lev Rozansky): Comparison with matrix factorizations	70
References	75

## 1. INTRODUCTION

Induction and restriction functors between categories of representations of finite groups are biadjoint and natural transformations between their compositions have a graphical presentation via systems of oriented arcs and circles in the plane, see [Kh3] for example. In these diagrams, regions are labelled by finite groups and lines by inclusions of groups.

In Section 2 we explain how such planar diagrams can be refined to foams when some of the groups have a direct product decomposition. Sections 3 and 4 treat a special case when the groups are iterated wreath products of the cyclic group  $C_2$  (equivalently, symmetric group  $S_2$ ).

Iterated wreath products have been studied, for example, in [CST, OOR, IW1, IW2, IO]. Natural transformations between compositions of induction and restriction functors between iterated wreath products of  $C_2$  can be depicted by suitable foams. Facets of this foam labelled  $n$  correspond to the  $n$ -th iterated wreath product group  $G_n$ , the group of symmetries of a full binary tree of depth  $n$ . Seams correspond to the induction and restriction for the inclusion  $G_n \times G_n \subset G_{n+1}$  as an index two subgroup. Graphical calculus for these foams and its relation to representation theory of  $G_n$  are developed in Sections 3 and 4.

These foams are different from  $SL(N)$  or  $GL(N)$  foams. The latter are commonly used in link homology and categorification. In particular, they can be used to describe the Soergel category [RWe, We, RW2] and to construct  $GL(N)$  link homology via foam evaluation [Kh2, RW1]; they also appear in categorified quantum groups [QR].

In Section 5 we explain how automorphisms of a commutative Frobenius algebra give rise to a decorated 2-dimensional topological quantum field theory (2D TQFT) with defect circles. A further refinement is sometimes possible, along the lines of Turaev's homotopy quantum field theories (QFTs) and Landau-Ginzburg orbifolds. We describe a useful way to encode a representation of the fundamental group of a surface, Poincare dual to the standard description. We explain that surfaces in decorated TQFTs that come from separable field extensions and the standard trace on them admits a straightforward evaluation.

Section 6 contains a couple of curious connections of foams to Galois theory and to polynomial interpolation. Suppose given a degree  $N$  irreducible polynomial  $f(x)$  over a ground field  $\mathbf{k}$  with the maximal for that degree Galois group  $\text{Gal}(F/\mathbf{k}) \cong S_N$ , where  $F$  is the splitting field. In Section 6.1 we identify  $F$  and suitable intermediate fields of the extension with state spaces of MOY theta-webs, upon a base change from the symmetric functions to  $\mathbf{k}$  via coefficients of  $f(x)$ . In Section 6.2 we interpret the Sylvester double sums [Sy] that describe subresultants and related identities and expressions in the field of polynomial interpolation [DHKS, DKSv, KSV] via evaluation of overlapping foams.

In the appendix (Section 7), written jointly with Lev Rozansky, we show that 2D TQFTs that come from matrix factorizations and Landau-Ginzburg models exhibit much more subtle behavior.

**Acknowledgments.** The authors are grateful to Johan De Jong, Louis-Hadrien Robert, Alvaro Martinez Ruiz and Lev Rozansky for valuable discussions. M.S.I. was partially supported by Naval Academy Research Council (NARC) at Annapolis, MD, and M.K. was partially supported by NSF grant DMS-1807425 while working on this paper.

## 2. FOAMS AND FUNCTORS BETWEEN REPRESENTATION CATEGORIES OF DIRECT PRODUCTS OF GROUPS

**2.1. Diagrammatics of induction and restriction.** Given an inclusion of finite groups  $H \subset G$  (or, more generally, an inclusion with  $H$  of finite index in  $G$ ) and a ground field  $\mathbf{k}$ , induction and restriction functors  $\text{Ind}_H^G$  and  $\text{Res}_G^H$  between categories of  $\mathbf{k}H$ -modules and  $\mathbf{k}G$ -modules are biadjoint, that is, adjoint on both left and right. Diagrammatics of these biadjoint functors are explained in [Kh3, Section 3.2]. Natural transformations between compositions of these functors can be depicted by planar diagrams of arcs and circles in the plane with regions labelled by  $G$  and  $H$  in a checkboard fashion.



FIGURE 2.1. Oriented cups and caps natural transformations, for induction and restriction between  $H$ - and  $G$ -modules, with  $H \subset G$  a finite index subgroup.

Biadjointness can be encoded by four natural transformations that can be depicted by the four oriented cup and cap diagrams in Figure 2.1. Biadjointness is equivalent to the isotopy invariance of diagrams or arcs and circles built from these diagrams, and the four generating isotopy relations are shown in Figure 2.2.

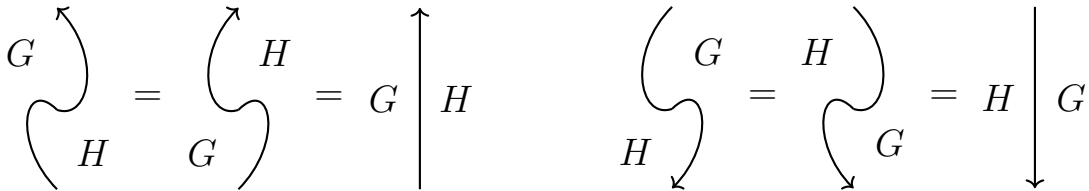


FIGURE 2.2. Biadjointness isotopy relations on compositions of cups and caps.

Further extension of this construction adds diagrammatics for induction and restriction between many finite groups and additional diagrams for functor isomorphisms and other natural transformations between compositions of these functors [Kh3, Section 3.2].

The induction functor and, more generally, a functor  $F : \mathbf{k}H\text{-mod} \rightarrow \mathbf{k}G\text{-mod}$ , for finite groups  $H$  and  $G$ , can be depicted by a dot on a horizontal line, with intervals to the right

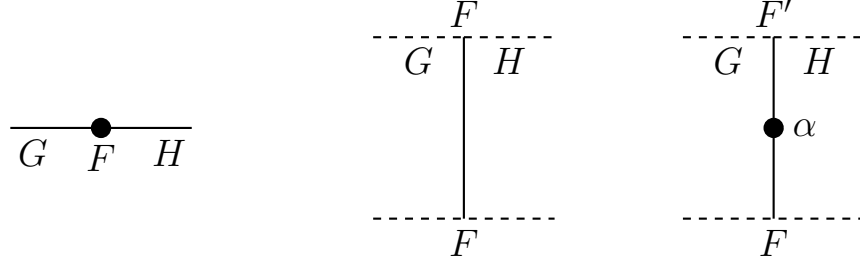


FIGURE 2.3. Left: functor  $F$ . Middle: identity map  $\text{id}_F : F \Rightarrow F$ . Right: natural transformation  $\alpha : F \Rightarrow F'$ .

and left of the dot labelled by  $H$  and  $G$ , respectively, see Figure 2.3 left. The identity natural transformation  $\text{id}_F$  of  $F$  is depicted by a vertical line in the plane, see Figure 2.3 middle. A natural transformation  $\alpha : F \Rightarrow F'$  between two such functors is depicted by a dot on a vertical line, with intervals below and above the dot labelled by  $F$  and  $F'$ , respectively, see Figure 2.3 right.

In these considerations, it's natural to restrict to functors  $F$  that admit biadjoint functors, that is, there exists a functor  $\overline{F}$  which is both left and right adjoint to  $F$ , with biadjointness isomorphisms fixed. This allows to add “cup” and “cap” diagrams, their compositions and suitable isotopies to our graphical calculus, see for instance [Kh3, Section 3.2] as well as the discussion of isotopies and biadjointness in [Kh1, La1, La2] and [KQ, Chapter 7].

**2.2. Extending to foams.** Starting from the planar diagrammatics of induction and restriction functors for finite groups one easily makes one step to its extension to foam diagrammatics for these functors, once direct products of groups are used.

Suppose that group  $H$  is the direct product,  $H \cong H_1 \times H_2$ . Then suitable endofunctors and natural transformations between them in the category of  $H$ -modules can be reduced to exterior tensor products of those in categories of  $H_1$ -modules and  $H_2$ -modules. Diagrammatically, the  $H$ -plane that carries information about natural transformations of endofunctors in the category of  $\mathbf{k}H$ -modules is converted into two parallel planes, one for each term  $H_1, H_2$  in the direct product.

For instance, a natural transformation  $\alpha_i : F_i \longrightarrow F'_i$  between endofunctors  $F_i, F'_i$  in the category of  $H_i$ -modules can be depicted by a dot on a vertical line in the  $H_i$ -plane, see Figure 2.4 left, for  $i = 1, 2$ . Bottom and top endpoints of the vertical line denote functors  $F_i$  and  $F'_i$ , respectively.

Then the natural transformation

$$\alpha_1 \boxtimes \alpha_2 : F_1 \boxtimes F_2 \longrightarrow F'_1 \boxtimes F'_2$$

between endofunctors in the category of  $H_1 \times H_2$ -modules can be depicted by placing the two diagrams in parallel next to each other, see Figure 2.4 right.

When some of the groups are direct products, diagrammatic presentation of functors and their compositions as sequences of dots on a line can be refined to presentations via suitable

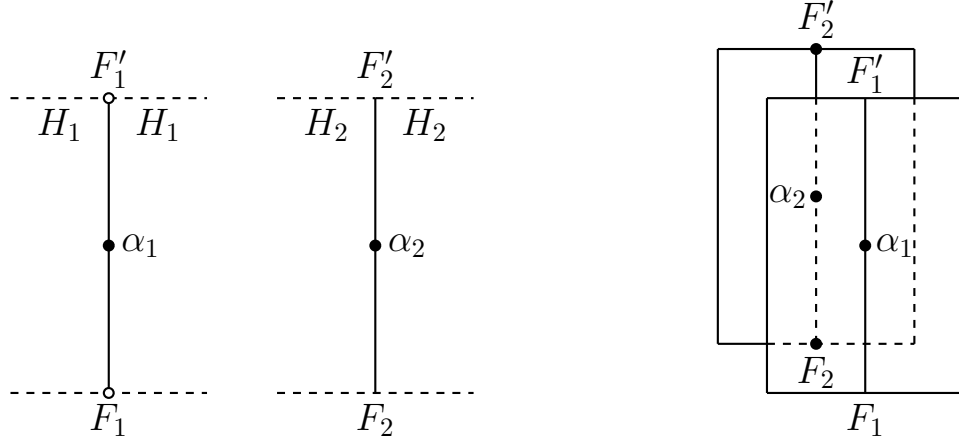


FIGURE 2.4. Diagrams of natural transformations  $\alpha_1, \alpha_2$  and of their exterior tensor product.

graphs that come with a projection on a line. Suppose we are given an inclusion of groups  $H_1 \times H_2 \subset G$ . Denote the induction functor  $\text{Ind}_{H_1 \times H_2}^G$  from  $H_1 \times H_2$ -modules to  $G$ -modules by a vertex with  $H_1, H_2$  lines flowing in and  $G$  line flowing out, see Figure 2.5 left. The restriction functor is depicted by having a  $G$ -line split into  $H_1$  and  $H_2$  lines, see Figure 2.5 middle. One can then build diagrams for compositions of these functors, see Figure 2.5 right, for instance. These graphs come with projections onto  $\mathbb{R}^1$ , to keep track of the order of composition of functors.

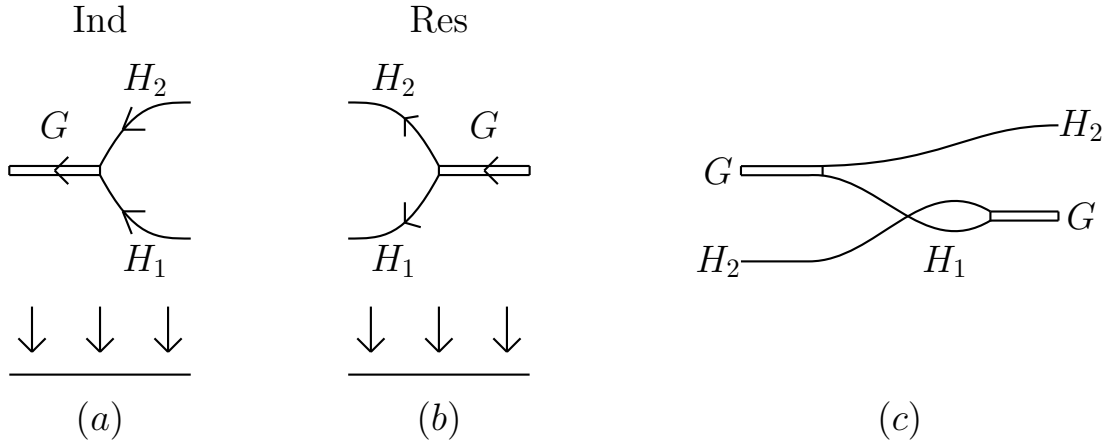


FIGURE 2.5. Diagrams of the induction (a) and restriction (b) functors. Diagram (c) is a composition of one restriction, one induction, and one permutation functor, going from the category of  $G \times H_2$ -modules to that of  $H_2 \times G$ -modules. Composition is depicted and read from right to left.

Natural transformations between these compositions can be naturally depicted by foams that extend between such diagrams. First off, identity natural transformation from the induction functor to itself (respectively, from the restriction functor to itself) is depicted by the direct product foam, the graph depicting this functor times the unit interval  $[0, 1]$ , see Figure 2.6.

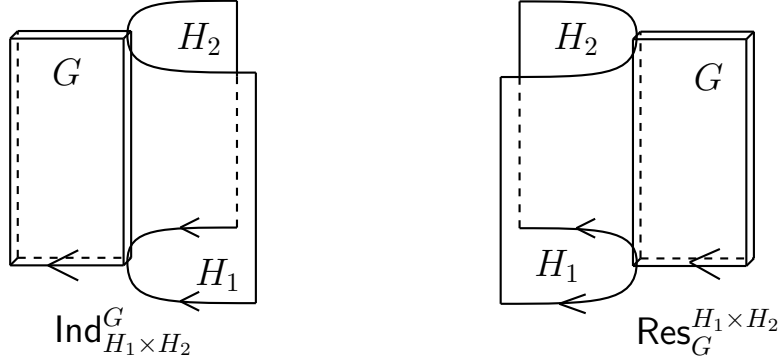


FIGURE 2.6. Identity natural transformations on induction and restriction functors  $\text{Ind}_{H_1 \times H_2}^G$ ,  $\text{Res}_G^{H_1 \times H_2}$ , respectively.

Singular lines in these foams are referred to as *seam* lines. A natural transformation  $a$  from the induction functor to itself may be denoted by a dot on a seam line, labelled  $a$ , see Figure 2.7 left, and likewise for an endomorphism of the restriction functor. A central element  $c \in Z(\mathbf{k}G)$  in the center  $Z(\mathbf{k}G)$  of the group algebra  $\mathbf{k}G$  is denoted by a dot floating in a facet  $G$  labelled  $c$ , see Figure 2.7 right.

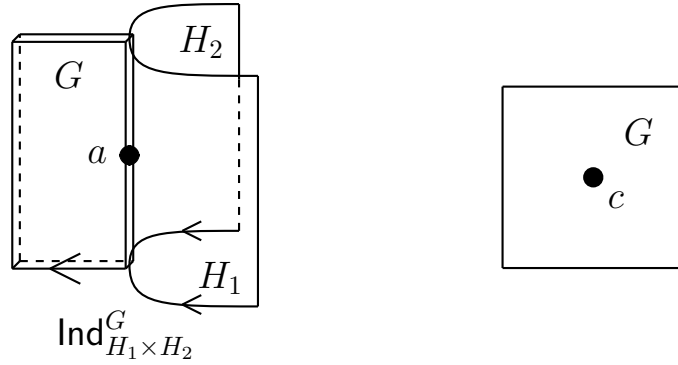


FIGURE 2.7. Left: natural transformation  $a$ , an endomorphism of the induction functor. Right: central element  $c$  of  $\mathbf{k}G$ .

The functor  $V \otimes -$  of the tensor product with a representation  $V$  of  $G$  is denoted by a dot on a line, with label  $V$  and the regions to the sides of the dot labelled  $G$ , see Figure 2.8 left. Identity natural transformation  $V \otimes - \Rightarrow V \otimes -$  is depicted by a vertical line (*defect or seam line*) labelled  $V$ , see Figure 2.8 middle. A homomorphism  $\gamma : V_1 \rightarrow V_2$  of  $G$ -modules induces

a natural transformation  $V_1 \otimes - \longrightarrow V_2 \otimes -$  of the functors  $V_1 \otimes -$  and  $V_2 \otimes -$ , which we also denote by  $\gamma$ ; it is depicted by a dot on a *defect line* for  $V$ , see Figure 2.8 right, with the defect line label changing from  $V_1$  to  $V_2$ .

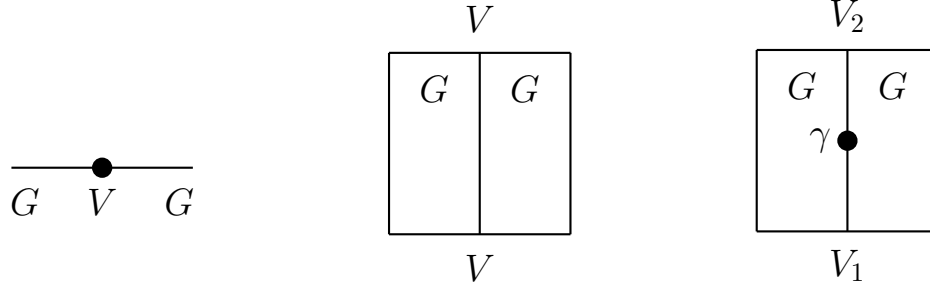


FIGURE 2.8. Left: notation for the functor  $V \otimes -$  of the tensor product with  $V$ . Middle: identity natural transformation on  $V \otimes -$ . Right: natural transformation  $\gamma: V_1 \otimes - \longrightarrow V_2 \otimes -$ .

### 3. FOAMS FOR THE ITERATED WREATH PRODUCTS OF $S_2$ 'S

**3.1. Iterated wreath products of  $S_2$ 's.** For some background on the wreath product, see [CST, OOR, IW1, IW2, IO]. Denote by  $G_n$  the  $n$ -th iterated wreath product of the symmetric group  $S_2$ . It can be defined as the group of symmetries of the full binary tree  $T_n$  of depth  $n$ . This binary tree has a root,  $2^n$  leaf vertices, and all paths from the root to leaf vertices have length  $n$ . Tree  $T_n$  has  $2^{n+1} - 1$  vertices. Leaf vertices can be naturally labelled from 1 to  $2^n$  inductively on  $n$  so that the vertices of the left branch are labelled by 1 through  $2^{n-1}$  and those of the right branch are labelled by  $2^{n-1} + 1$  through  $2^n$ . See Figure 3.1 for the case when  $n = 4$ .

For small values of  $n$ , the group  $G_n$  has the following form:

- $G_0 = \{1\}$  is the trivial group,
- $G_1 = S_2$  is the symmetric group of order two,
- $G_2 = S_2 \wr S_2 = (S_2 \times S_2) \rtimes S_2$  has order 8 and is isomorphic to the dihedral group  $D_4$ .

Note that group  $G_n$  has order  $2^{2^n - 1}$ .

The group  $G_n$  has an index two subgroup naturally isomorphic to  $G_{n-1} \times G_{n-1}$ , which we also denote by

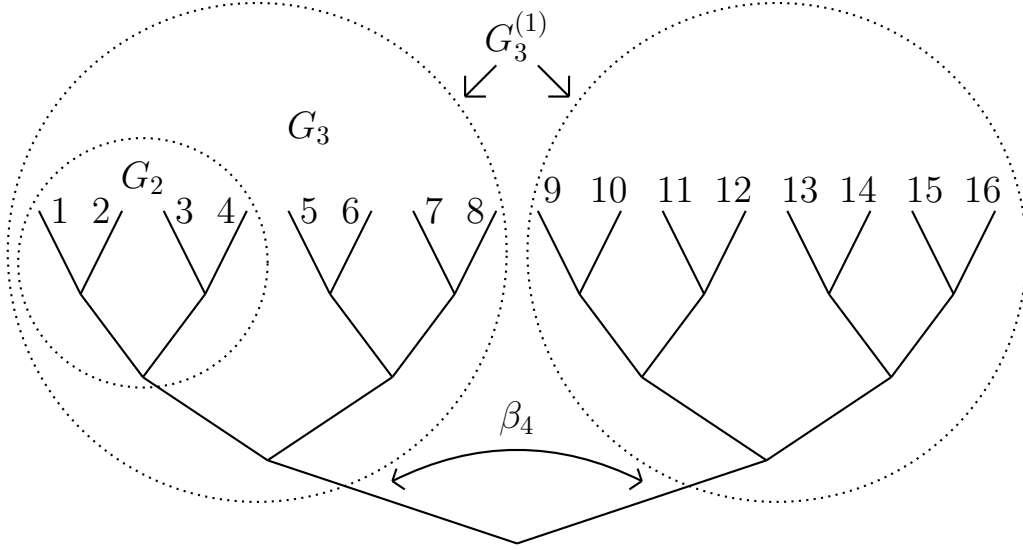
$$(1) \quad G_{n-1}^{(1)} := G_{n-1} \times G_{n-1} \xrightarrow{\iota_{n-1}} G_n.$$

The embedding consists of symmetries that fix the two branches of the tree, one to the left and the other to the right, of the root. The inclusion of this subgroup is denoted by  $\iota_{n-1}$ . There is a coset decomposition

$$(2) \quad G_n = G_{n-1}^{(1)} \sqcup G_{n-1}^{(1)} \beta_n = G_{n-1}^{(1)} \sqcup \beta_n G_{n-1}^{(1)},$$

where  $\beta_n$  is the involution that transposes the left and right branches of  $T_n$ . Notice the coincidence of left and right cosets

$$(G_{n-1} \times G_{n-1}) \beta_n = \beta_n (G_{n-1} \times G_{n-1}),$$

FIGURE 3.1. Tree  $T_4$ .

which holds for cosets of any index two subgroup. In particular, the left and right cosets are also double cosets. Furthermore, for  $g_1, g_2 \in G_{n-1}$ ,

$$(g_1, g_2) \beta_n = \beta_n (g_2, g_1),$$

that is, moving through  $\beta_n$  switches the order of the two terms in the product  $G_{n-1} \times G_{n-1}$ . Denote by  $\tau$  the transposition involution of  $G_{n-1}^{(1)} = G_{n-1} \times G_{n-1}$ ,

$$(3) \quad \tau(g_1, g_2) := (g_2, g_1), \quad g_1, g_2 \in G_{n-1}.$$

Then

$$(4) \quad \tau(g) = \beta_n g \beta_n, \quad g \in G_{n-1}^{(1)}.$$

By induction on  $n$ , we can canonically identify  $G_n$  with a subgroup of the symmetric group  $S_{2^n}$ . When  $n = 0$ , both  $G_0$  and  $S_{2^0} = S_1$  are the trivial group. For the induction step, given an inclusion  $j_{n-1} : G_{n-1} \hookrightarrow S_{2^{n-1}}$ , we realize  $G_n \subset S_{2^n}$  as the subgroup generated by:

- permutations of  $\{1, \dots, 2^{n-1}\}$  in  $G_{n-1}$ ,
- permutations of  $\{2^{n-1} + 1, \dots, 2^n\}$  in  $G_{n-1}$  (obtained by shifting all indices by  $2^{n-1}$ ),
- permutation  $\beta_n = (1, 2^{n-1} + 1)(2, 2^{n-1} + 2) \cdots (2^{n-1}, 2^n)$ .

Here we inductively identify  $\beta_n \in G_n$  with its image in  $S_{2^n}$ . The subgroup  $G_{n-1}^{(1)}$  is given by products of permutations of the first and the second type on the above list. As we've already mentioned, it's a normal subgroup of index 2, with  $\{1, \beta_n\}$  a set of coset representatives.

**3.2. A description of the center of  $G_n$ .** The center of  $G_n$  is an order two subgroup,

$$(5) \quad Z(G_n) = \{1, c_n\}, \quad c_n := (1, 2)(3, 4) \cdots (2^n - 1, 2^n),$$

see [IO, Lemma 3.6].



Define  $G_{n-k}^{(k)}$  as the subgroup  $(G_{n-k})^{\times 2^k} \subset G_n$  given by permutations that fix all nodes of the full binary tree at distance at most  $k-1$  from the root. There is a chain of inclusions

$$(6) \quad \{1\} = G_0^{(n)} \subset G_1^{(n-1)} \subset \dots \subset G_{n-2}^{(2)} \subset G_{n-1}^{(1)} \subset G_n^{(0)} = G_n.$$

Each inclusion

$$(7) \quad G_{n-k-1}^{(k+1)} \subset G_{n-k}^{(k)}$$

is that of an index  $2^{2^k}$  normal subgroup, with the quotient isomorphic  $C_2^{\times 2^k}$ .

**3.3. Induction and restriction bimodules.** We denote  $\mathbf{k}G_n$ , viewed as a bimodule over itself, by  $(n)$ . Denote  $\mathbf{k}G_{n-1}^{(1)} := \mathbf{k}(G_{n-1} \times G_{n-1})$  by  $(n-1, n-1)$  and even by  $(n-1)^{(1)}$ , to further compactify the notation, and extend these notations to tensor products of bimodules. For instance

$$(n)_{(n-1)^{(1)}}(n) := \mathbf{k}G_n \otimes_{\mathbf{k}G_{n-1}^{(1)}} \mathbf{k}G_n,$$

is naturally a  $\mathbf{k}G_n$ -bimodule.

Using notations from [Kh1, Section 3.2], we write down the biadjointness maps:

- (1)  $\alpha_{n-1}^n : (n)_{(n-1)^{(1)}}(n) \longrightarrow (n)$ , where  $x \otimes y \mapsto xy$ ,  $x, y \in (n) = \mathbf{k}G_n$ ,
- (2)  $\gamma_{n-1}^n : (n-1)^{(1)} \longrightarrow (n-1)^{(1)}(n)_n(n)_{(n-1)^{(1)}}$ , where  $x \mapsto x \otimes 1 = 1 \otimes x$ ,  $x \in (n-1)^{(1)}$ ,
- (3)  $\alpha_n^{n-1} : (n-1)^{(1)}(n)_n(n)_{(n-1)^{(1)}} \cong (n-1)^{(1)}(n)_{(n-1)^{(1)}} \longrightarrow (n-1)^{(1)}$  takes  $g \in (n)$  to  $p_{n-1}(g) \in (n-1)^{(1)}$  by  $p_{n-1}(g) = \begin{cases} g & \text{if } g \in (n-1)^{(1)}, \\ 0 & \text{otherwise.} \end{cases}$
- (4)  $\gamma_n^{n-1} : (n) \longrightarrow (n)_{(n-1)^{(1)}}(n)$ , where  $x \mapsto 1 \otimes x + \beta_n \otimes \beta_n x$ , and  $x \in (n)$ .

These four bimodule maps (or morphisms of functors) are represented by the four diagrams in Figure 3.2.

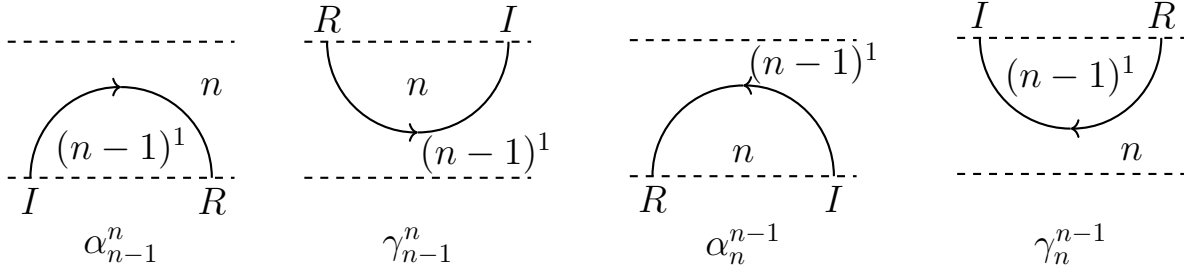


FIGURE 3.2. Diagrams for natural biadjointness transformations. Letters  $R$  and  $I$  stand for *restriction* and *induction* functors, respectively.

**Proposition 3.1.** *These four natural transformations turn functors  $I_{n-1}^n$  and  $R_n^{n-1}$  into a cyclic biadjoint pair.*

We refer the reader to [Kh1, Section 3.2] for details, in the general case of a finite index subgroup. In particular, planar isotopy relations between compositions of these cups and caps hold, see Figure 2.2, where the general case of  $H \subset G$  of finite index is shown.

For our specific case, we have obvious relations in Figure 3.3.

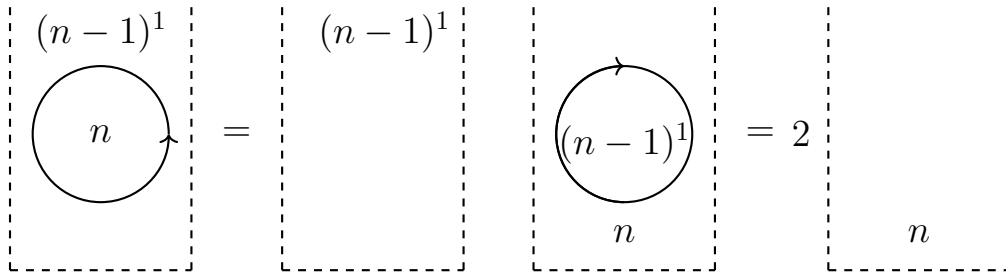


FIGURE 3.3. Some simple relations on diagrams.

We now refine these planar diagrams to a foam description for these and related intertwiners between compositions of induction and restriction functors  $I_{n-1}^n$  and  $R_n^{n-1}$ . We denote the induction and restriction functors by trivalent vertices in graphs as shown in Figure 3.4 left.

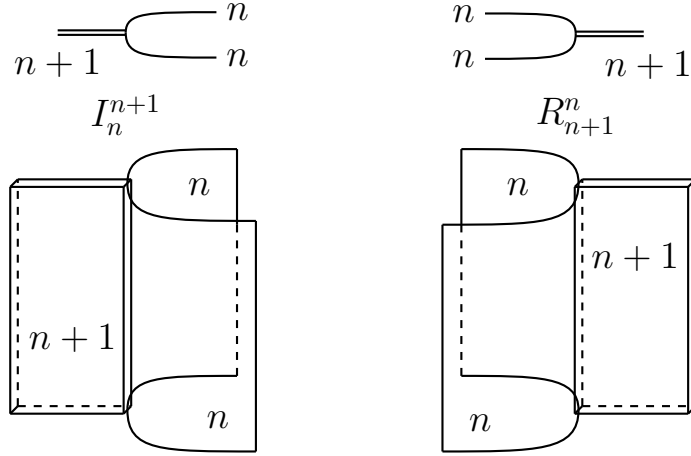


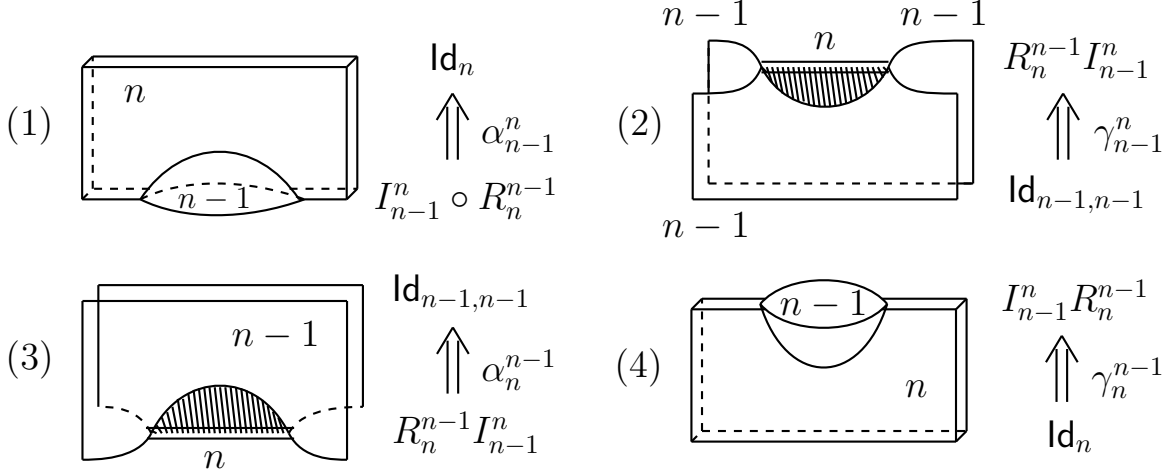
FIGURE 3.4. Induction and restriction functors  $I_n^{n+1}, R_{n+1}^n$  (top figures) and identity natural transformation on them (bottom figures).

Identity natural transformations for these functors are shown in Figure 3.4 right. The four biadjointness transformations are shown in Figure 3.5.

Biadjointness relations translate into the isotopy properties of foam glued from these four foams. One out of four possible isotopy relations is shown in Figure 2.2.

### 3.4. Mackey induction-restriction formula and decomposition of Ind-Res functor.

To the transposition automorphism  $\tau$  of  $G_{n-1,n-1}$  taking  $g_1 \times g_2$  to  $g_2 \times g_1$ , we associate  $\mathbf{k}G_{n-1,n-1}$ -bimodule  $B_{12}$  given by  $\mathbf{k}G_{n-1,n-1}$  with the left action twisted by  $\tau$ . Denote by  $T_{12}$  the invertible endofunctor of  $\mathbf{k}G_{n-1,n-1}\text{-mod}$  given by tensoring with  $B_{12}$ .

FIGURE 3.5. The four biadjointness transformations for  $I_{n-1}^n, R_n^{n-1}$ .

**Proposition 3.2.** *There is a canonical decomposition of functors*

$$(8) \quad R_n^{n-1} \circ I_{n-1}^n \cong \text{Id} \oplus T_{12}.$$

Diagrams for the three functors in this isomorphism are shown in Figure 3.6. In Figure 3.7, we describe the direct sum decomposition via foams.

The composition  $R_n^{n-1} \circ I_{n-1}^n$  is given by tensoring with the  $G_{n-1,n-1}$ -bimodule  $G_n$ . The proposition follows from the Mackey induction-restriction formula.

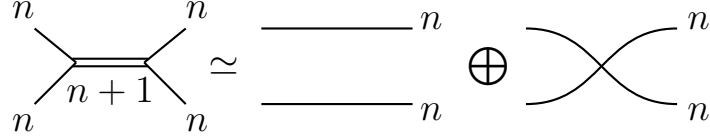


FIGURE 3.6. Diagrams for the three functors in (8).

The direct sum decomposition property translates into the following relations:

$$\begin{aligned} y_1 x_1 + y_2 x_2 &= \text{id}_{RI}, \\ x_1 y_1 &= \text{id}, & x_2 y_2 &= \text{id}, \\ x_1 y_2 &= 0, & x_2 y_1 &= 0. \end{aligned}$$

Foam equivalents of these relations are shown in Figure 3.8.

When depicted in  $\mathbb{R}^3$ , foams for maps  $x_2, y_2$  are immersed, and contain “overlap” or “intersection” lines or seams. Using biadjointness of the induction and restriction functors, these immersed foams can be converted into foams in Figure 3.9, depicting mutually-inverse natural transformations, denoted  $\ell(\beta_n)$  and  $\ell(\beta_n)'$ , respectively, between functors  $R_n^{n-1}$  and  $T_{12}R_n^{n-1}$ .

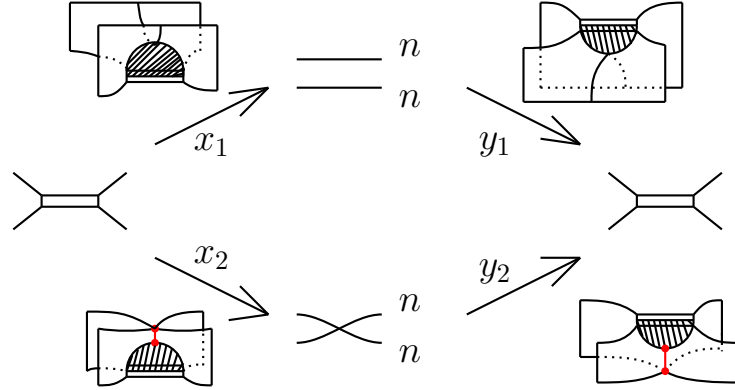


FIGURE 3.7. Maps (foams) describing the direct sum decomposition in (8).

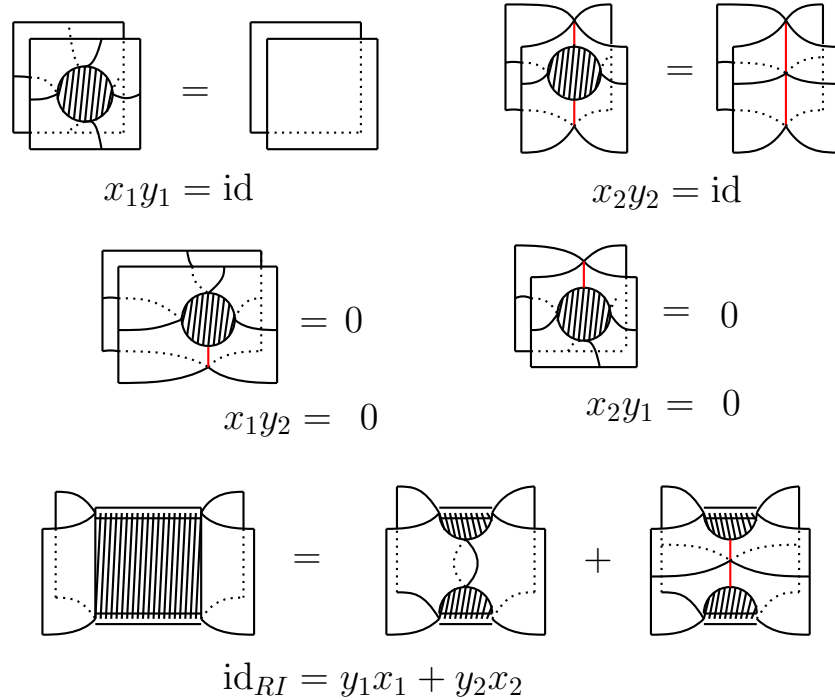


FIGURE 3.8. Direct sum decomposition relations.

Reflecting these diagrams about the  $yz$ -plane gives dual (biadjoint) mutually-inverse natural transformations between the functors  $I_{n-1}^n$  and  $I_{n-1}^n T_{12}$ . Figures 3.10 and 3.11 depict relations that these two maps are mutually-inverse isomorphisms.

Endpoints of immersion seams can move freely along the  $(n, n-1)$ -seam lines, see Figure 3.12. Deforming intersecting facets of these foams embedded in  $\mathbb{R}^3$  gives a number of obvious relations, one of which is shown in Figure 3.13.

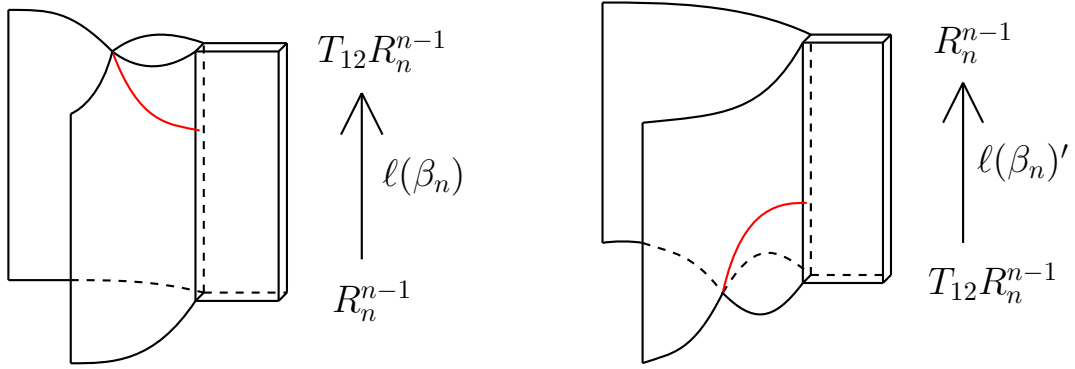


FIGURE 3.9. Intersection seams giving mutually-inverse functor isomorphisms  $T_{12}R_n^{n-1} \cong R_n^{n-1}$ .

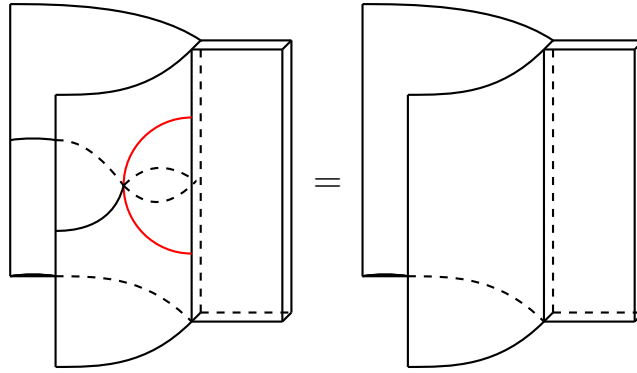


FIGURE 3.10. Relation  $\ell(\beta_n)'\ell(\beta_n) = \text{id}$  allows to undo an immersion seam that goes out and back into an  $(n, n-1)$ -seam.

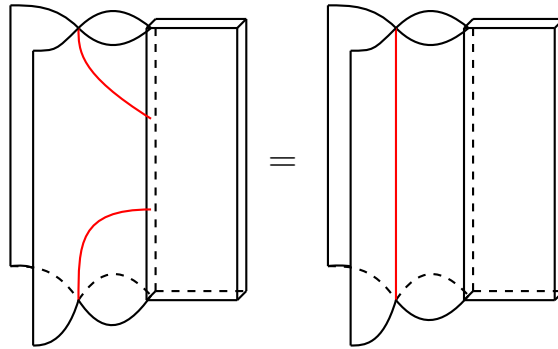


FIGURE 3.11. Relation  $\ell(\beta_n)\ell(\beta_n)' = \text{id}$  cancels two adjacent immersion points on an  $(n, n-1)$ -seam.

Together, these relations allow to reduce the number of immersion points along an  $(n, n-1)$ -seam to one or none. If such a seam closes into a disk which carries no additional decorations,

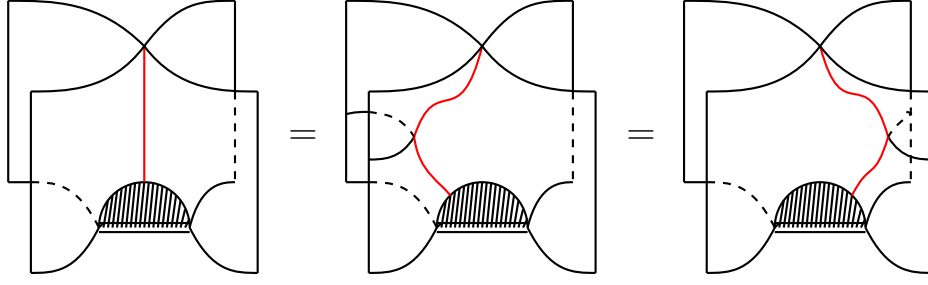
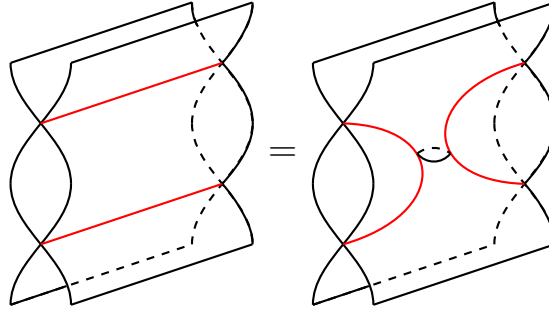


FIGURE 3.12. Deforming an immersion seam and moving its endpoint.

FIGURE 3.13. An isotopy of immersed surfaces in  $\mathbb{R}^3$ . Intersection lines are shown in red.

it can then be reduced to either two parallel planes (top left relation in Figure 3.8), if the original number of immersion endpoints along a seamed circle is even, or to 0 (either one of the middle row relations in Figure 3.8), if the number of immersion endpoints along a seamed circle is odd.

Functor  $T_{12}$  is just the permutation functor, induced by the transposition of two copies of the group  $G_{n-1}$  in the direct product, and satisfies the relations

$$T_{12}T_{12} = \text{id}, \quad T_{12}T_{23}T_{12} = T_{23}T_{12}T_{23}.$$

We leave it to the reader to draw the corresponding relations on immersed foams. The second relation is induced by a foam with three facets and a triple intersection point of these facets, where three intersection seams meet.

For a seam  $C$  that's closed into a circle and bounds a disk  $D$ , as in the two top rows of Figure 3.8, consider the number  $m$  of immersion points on it (points where a red segment ends). Using the above relations preserving the parity of  $m$  we can reduce the foam to have at most one immersion point along  $C$ . From Figure 3.8 relations we then see that a diagram evaluates to 0 if  $m$  is odd. If  $m$  is even, diagram can be simplified to one without  $C$  and disk  $D$ , and immersion endpoints along  $C$  matched in pairs.

There are also obvious isotopy relations, some of which can be obtained from Figure 2.2 by substituting a direct product  $H_1 \times H_2$  for  $H$  and converting diagrams into foams, see also [Kh3].

**3.5. Central elements and bubbles.** Recall that the center  $Z(G_n) \cong C_2$  is the cyclic group of order two, with the nontrivial element  $c_n = (1, 2)(3, 4) \cdots (2^n - 1, 2^n)$ . Via the inclusion  $\iota_{n-1}$  this element can be defined inductively as  $c_n = \iota_{n-1}(c_{n-1} \times c_{n-1})$ . We denote  $c_n$  by a dot on a facet labelled  $n$ , see Figure 3.14 left. Square of the dot is the identity, see Figure 3.14 right. Element  $c_n$  can also be thought of as an endomorphism of the identity functor on  $\mathbf{k}G_n\text{-mod}$ .

The center  $Z(\mathbf{k}G_n)$  is a commutative algebra with a basis parametrized by conjugacy classes of  $G_n$ . Iterating the bubbles and dots construction allows us to construct various elements of the center.

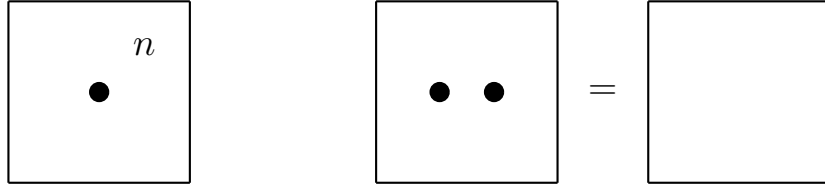


FIGURE 3.14. Central element  $c_n$  and a relation on it: the square of the dot is the identity.

As a first example, taking an  $n$ -facet, we can create an  $(n-1)$ -bubble on it and insert a dot into one or both facets of the bubble, see Figures 3.15 and 3.16.

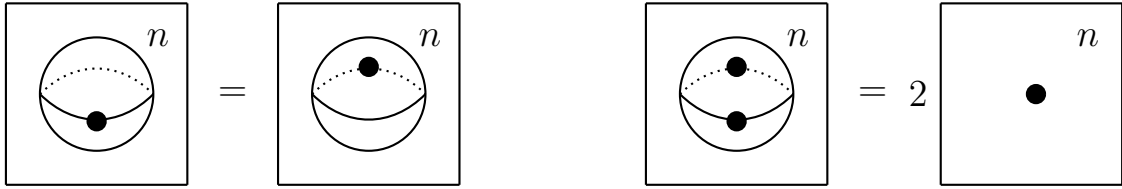


FIGURE 3.15. The simplest relations on  $c$ -bubbles.

To compute the corresponding central elements, we factor these foams into a composition of elementary foams and compute the corresponding natural transformations. For instance, bubble with a single dot is a composition of three elementary foams, see Figure 3.16.

These three foams are local singular maximum and minimum, and adding a dot to a facet. The corresponding bimodule map is composition

$$\mathbf{k}G_n \xrightarrow{\gamma_n^{n-1}} \mathbf{k}G_n \otimes_{n-1} \mathbf{k}G_n \xrightarrow{c_{n-1} \times 1} \mathbf{k}G_n \otimes_{n-1} \mathbf{k}G_n \xrightarrow{\alpha_{n-1}^n} \mathbf{k}G_n,$$

where  $\otimes_{n-1}$  denotes the tensor product over the subalgebra  $\mathbf{k}G_{n-1}^{(1)}$  and  $\gamma_n^{n-1}$  and  $\alpha_{n-1}^n$  are given by formulas (1) and (4), see also Figure 3.5.

For  $x \in \mathbf{k}G_n$  we compute the composition

$$x \mapsto 1 \otimes x + \beta_n \otimes \beta_n x \mapsto 1 \otimes c_{n-1}^{(1)} x + \beta_n \otimes c_{n-1}^{(1)} \beta_n x \mapsto c_{n-1}^{(1)} x + \beta_n c_{n-1}^{(1)} \beta_n x.$$

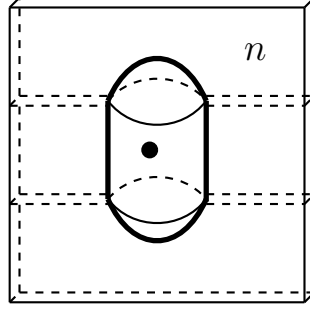


FIGURE 3.16. An example of the composition  $\mathbf{k}G_n \rightarrow \mathbf{k}G_n \otimes \mathbf{k}G_{n-1}^{(1)} \otimes \mathbf{k}G_n \rightarrow \mathbf{k}G_n$ .

This endomorphism of the identity functor is the multiplication by the central element

$$c_{n-1}^{(1)} + \beta_n c_{n-1}^{(1)} \beta_n = c_{n-1}^{(1)} + c_{n-1}^{(2)} = c_{n-1} \times 1 + 1 \times c_{n-1}$$

(where we skipped the inclusion map  $\iota_n$ ), also implying the first relation in Figure 3.15. Another easy computation gives the second relation in Figure 3.15.

Iterating the bubble construction, one can produce more general central elements of the group algebra  $\mathbf{k}G_n$ . One can keep splitting some facets of the bubble into thinner facets and placing dots on some of these facets. An example is shown in Figure 3.17, with the foam there describing the central element

$$(9) \quad c_{n-2}^{(1)} + c_{n-2}^{(2)} + c_{n-2}^{(3)} + c_{n-2}^{(4)}.$$

Here  $c_{n-2}^{(i)}$  stands for the  $i$ -th copy of  $c_{n-2}$  in the direct product  $G_{n-2}^{\otimes 4} \subset G_n$ .

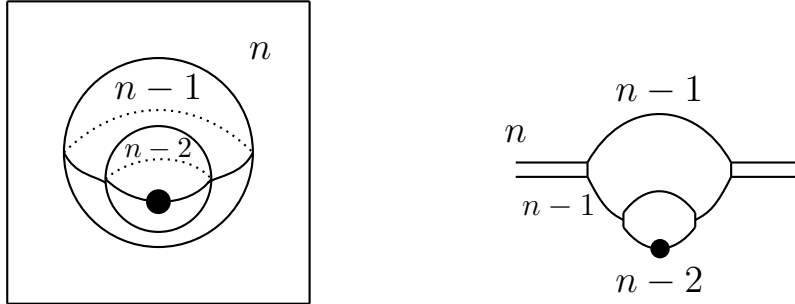


FIGURE 3.17. A more complicated bubble describing a central element. The middle cross-section of this bubble is shown on the right.

#### 4. DEFECT LINES AND NETWORKS

##### 4.1. Tensoring with induced representations.

**Lemma 4.1.** *Let  $H \subseteq G$  be a subgroup, and  $M$  a  $G$ -module. There is a natural in  $M$  isomorphism*

$$(10) \quad \mathrm{Ind}_H^G \circ \mathrm{Res}_G^H(M) \xrightarrow{\sim} \mathrm{Ind}_H^G(\underline{\mathbf{k}}) \otimes M.$$



Consequently, the composition of restriction and induction functors is isomorphic to the functor of tensor product with the induced representation  $\text{Ind}_H^G(\underline{\mathbf{k}})$ .

Here  $\underline{\mathbf{k}}$  denotes the trivial representation of  $H$ .

*Proof.* Define the map

$$(11) \quad \varphi : \mathbf{k}G \otimes_{\mathbf{k}H} M \rightarrow (\mathbf{k}G \otimes_{\mathbf{k}H} \underline{\mathbf{k}}) \otimes_{\mathbf{k}} M, \quad g \otimes m \mapsto (g \otimes \underline{1}) \otimes gm.$$

The module on the left is  $\text{Ind}_H^G \circ \text{Res}_G^H(M)$ , the one on the right is  $\text{Ind}_H^G(\underline{\mathbf{k}}) \otimes M$ . The map is a module map, natural in  $M$ .

Conversely, let  $\psi : (\mathbf{k}G \otimes_{\mathbf{k}H} \underline{\mathbf{k}}) \otimes_{\mathbf{k}} M \rightarrow \mathbf{k}G \otimes_{\mathbf{k}H} M$  be given by  $(g \otimes \underline{1}) \otimes n \mapsto g \otimes g^{-1}n$ . One can easily check that  $\varphi$  and  $\psi$  are inverses.  $\square$

Thus  $H \subseteq G$  being a subgroup of  $G$ ,

$$(12) \quad \text{Ind}_H^G \circ \text{Res}_G^H \simeq V_H^G \otimes -$$

is an isomorphism of functors. We denote by  $\mathbf{V}_H^G := \text{Ind}_H^G(\underline{\mathbf{k}})$  the induced representation of  $G$ .

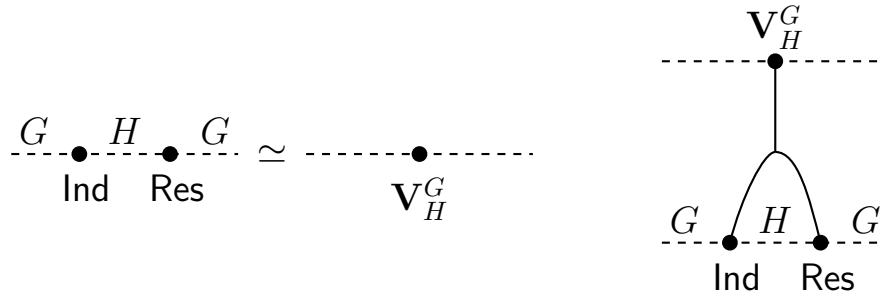


FIGURE 4.1. Left: diagrammatic notations for the two functors. Right: a vertex to denote their isomorphism.

Isomorphism  $\varphi$  of functors can be represented by an invertible trivalent vertex in Figure 4.1 going two marks on a dashed line, representing composition of induction and restriction functors, to a single mark, labeling the tensor product functor. The inverse isomorphism can be represented by a reflected diagram.

Assume that  $\text{char}(\mathbf{k}) = 0$ , so representations of finite groups over  $\mathbf{k}$  are completely reducible. Given a subrepresentation  $V \subseteq \mathbf{V}_H^G$ , choose an idempotent endomorphism  $e_V \in \text{End}(\mathbf{V}_H^G)$  of projection on  $V$ . It can be described by a box labelled  $e_V$  on the vertical line depicting the identity natural transformation of the functor  $\mathbf{V}_H^G \otimes -$ , see Figure 4.2.

The quotient group  $G_n/G_{n-1}^{(1)}$  is the cyclic group  $C_2$ , and its two-dimensional regular representation, viewed as a representation of  $G_n$ , will be denoted  $V_1$ . The latter representation is the induced from the trivial representation of  $G_{n-1}^{(1)}$ ,

$$V_1 \cong \text{Ind}_{G_{n-1}^{(1)}}^{G_n}(\underline{\mathbf{k}}).$$

We depict the corresponding isomorphism of functors in Figure 4.3.

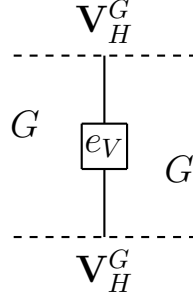
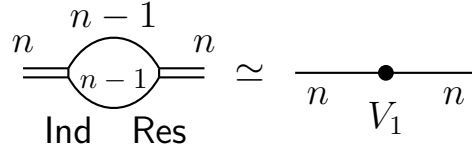
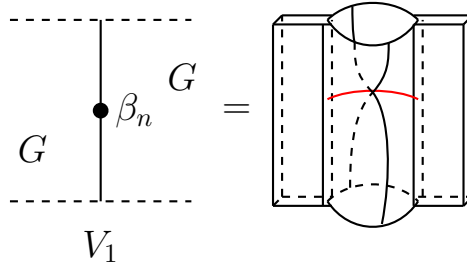

 FIGURE 4.2. Idempotent  $e_V$  on the endomorphism of  $\mathbf{V}_H^G$ .


FIGURE 4.3. Functor isomorphism.

Under the quotient map,  $\beta_n \in G_n$  becomes the nontrivial element of  $C_2$ , which we may also denote  $\underline{\beta}_n$ . Multiplication by  $\beta_n$  is an involutive endomorphism of  $V_1$ , see Figures 4.4 left and Figure 4.5. Figure 4.4 right describes the foam that represents the corresponding endomorphism of  $\text{Ind} \circ \text{Res}$ , under its isomorphism with the tensor product functor. The foam consists of a flip between two  $(n-1)$  facets, with the intersection interval shown in red.


 FIGURE 4.4. Foam representation of the endomorphism of the functor  $V_1 \otimes - \cong \text{Ind} \circ \text{Res}$  given by multiplication by  $\beta_n$ . Two lines on thin facets are used to better depict these facets.

Relation  $\beta_n^2 = 1$  translates into the foam identity in Figure 4.6 that can be obtained as a composition of Figure 3.13 and 3.10 relations.

**4.2. Foams for idempotents and basic relations on them.** Idempotents  $e_+ = \frac{1+\beta_n}{2}$  and  $e_- = \frac{1-\beta_n}{2}$  in the group algebra  $\mathbf{k}G_n$  give corresponding idempotents, also denoted  $e_+, e_-$ , in the quotient algebra  $\mathbf{k}C_2 \cong \text{End}_{G_n}(V_1)$ . These idempotents produce direct summands of

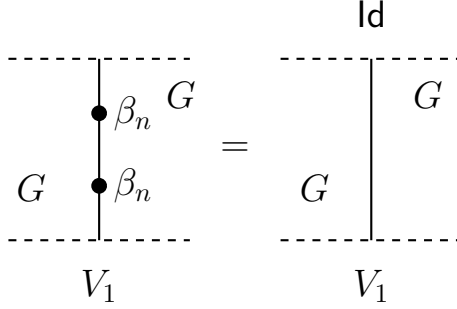


FIGURE 4.5.  $\beta_n^2 = 1$ , and endomorphism of  $V_1$  it induces squares to identity.

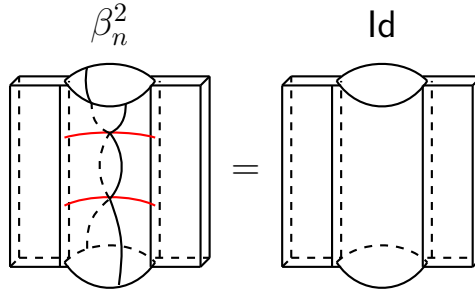


FIGURE 4.6. Equality of foams corresponding to the relation  $\beta_n^2 = 1$  (as endomorphisms of  $\text{Ind} \circ \text{Res}$  functor).

representation  $V_1$ , the trivial and the sign representations, that we denote  $V_+$  and  $V_-$ , so that

$$V_1 \cong V_+ \oplus V_-.$$

Note that  $V_+ \cong \underline{\mathbf{k}}$ , which is our two notations for the trivial representation.

Under functor isomorphism  $V_1 \otimes \bullet \cong \text{Ind} \circ \text{Res}$  these idempotents become idempotents in the endomorphism algebra of the latter functor, also denoted  $e_+$  and  $e_-$ . In the foam notation, we represent these idempotents in  $\text{End}(\text{Ind} \circ \text{Res})$  by disks, green and blue, respectively, that intersect two opposite seam lines, with labels  $+$  and  $-$ , respectively, see Figures 4.7 and 4.8.

Some of the obvious relations

$$1 = e_+ + e_-, \quad e_+ e_- = e_- e_+ = 0, \quad e_+^2 = e_+, \quad e_-^2 = e_-$$

are shown in Figures 4.9, and 4.10. Figure 4.11 shows how to convert from a planar to a foam representation of the identity endomorphism of  $V_-$ , also see Section 4.3.

Figure 4.12 shows two more immediate foam relations or simplifications for these idempotent disks. Figure 4.13 and 4.14 relations now follow.

The last relation implies the relation in Figure 4.15. Converting into the language of tensoring with representations, we can interpret it as saying that functor isomorphisms between tensoring with  $V_- \otimes V_-$  and  $V_+$  given by the two tubes at the top and bottom halves of Figure 4.15 left are mutually-inverse on one side. Consequently, they are mutually-inverse on

$$e_+ = \frac{1}{2} \left( \text{Id} + \beta_n \right)$$

 FIGURE 4.7. Idempotent  $e_+ = \frac{1 + \beta_n}{2}$ .

$$e_- = \frac{1}{2} \left( \text{Id} - \beta_n \right)$$

 FIGURE 4.8. Idempotent  $e_- = \frac{1 - \beta_n}{2}$ .

$$\text{Id} = e_+ + e_-$$

 FIGURE 4.9. The sum of two idempotents  $e_+$  and  $e_-$  gives the identity foam.

the other side as well, as shown in Figure 4.16, which can also be derived directly. Note that multiple blue disks along the tube in that figure can be reduced to a single one, via Figure 4.10 relation.

**4.3. Simplified (planar) notation.** Much simpler (and conventional) diagrammatics for representations of  $C_2 \simeq G_n/G_{n-1}^{(1)}$  are shown in Figures 4.17, 4.18, 4.19, 4.20, and 4.21. Lines for the identity endomorphism of the trivial representation can be erased, see Figure 4.18. We are essentially left with the sign representation  $V_-$  and isomorphisms given by a cup and a cap between its tensor square and the trivial representation.

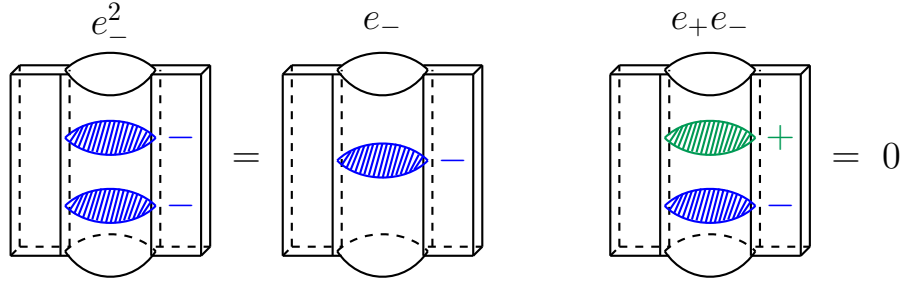


FIGURE 4.10. Left: idempotency relation  $e_-^2 = e_-$  via foams. Right: orthogonality relation  $e_+ e_- = 0$  via foams.

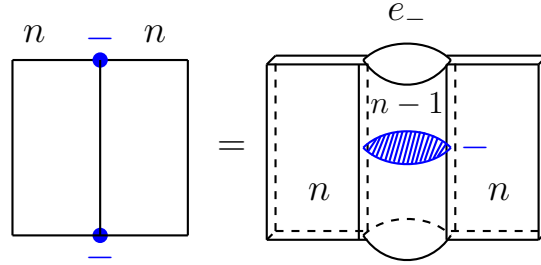


FIGURE 4.11. Converting from the planar to the foam presentation of the identity endomorphism of  $V_-$ .

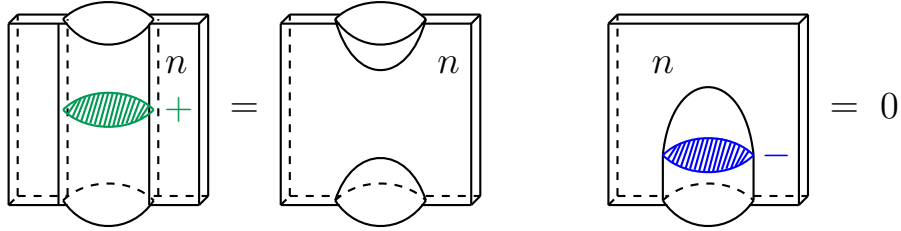


FIGURE 4.12. Left equality: symmetrizer  $e_+$  is the projection onto the trivial representation; the foam interpretation is shown. In the second equality, absence of homs between the trivial and the sign representations implies this relation, or one can use Figure 3.10 relation.

To convert between the two presentations, we need to replace  $V_-$  lines in the second diagrammatics by tubes spanned by one or more blue “minus” disks, see Figure 4.22 for the conversion of the “cap” morphism.

The correspondence on the level of objects is further clarified in Figure 4.23, with blue dot denoting the sign representation and the green dot the trivial representation (when it’s convenient to keep track of the latter).

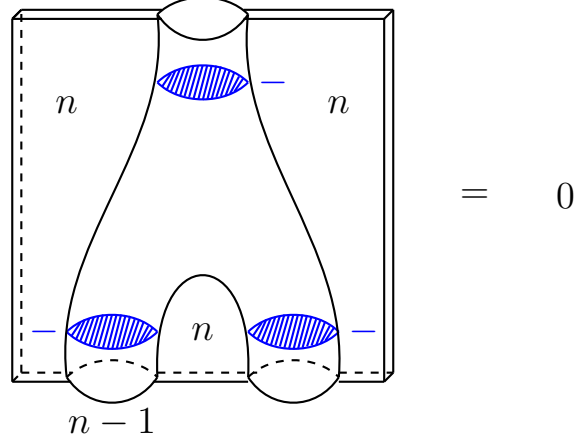


FIGURE 4.13. The only hom between irreducible representations  $V_- \otimes V_- \cong V_+$  and  $V_-$  is 0. This equality can also be checked by expanding three blue disks and canceling the terms.

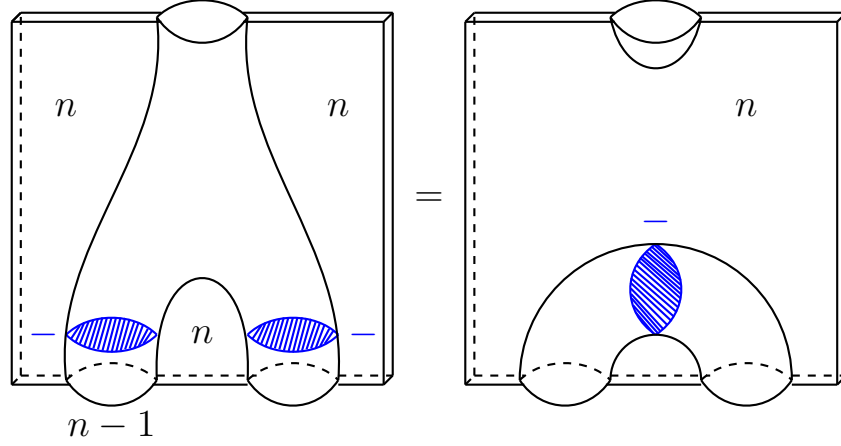


FIGURE 4.14. This relation follows by expanding the “neck” on top left as in Figure 4.9 and applying relations in Figures 4.12 and 4.13.

**4.4. Dihedral groups.** Consider the two diagrams in Figure 4.24. Each of them describes a summand of a composition of restriction and induction functors. In the diagram on the left, we first restrict from  $G_n$  to  $G_{n-1} \times G_{n-1}$ , then further restrict to  $G_{n-2} \times G_{n-2} \times G_{n-1}$ . After that we induce back to  $G_n$ . The “minus” idempotent is applied for the composition of restriction and induction between  $G_{n-1}$  and  $G_{n-2} \times G_{n-2}$ . In the diagram on the right, a similar functor is described, but the inner induction and restriction is for the other factor of the product  $G_{n-1} \times G_{n-1}$ .

**Proposition 4.2.** *The isomorphism in Figure 4.24 holds.*

*Proof.* Mutually-inverse isomorphisms between these functors are given by the foam in Figure 4.25 and its reflection about the  $xy$ -plane.  $\square$

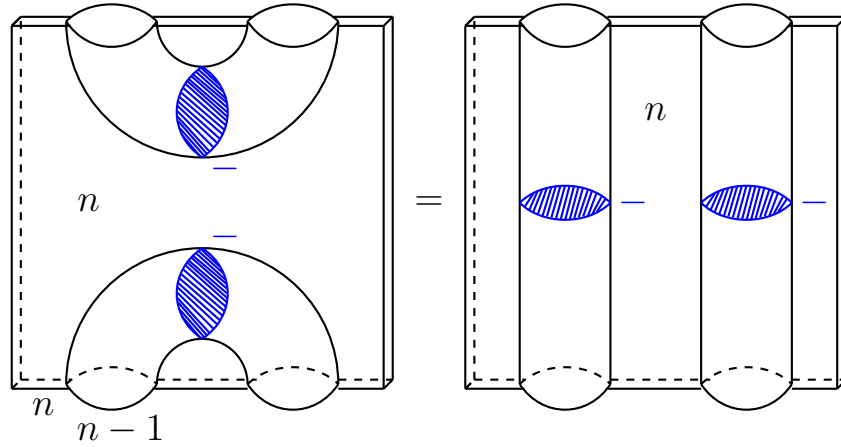
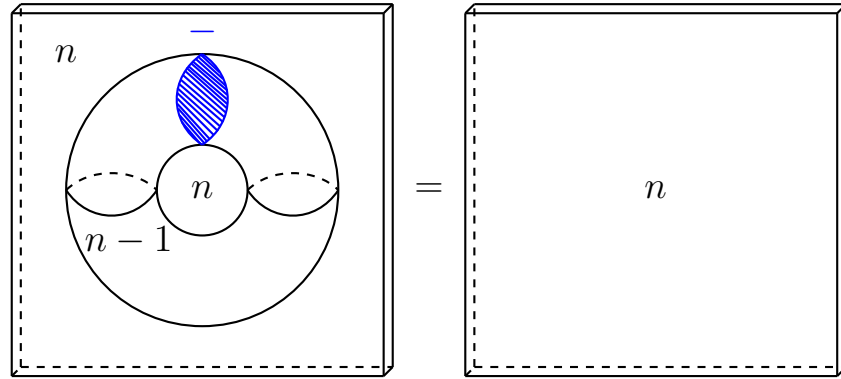
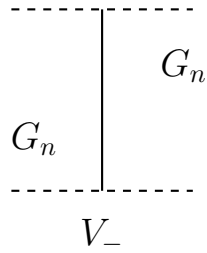


FIGURE 4.15. Foam equivalent of Figure 4.20 relation.

FIGURE 4.16. Horizontal circles indicate that the two  $(n-1)$ -facets on the left picture constitute a 2-torus inside the foam. Figure 4.10 relation allows to duplicate the  $e_-$ -disk, if desired. Compare with Figure 4.21 below.FIGURE 4.17. The sign representation  $V_-$  corresponds to the idempotent  $e_- = (1 - \beta_n)/2$ . The group  $G_{n-1}^{(1)}$  acts trivially on  $V_-$  and  $\beta_n$  acts by  $-1$ .

Denote by  $\mathcal{V}$  the functor given by the diagram on the left of Figure 4.24.

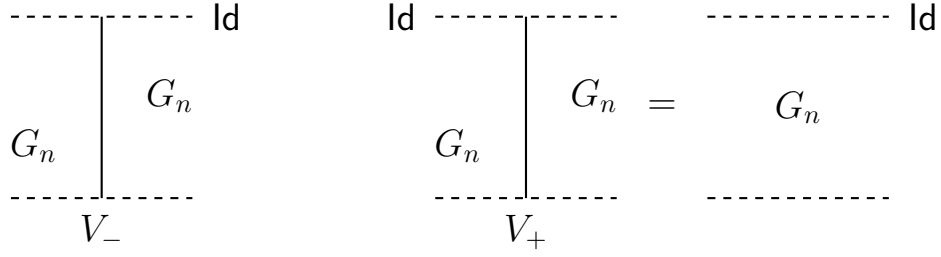


FIGURE 4.18.  $V_-$  is the sign and  $V_+$  is the trivial representation. Left: the identity endomorphism of the sign representation (and of the corresponding functor  $V_- \otimes \bullet$ ). Right: the identity endomorphism of the trivial representation. Lines representing the identity map of the trivial representation can be erased, simultaneously with removing dots denoting  $V_+$  on dashed lines.

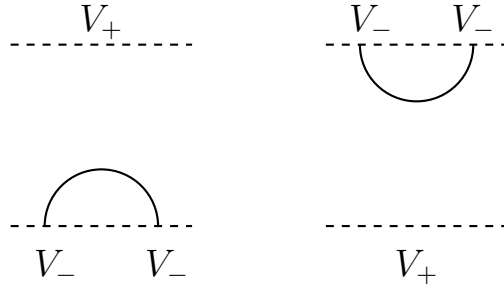


FIGURE 4.19. Mutually-inverse isomorphisms between  $V_- \otimes V_-$  and the trivial representation  $V_+$  since  $V_- \otimes V_- \simeq V_+$ .

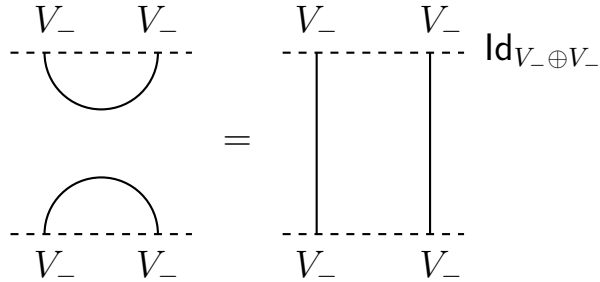


FIGURE 4.20. Composition of the two isomorphisms is the identity.

The quotient group  $G_n/G_{n-2}^{(2)}$  is naturally isomorphic to the dihedral group  $D_4$  of symmetries of the square,

$$(13) \quad G_n/G_{n-2}^{(2)} \cong D_4.$$

The quotient map

$$(14) \quad G_n/G_{n-2}^{(2)} \longrightarrow G_n/G_{n-1}^{(1)} \cong C_2$$



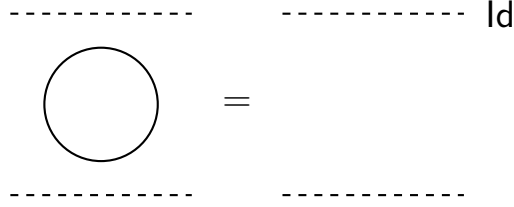


FIGURE 4.21. Composition of isomorphisms is the identity.

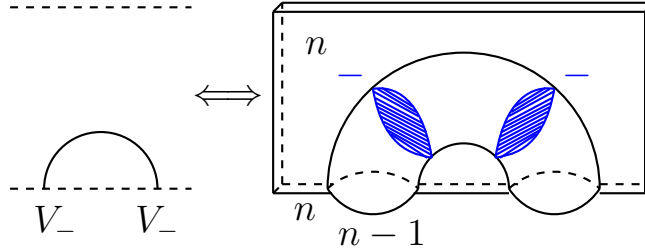
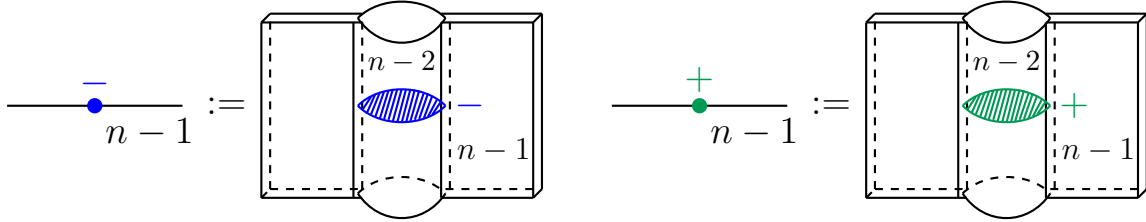
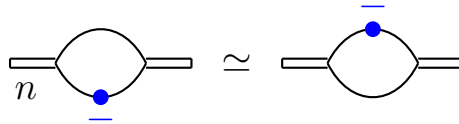
FIGURE 4.22. This correspondence represents the isomorphism  $V_-^{\otimes 2} \cong V_+$  given by a foam. Two  $e_-$  disks may be reduced to one, see Figure 4.10.FIGURE 4.23. Compact notations for idempotents  $e_-$  and  $e_+$ . For the equality on the right, the right hand side is isomorphic to the identity functor.

FIGURE 4.24. A functor isomorphism.

corresponds to the homomorphism  $D_4 \rightarrow C_2$  where to a symmetry of  $D_4$  one associates the induced permutation of the two diagonals. Thinking of the quotient group  $G_n/G_{n-2}^{(2)}$  as all symmetries of a full binary tree of depth 2, to get the homomorphism we map the tree to the square so that the two depth one branches correspond to the diagonals of the square, see Figure 4.26.

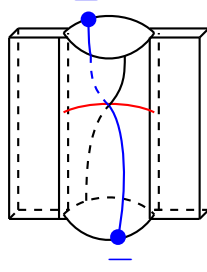


FIGURE 4.25. Foam for the functor isomorphism in Figure 4.24. The blue line depicts the identity endomorphism of the “blue point” functor (direct summand of the induction-restriction functor isomorphic to  $V_- \otimes -$ ). The black line on the other thin facet is drawn to help see the facet. The two thin facets intersect along the red interval.

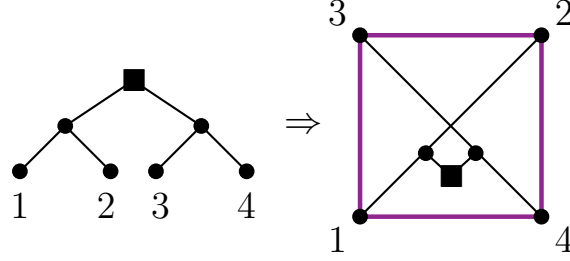


FIGURE 4.26. An identification of symmetries of a depth 2 full binary tree with those of a square. Nodes 1, 2, 3, 4 of the tree are mapped to vertices of the square.

Denote by  $V$  the unique (up to isomorphism) two-dimensional irreducible representation of  $D_4$ , the rotation representation.

**Proposition 4.3.** *Under the above group isomorphism, the functor of tensor product with  $V$  is isomorphic to the functor  $\mathcal{V}$  given in Figure 4.24.*

*Proof.* Functor  $\mathcal{V}$  is a direct summand of the composition  $\text{Ind} \circ \text{Res}$  for restricting from  $G_n$  to the subgroup  $G_{n-2} \times G_{n-2} \times G_{n-1}$  and inducing back. In  $D_4$ , the corresponding subgroup is  $H - \{1, (34)\}$ . The complement to  $\mathcal{V}$  in the above functor is  $\text{Ind} \circ \text{Res}$  for the subgroup  $G_{n-1}^{(1)}$  (since the complement is given by putting the “plus” label on the dot in Figure 4.24 left and “+” labels may be erased). Thus, the complementary functor is isomorphic to the direct sum of tensoring with the trivial  $V_+$  and the sign representation  $V_-$ .

The composition functor of restriction then induction for the subgroup  $H$  in  $D_4$  is isomorphic to the functor of the tensor product with the four-dimensional representation  $\mathbf{k}[D_4/H]$ . It’s easy to decompose this representation into the direct sum

$$(15) \quad \mathbf{k}[D_4/H] \cong V \oplus V_+ \oplus V_-,$$

using characters (in characteristic 0, see the table below) or directly (as long as  $\text{char}(\mathbf{k}) \neq 2$ ).  $\square$

So far we have accounted for the fundamental representation  $V$  of  $D_4$  and two one-dimensional representations: the trivial  $V_+$  and the sign representation  $V_-$ , on which the normal subgroup  $\{1, (12), (34), (12)(34)\}$  acts trivially.

Denote the remaining two one-dimensional representations of  $D_4$  by  $V_{-+}$  and  $V_{--}$ . On  $V_{-+}$  generators (12) and (1324) act by  $-1$ , and on  $V_{--}$  generators (12) and (13)(24) act by  $-1$ .

The table below lists the characters of the five irreducible representations of  $D_4$  and of representation  $\mathbf{k}[D_4/H]$ .

	1	(12)	(12)(34)	(1324)	(13)(24)
$V$	2	0	-2	0	0
$V_+$	1	1	1	1	1
$V_-$	1	1	1	-1	-1
$V_{-+}$	1	-1	1	-1	1
$V_{--}$	1	-1	1	1	-1
$\mathbf{k}[D_4/H]$	4	2	0	0	0

Consider the endofunctor  $\mathcal{V}'$  in the category of  $G_n$ -modules given by the diagram in Figure 4.27 left. This functor is a direct summand of the composition of restriction to  $G_{n-2}^{(2)}$  then induction back to  $G_n$  functor. The latter composition is isomorphic to the tensor product with the 8-dimensional representation  $\mathbf{k}[G_n/G_{n-2}^{(2)}]$ . The minus idempotents on both thin edges pick out a direct summand functor given by the tensor product with a two-dimensional representation.

One way to understand functor  $\mathcal{V}'$  is by computing the composition  $\mathcal{V} \circ \mathcal{V}$ , see Figure 4.29. The computation uses the relations in Figure 4.30. The square  $\mathcal{V}^2$  decomposes as the sum of two functors,

$$(16) \quad \mathcal{V}^2 \cong (\text{Ind}_{n-1}^n \circ \text{Res}_n^{n-1}) \oplus \mathcal{V}' \cong (V_+ \otimes *) \oplus (V_- \otimes *) \oplus \mathcal{V}',$$

since  $\text{Ind}_{n-1}^n \circ \text{Res}_n^{n-1}$  is isomorphic to the functor of tensoring with  $V_+ \oplus V_-$ . At the same time, we have decomposition of tensor product of representations

$$(17) \quad V \otimes V \cong V_+ \oplus V_- \oplus V_{-+} \oplus V_{--},$$

(tensor square of the fundamental  $D_4$  representation  $V$  is the sum of the four irreducible one-dimensional  $D_4$  representations).

Thus, functor  $\mathcal{V}'$  is isomorphic to the functor of tensoring with  $V_{-+} \oplus V_{--}$ ,

$$(18) \quad \mathcal{V}' \cong (V_{-+} \oplus V_{--}) \otimes *.$$

Foam that transposes the two thin edges of this diagram, together with the minus dots on them, see Figure 4.27, is an endomorphism of the diagram of order two. The two idempotents (symmetrizer and antisymmetrizer) made off this endomorphism give functors isomorphic to functors of tensor product with  $V_{-+}$  and  $V_{--}$ , respectively.

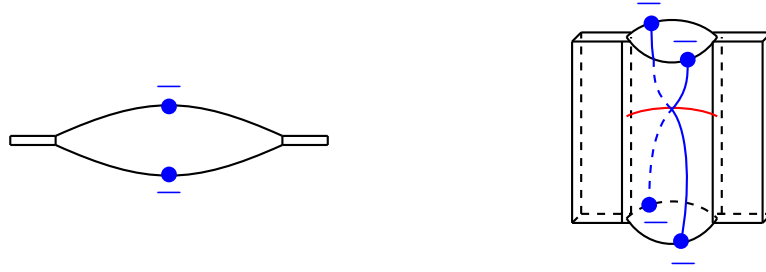


FIGURE 4.27. Left: An endofunctor  $\mathcal{V}'$  of  $G_n\text{-mod}$ . Right: an order two endomorphism  $\beta'$  of  $\mathcal{V}'$  (the flip). Symmetrizing or antisymmetrizing via  $\beta'$  decomposes  $\mathcal{V}'$  into a direct sum of two functors.

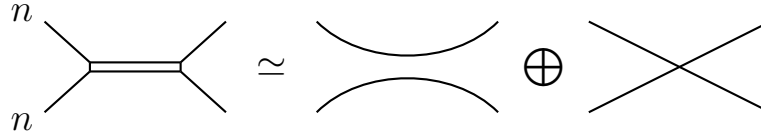


FIGURE 4.28. Direct sum decomposition of  $\text{Res} \circ \text{Ind}$  into the identity and the transposition functors, see earlier and Figure 3.6.

Figure 4.28 gives a direct sum decomposition of  $\text{Res} \circ \text{Ind}$  as the identity and the transposition functors, and Figure 4.31 shows that functors  $\mathcal{V}'$  and tensoring with  $V_{-+} \oplus V_{--}$  are isomorphic.

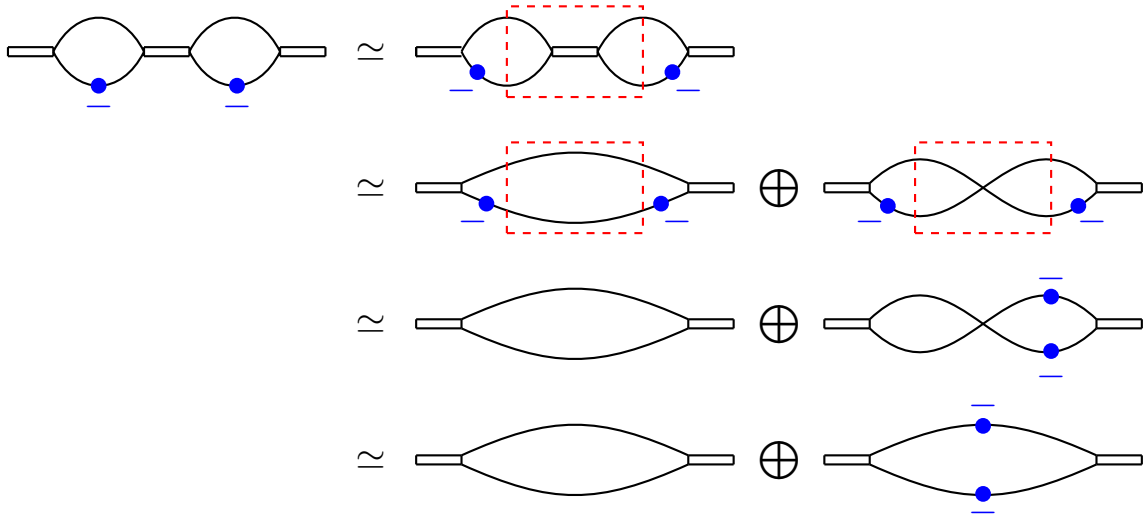


FIGURE 4.29. We apply relations in Figures 4.28 and 4.30 to decompose the square of the functor  $\mathcal{V}$ . Figure 4.28 relation is applied inside the dotted red rectangle.



FIGURE 4.30. Left: tensor square of  $V_-$  is the trivial representation,  $V_-^{\otimes 2} \cong V_+$ . Right: functor isomorphism  $\text{Ind} \circ T_{12} = \text{Ind}$ , where  $T_{12}$  is the transposition, given by Figure 3.9 foams reflected in the vertical plane.

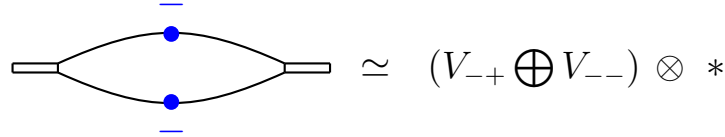


FIGURE 4.31. Functor  $\mathcal{V}'$  is isomorphic to the functor of tensoring with  $V_{-+} \oplus V_{--}$ .

We thus have five irreducible representations of  $D_4$ : trivial rep  $V_+$ , sign rep  $V_-$ , fundamental two-dimensional representation  $V$  and two more one-dimensional irreducible representations  $V_{-+}, V_{--}$ . Each of them can be described by a suitable graph, together with an idempotent linear combination of foams assigned to it. The graphs together with the idempotents, in our notations, are shown in Figure 4.32.

Figure 4.29 computation, together with direct decompositions for the two terms at the bottom line of the figure, can be translated into the direct sum decomposition (17) for the tensor square  $V^{\otimes 2}$ . Decompositions of tensor products of other pairs of irreducible representations of  $D_4$  can be derived in a similar way. For instance, an isomorphism  $V \otimes V_- \cong V$  can be related to the identity in Figure 4.33 and a similar identity obtained by reversing the order of the two halves of the left picture and changing the right hand side to the identity natural transformation of the functor  $\text{Res} \circ \text{Ind} \circ \text{Res}$ .

**4.5. Rooted trees and higher depth representations.** Consider the chain of inclusions

$$G_n \supset G_{n-1}^{(1)} \supset G_{n-2}^{(2)} \supset \dots \supset G_0^{(n)} = \{1\}.$$

In particular,  $G_n/G_{n-1}^{(1)} \simeq C_2$ , the cyclic group of order 2, and  $G_n/G_{n-2}^{(2)} \simeq D_4$ , the dihedral group of order 4. To describe irreducible representations of  $D_4$  via foams we had to use foams that go between  $n$ -facets but in the middle may have facets of thickness  $n-2$  (a dot labelled  $-$  on an  $(n-1)$ -facet, as in Figure 4.32, requires descending to  $(n-2)$ -facets to define it).

Let us say that a representation of  $G_n$  has *depth*  $k$  if the subgroup  $G_{n-k}^{(k)}$  acts nontrivially on it, while  $G_{n-k-1}^{(k+1)}$  acts trivially. To create functors of tensoring with depth  $k$  representations using foams, apply enough restriction functors to get from a line of thickness  $n$  to a line of thickness  $n-k-1$  in at least one location of the diagram, and then go back to a single line of thickness  $n$ . Denote the resulting graph by  $\Gamma$ . There's a composition  $F(\Gamma)$  of restriction and induction functors associated with  $\Gamma$ , and  $F(\Gamma)$  is isomorphic to tensoring with a suitable induced representation  $W$  of  $G_n$ . One can then introduce some idempotent  $e \in \text{End}(F(\Gamma))$  given by a linear combination of foams with boundary  $\Gamma$  on bottom and top. Idempotent  $e$

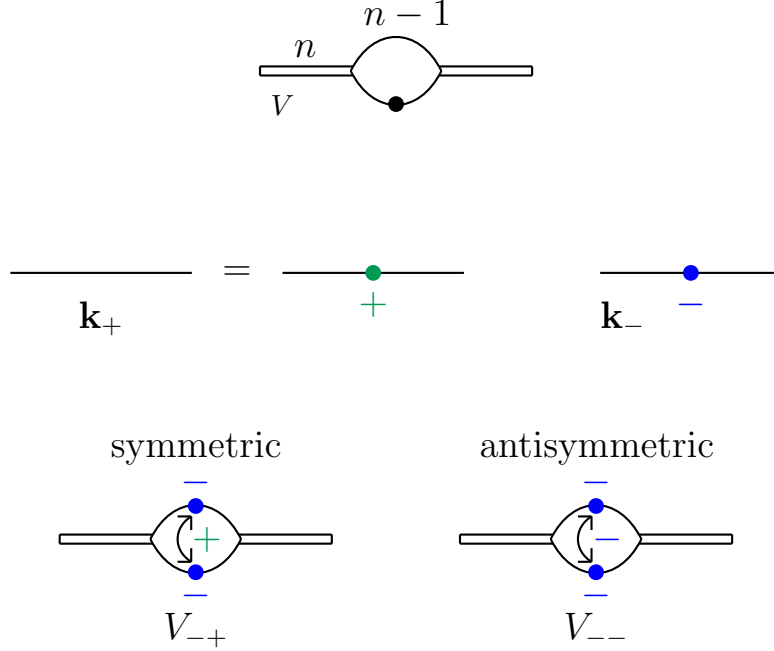


FIGURE 4.32. This figure lists foam idempotents for all 5 irreducible representations of  $D_4 \simeq G_n/G_{n-2}^{(2)}$ . Top to bottom and left to right, these correspond to representations  $V$  (fundamental),  $V_+$  (trivial),  $V_-$  (sign),  $V_{-+}$  and  $V_{--}$ , respectively.

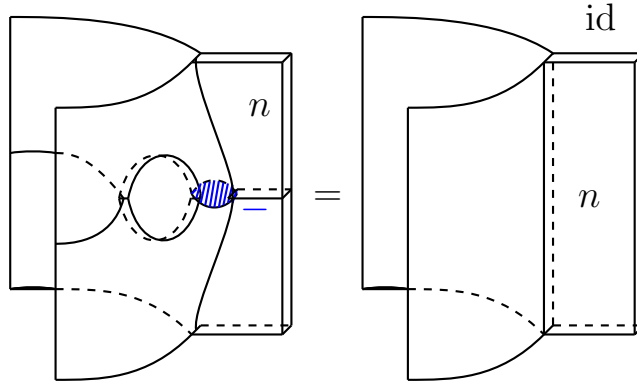


FIGURE 4.33. The two vertical halves of the image on the left are mutually inverse isomorphisms.

defines a direct summand of  $F(\Gamma)$  as well as a direct summand of  $W$  once an isomorphism between  $F(\Gamma)$  and  $W \otimes -$  is fixed.

Irreducible representations of the  $n$ -th wreath product  $G_n$  over a field  $\mathbf{k}$  of characteristic different from 2 were classified by Orellana, Orrison, and Rockmore [OOR, Proposition 3.1], as a special case of their classification of iterated wreath products of the cyclic group  $C_m$ ,

for  $m = 2$ . Their classification gives a bijection between isomorphism classes of irreducible representations and isomorphism classes of complete binary trees of depth  $n - 1$  with vertices labelled by signs  $+$ ,  $-$  and an additional assumption that at each vertex  $v$  labelled by the minus sign  $-$  the standard symmetry  $\beta_k$ , see Section 3.1, applied to the subtree at the vertex  $v$ , preserves signs of vertices.

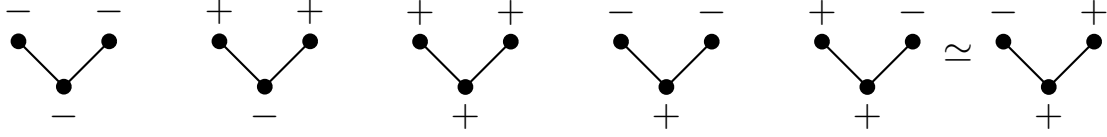


FIGURE 4.34. Above are the labeled trees corresponding to the irreducible representations of the dihedral group  $D_4$ , with the labelling as in [OOR]. Representations corresponding to these trees, going from left to right, are  $V_{--}$ ,  $V_-$ ,  $V_+$ ,  $V_{-+}$ ,  $V$ , respectively. The rightmost two labeled trees are isomorphic via the swap at the root of the tree.

When depth  $n = 2$ , the five labelled trees corresponding to irreducible representations of the dihedral group  $D_4 \cong G_2$  are shown in Figure 4.34.

Let us write an irreducible representation of  $D_4$  in the notation of [OOR] as  $V^{(\beta\alpha\gamma)}$ , where  $\alpha, \beta, \gamma \in \{+, -\}$ . The two-dimensional irreducible representation is  $V^{(+ + -)}$  which corresponds to the tree on the left in Figure 4.35. By [OOR], notation  $V^{(+ - -)}$  corresponding to the labeled tree on the right in Figure 4.35 does not correspond to any representation since there is a minus sign at the root; if there is a minus sign at the root, then the two subtrees must be identical, via a swap of the subtrees that preserves the order of lowest nodes (from left to right). If the sign at the root is  $+$ , then the two subtrees do not need to be identical. So the irreducible representations of the dihedral group  $D_4$  are given in Figure 4.34. Note that  $V^{(+ + -)} \simeq V^{(- + +)}$  since the two subtrees are canonically isomorphic (via a swap at the root of the tree).

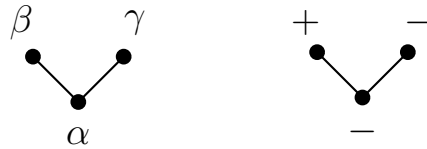


FIGURE 4.35. A labeled tree of height 1, where  $\alpha, \beta, \gamma \in \{+, -\}$ . The labeled tree on the right corresponds to the notation  $+^- -$ .

**Remark 4.4.** We can send  $n$  to infinity and consider the profinite limit

$$(19) \quad \widehat{G} = \lim_{n \rightarrow \infty} G_n.$$

The profinite limit has an open subgroup isomorphic to  $(\widehat{G})^{\times 2^n}$ , with the quotient  $G_n$ , for each  $n \geq 1$ . One can then consider foams as above without any restrictions on the number of times a facet can be split into a pair of “thinner” facets. Such foams will encode natural

transformations between induction and restriction functors for suitable inclusions between direct products of groups  $\widehat{G}$ .

## 5. PATCHED SURFACES, SEPARABLE EXTENSIONS, AND FOAMS

### 5.1. Defect circles and Frobenius algebra automorphisms.

5.1.1. *Commutative Frobenius algebras and 2D TQFTs.* A commutative Frobenius algebra  $A$  over a field  $\mathbf{k}$  is a commutative  $\mathbf{k}$ -algebra together with a nondegenerate linear functional (trace map)  $\varepsilon : A \rightarrow \mathbf{k}$ . Algebra  $A$  is necessarily finite dimensional. Such algebra gives rise to a 2-dimensional TQFT, a tensor functor  $\mathcal{F}$  from the category of oriented 2-dimensional cobordisms to the category of  $\mathbf{k}$ -vector spaces, see [Ab, Kc1, Kc2, LP]. This functor  $\mathcal{F}$  associates  $A^{\otimes k}$  to the 1-manifold which is the union of  $k$  circles. To the generating morphisms *cup*, *cap*, *pants*, *copants*, and *transposition*, it associates the unit, counit (trace), multiplication, comultiplication maps and transposition of factors in  $A^{\otimes 2}$ , respectively, see Figure 5.1.

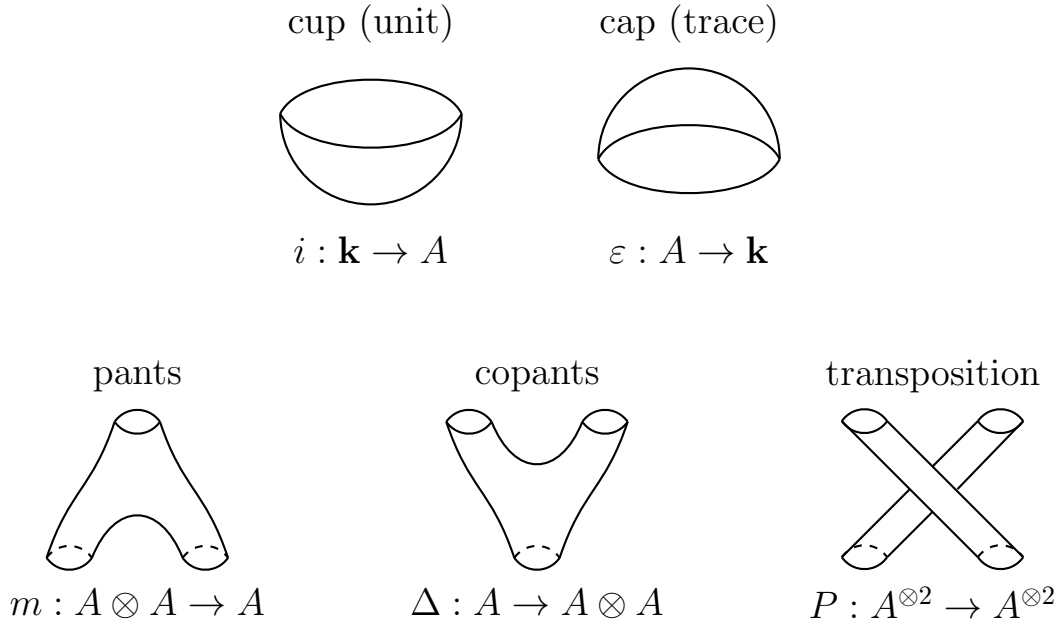


FIGURE 5.1. Generating cobordisms are taken by  $\mathcal{F}$  to the structure maps of  $A$ : identity  $\iota : \mathbf{k} \rightarrow A$ , trace  $\varepsilon : A \rightarrow \mathbf{k}$ , multiplication  $m : A^{\otimes 2} \rightarrow A$ , comultiplication  $\Delta : A \rightarrow A^{\otimes 2}$  and the transposition of factors in the tensor product  $P : A^{\otimes 2} \rightarrow A^{\otimes 2}$ .

Given  $A$ , two-dimensional cobordisms can be refined by allowing elements of  $A$ , which are represented by dots, to float on surfaces. Functor  $\mathcal{F}$  is extended to such cobordisms by associating to a tube with a dot labelled by  $a \in A$  the multiplication map  $m_a : A \rightarrow A$ ,  $m_a(b) = ab$ . Dots  $a, b$  floating on a component may be merged into a single dot  $ab$ . Dots can also be called *0-dimensional defects*.



A closed surface of genus  $g$  (possibly with elements of  $A$  floating on it) evaluates to an element of  $\mathbf{k}$ . One way to compute the evaluation and, more generally, simplify the topology of the cobordism (at the cost of working with linear combinations of cobordisms) is via the *neck-cutting relation*. That is, pick a basis  $x_1, \dots, x_n$  of  $A$  and let  $y_1, \dots, y_n$  be the dual basis, with  $\varepsilon(x_i y_j) = \delta_{i,j}$  for  $1 \leq i, j \leq n$ . Then a tube can be “cut” to a sum of decorated cups and caps, see Figure 5.2, right.

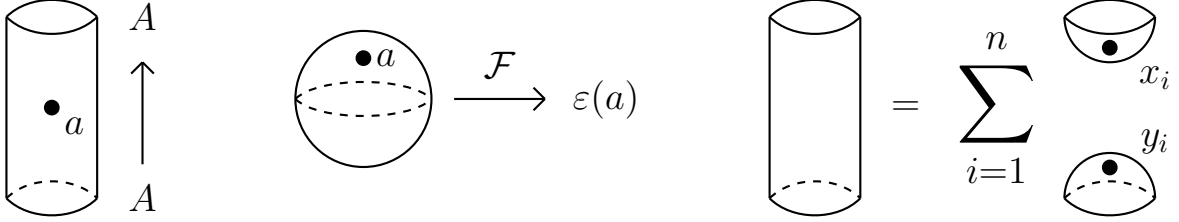


FIGURE 5.2. Left: a dot labelled  $a$  on a tube goes to multiplication by a map  $m_a : A \rightarrow A$ . Middle: a 2-sphere dotted by  $a$  evaluates to  $\varepsilon(a)$ . Right: the neck-cutting relation, where  $\{x_i\}_i$  and  $\{y_i\}_i$  are dual bases of  $A$  relative to  $\varepsilon$ .

Neck-cutting relation can be written algebraically:

$$(20) \quad \text{Id}_A = \sum_{i=1}^n x_i \varepsilon(y_i *), \quad \text{or} \quad a = \sum_{i=1}^n x_i \varepsilon(y_i a), \quad a \in A.$$

See [KQR] for more detail on evaluating thin flat surfaces.

**5.1.2. Defect lines and Frobenius automorphisms.** An automorphism  $\sigma$  of  $A$  is called a *Frobenius automorphism* or an  $\varepsilon$ -*automorphism* if  $\varepsilon \circ \sigma = \varepsilon$  as maps  $A \rightarrow \mathbf{k}$ . The second way of referring to  $\sigma$  may be preferable to avoid possible confusion with the Frobenius endomorphism of commutative rings in finite characteristic. The group of  $\varepsilon$ -automorphisms may be denoted  $G(A)$  or  $G(A, \varepsilon)$ , to emphasize dependence on  $\varepsilon$ .

Two-dimensional TQFT  $\mathcal{F}$  may be further refined by adding one-dimensional defects to surfaces. These defects are co-oriented circles labelled by  $\varepsilon$ -automorphisms of  $A$ . An example is worked out in [KR2, Section 2.2].

Functor  $\mathcal{F}$  is extended to such cobordisms with defects. It takes a circle labelled  $\sigma$  on a tube with upward coorientation to the map  $\sigma : A \rightarrow A$ , see Figure 5.3. Coorientation of a circle may be reversed simultaneously with replacing  $\sigma$  by  $\sigma^{-1}$ . Given that the underlying surface is oriented, co-orientation of a circle on it induces an orientation on the circle and vice versa, so it's also possible to describe this setup via oriented rather than co-oriented circles.

A dot labelled  $a$  may cross over a defect line  $\sigma$  simultaneously with changing its label to  $\sigma(a)$ , see Figure 5.3. An innermost circle around a dot  $a$  reduces to the dot  $\sigma^{\pm 1}(a)$  depending on its coorientation, see Figure 5.4. An innermost circle not containing any dots can be removed, since  $\sigma(1) = 1$ , see Figure 5.4.

Two parallel defect lines labelled  $\sigma_1, \sigma_2$ , co-oriented in the same direction can be converted to a single line labelled  $\sigma_1 \sigma_2$ , see Figure 5.5.

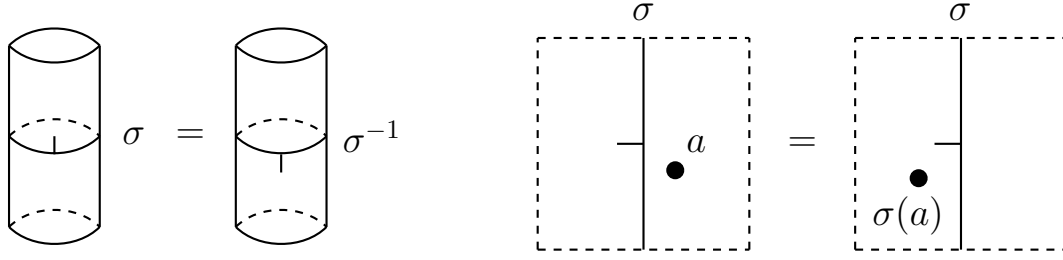


FIGURE 5.3. Dot crossing a defect circle. If crossing in the opposite direction,  $b$  will become  $\sigma^{-1}(b)$ .

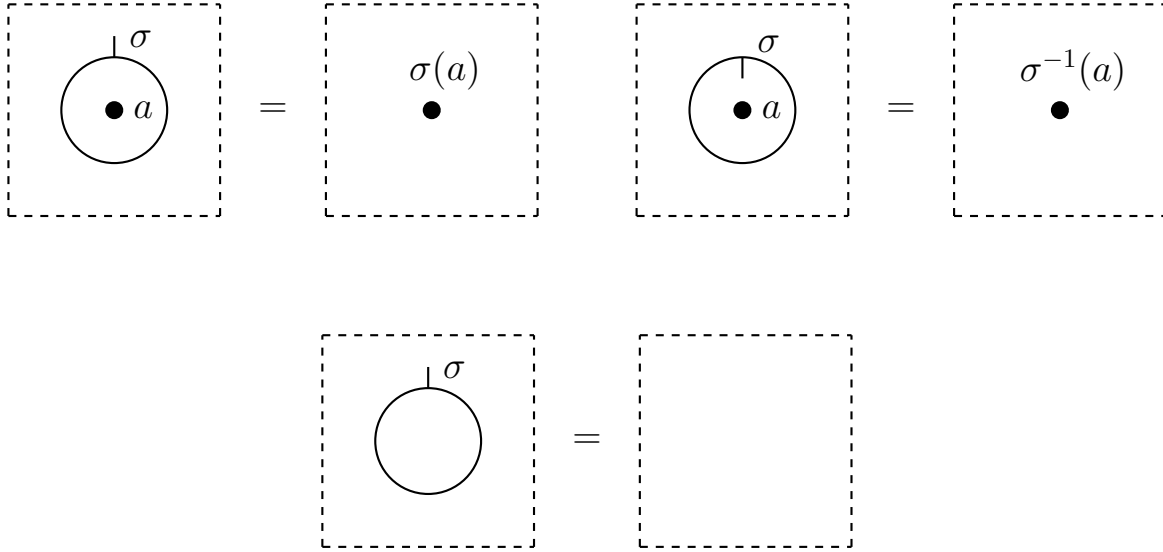


FIGURE 5.4. Defect circle  $\sigma$  around dot  $a$  without coorientation evaluates to dot  $\sigma(a)$ .

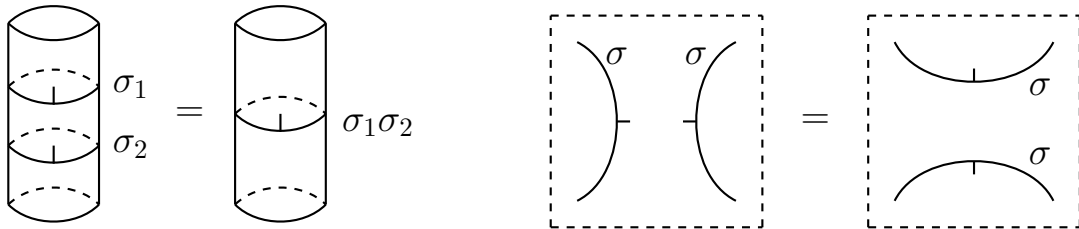


FIGURE 5.5. Left: merging two parallel circles into one. Right: Merging and splitting circles with the same label.

Suppose we are given an oriented closed surface  $S$  with  $A$ -labelled dots and  $G(A, \varepsilon)$ -labelled defect circles. Evaluation  $\mathcal{F}(S) \in \mathbf{k}$  is multiplicative under disjoint union of surfaces so we can assume  $S$  is connected. To evaluate  $S$ , we do two surgeries (neck-cutting) on each side of each defect line in  $S$  to reduce  $S$  to a linear combination of products of dotted spheres

with a single defect line and dotted surfaces, see Figure 5.6 and Figure 5.7. Each connected component of genus  $g > 0$  can be further simplified via neck-cutting into a linear combination of dotted 2-spheres, see Figure 5.7 right.

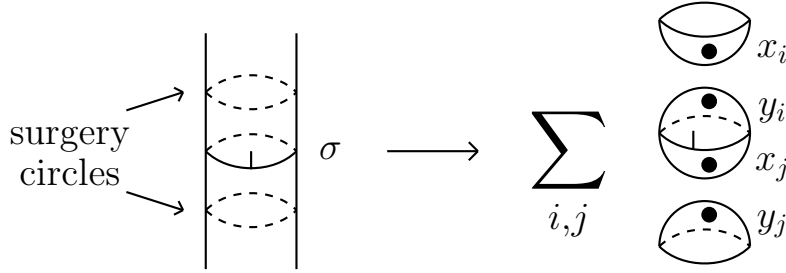


FIGURE 5.6. Separating defect lines into different connected components via neck-cutting.

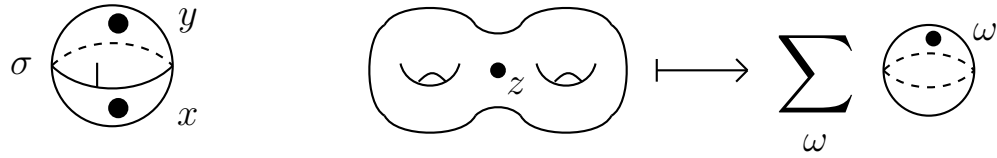


FIGURE 5.7. Left: a 2-sphere with a single defect circle and two dots. Right: reducing higher genus components via neck-cutting.

To evaluate a sphere with a  $\sigma$ -defect and dots  $x, y$  on it, as in Figure 5.8 center, we can push one of the dots across  $\sigma$ -circle into the region with the other dot, remove the circle (since it now circles an empty region), multiply the dots and apply the trace, see Figure 5.8. Since  $\sigma$  respects  $\epsilon$ , the two ways of doing it result in the same answer.

We record this as a proposition and denote the resulting evaluation of a decorated surface  $S$  as  $\langle F \rangle$  of  $\mathcal{F}(S)$ .

**Proposition 5.1.** *A closed oriented surface  $S$  with floating  $A$ -dots and co-oriented disjoint  $\sigma$ -circles for  $\sigma \in G(A, \epsilon)$  has a well-defined evaluation  $\mathcal{F}(S)$ .*

**Example 5.2.** *A dotless 2-torus  $T$  with a non-contractible  $\sigma$ -defect circle evaluates to the trace of  $\sigma$  on  $A$ , see Figure 5.9. For example,  $\text{tr}(\sigma) = \lambda + 2 + \lambda^{-1}$  for the automorphism  $\sigma$  on  $A$  given by (30) and (31) below since  $1, a, b, ab$  have eigenvalues  $1, \lambda, \lambda^{-1}, 1$ , respectively.*

More generally, given a decorated cobordism  $C$  between one-manifolds, neck-cutting and consequent evaluation reduces its image under  $\mathcal{F}$  to a linear combination of dotted cup and cap cobordisms, see Figure 5.10, where we assume that one-manifolds are not decorated. Such a decorated cobordism between unions of circles induces a linear map  $A^{\otimes k_0} \rightarrow A^{\otimes k_1}$ , where  $k_0, k_1$  is the number of bottom and top boundary circles of  $C$ . In this way, the original 2-dimensional TQFT associated to  $(A, \epsilon)$  allows an extension with these decorations. This TQFT associated  $A^{\otimes k}$  to a union of  $k$  undecorated circles.

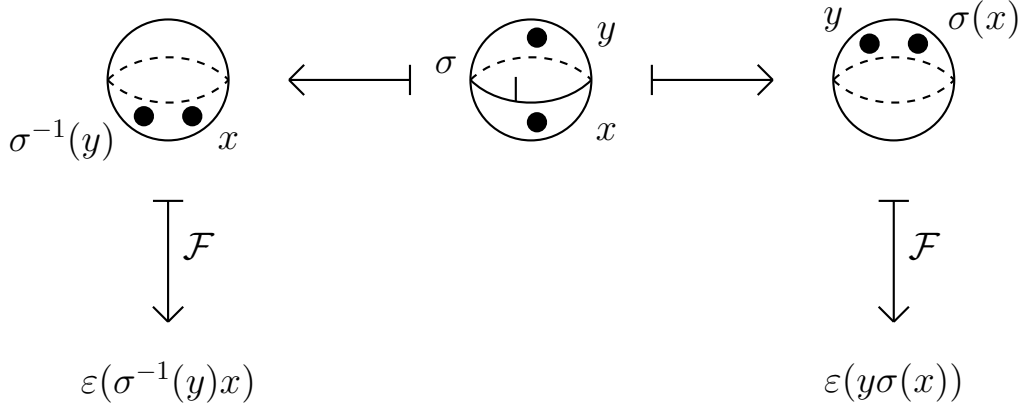


FIGURE 5.8. Two ways to evaluate a sphere with a  $\sigma$ -defect circle give the same answer since  $\sigma$  is an  $\varepsilon$ -automorphism,  $\varepsilon(\sigma^{-1}(y)x) = \varepsilon(y\sigma(x))$ .

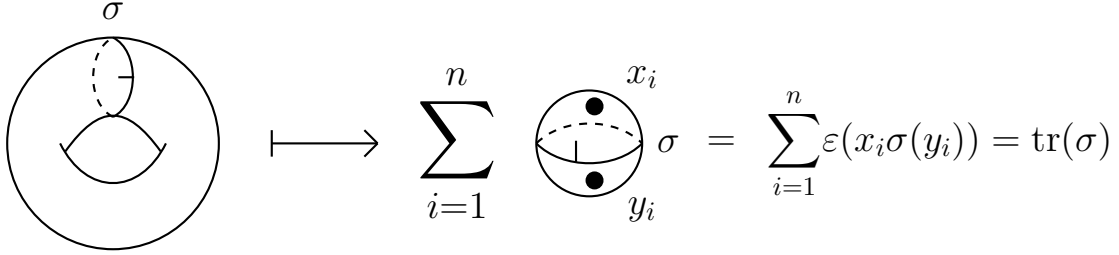


FIGURE 5.9. Torus with an essential  $\sigma$ -defect circle evaluates to  $\text{tr}(\sigma)$ . Note that  $\text{tr}(\sigma) = \text{tr}(\sigma^{-1})$  in view of Corollary 1.

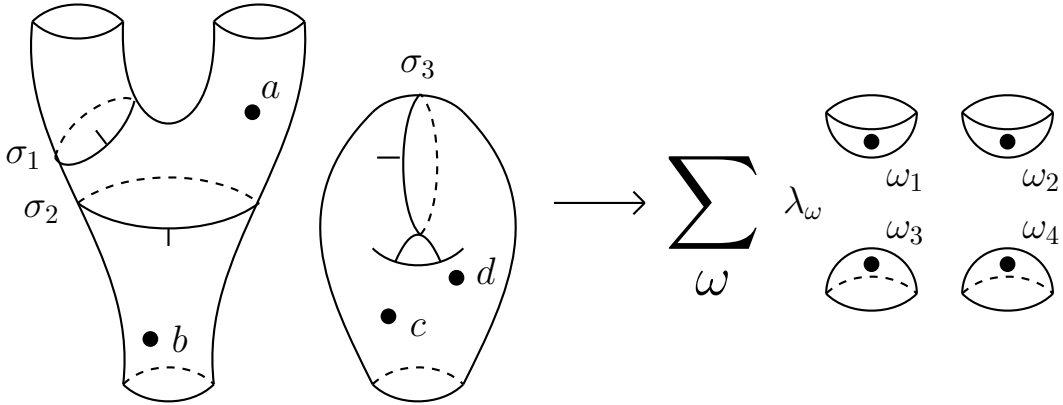


FIGURE 5.10. Reducing a decorated cobordism to a linear combination of cups and caps, by neck-cutting near each boundary circle and evaluating closed components.

5.1.3. *State spaces of decorated 1-manifolds.* One can use the language of universal constructions, see [Kh4] and references there, to extend the evaluation  $\mathcal{F}(S)$  for closed decorated

surfaces  $S$  to state spaces of one-manifolds that inherit decorations from surfaces. Namely, a generic codimension one submanifold of  $S$  may intersect  $\sigma$ -circles in finitely-many points. Local intersection information at such point consists of a co-orientation and choice of  $\sigma$ .

Vice versa, to a union  $L$  of circles with co-oriented  $\sigma$ -dots one can assign the state space  $\mathcal{F}(L)$  as follows. Start with a  $\mathbf{k}$ -vector space  $\text{Fr}(L)$  with a basis of oriented decorated surfaces  $S$  with  $\partial(S) \cong L$ , see Figure 5.11. These surfaces contain co-oriented  $\sigma$ -intervals,  $\sigma$ -circles and  $A$ -dots. Denote by  $[S]$  the basis element for the surface  $S$ .

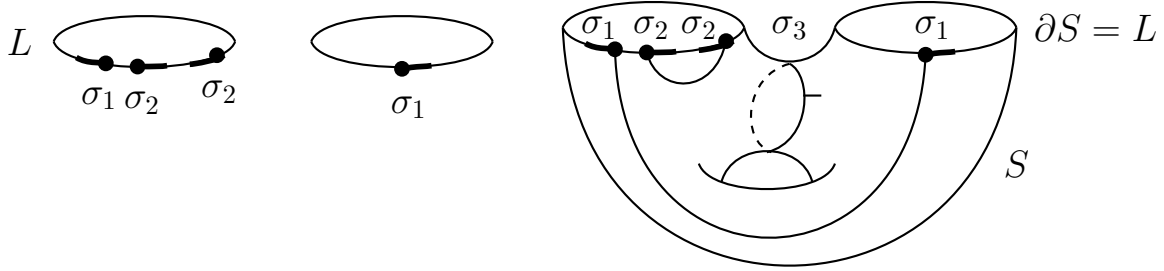


FIGURE 5.11. Decorated 1-manifold  $L$  and decorated surface  $S$  with  $\partial(S) = L$ .

Two decorated surfaces  $S_1, S_2$  with  $\partial S_1 \cong \partial S_2 \cong L$  can be glued together along the common boundary resulting in a closed decorated surface denoted  $\overline{S_2}S_1$ , see Figure 5.12.

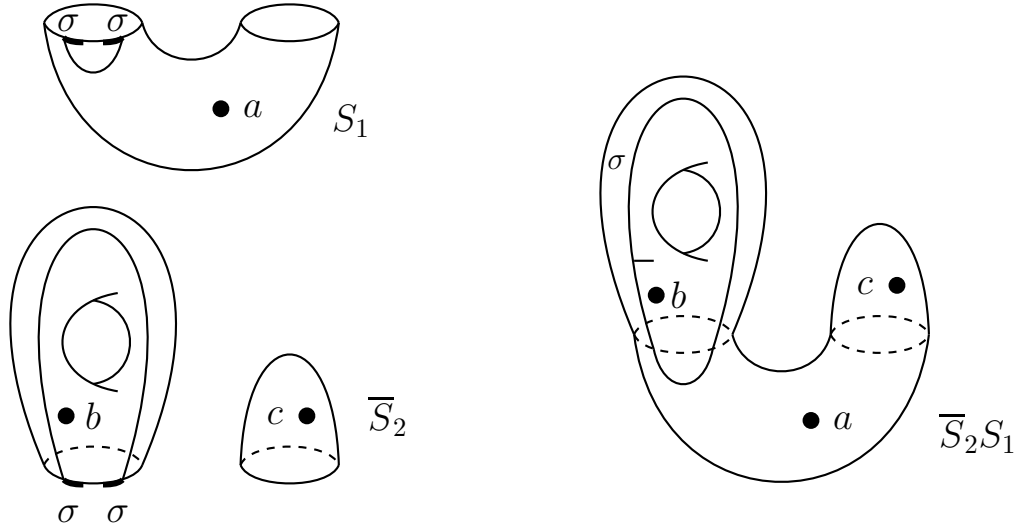


FIGURE 5.12. Gluing surfaces  $S_1$  and  $S_2$  along the common boundary.

Define a bilinear form  $(\ , \ )$  on  $\text{Fr}(L)$  by

$$(21) \quad ([S_1], [S_2]) = \mathcal{F}(\overline{S_2}S_1).$$

This bilinear form is symmetric. Define the state space of  $L$  as the quotient of  $\text{Fr}(L)$  by the kernel of this bilinear form:

$$(22) \quad \mathcal{F}(L) := \text{Fr}(L) / \ker((\ , \ )).$$

This is an example of universal construction of topological theories [Kh4, BHMV]. Any decorated oriented 2-dimensional cobordism  $S$  induces a map

$$(23) \quad \mathcal{F}(S) : \mathcal{F}(\partial_0 S) \longrightarrow \mathcal{F}(\partial_1 S)$$

given by composing a cobordism representing an element in  $\mathcal{F}(\partial_0 S)$  with  $S$ .

In general, the state spaces  $\mathcal{F}(L)$  are not multiplicative under disjoint union, and there are only inclusions

$$(24) \quad \mathcal{F}(L_1) \otimes \mathcal{F}(L_2) \subset \mathcal{F}(L_1 \sqcup L_2).$$

Due to the neck-cutting formula, which can be applied only if the cutting circle is disjoint from  $\sigma$ -circles, there is a restrictive case of multiplicativity,

$$(25) \quad \mathcal{F}(L \sqcup \mathbb{S}^1) \cong \mathcal{F}(L) \otimes \mathcal{F}(\mathbb{S}^1),$$

where  $\mathbb{S}^1$  denotes an undecorated circle. State spaces  $\mathcal{F}(L)$  are trivial for many decorated one-manifolds  $L$ , for instance if the endpoint labels  $\sigma$  cannot be matched in pairs, keeping track of co-orientations. Here it's convenient to at least allow co-orientation reversal together with changing  $\sigma$  to  $\sigma^{-1}$ . Such a reversal (or flip) may happen anywhere along a defect circle or line. Along a defect circle, the total number of reversals must be even, so that locally along a circle there's a well-defined co-orientation, with flips along reversal points, see Figure 5.13.

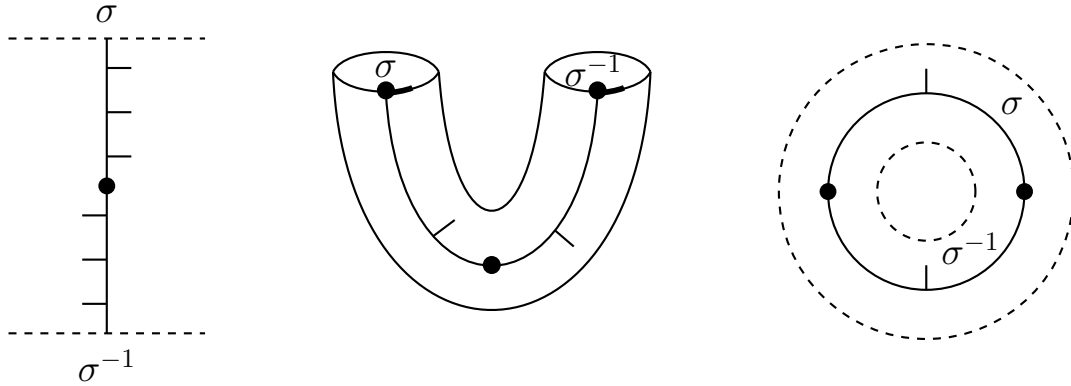


FIGURE 5.13. Left and center: co-orientation and  $\sigma \leftrightarrow \sigma^{-1}$  flip along a seam. Right: There is an even number of flips along a  $\sigma$ -circle, even if  $\sigma = \sigma^{-1}$ .

In general, we don't know much about the state spaces  $\mathcal{F}(L)$  for collections of decorated circles as above. Furthermore, it would be natural to look for extensions of these theories to networks, where lines labelled  $\sigma$  and  $\tau$  can merge into a line labelled  $\sigma\tau$ , as we now explain.

5.1.4. *Turaev’s homotopy TQFTs and universal theories.* One can think of a  $\sigma$ -circle on  $S$  as describing a sort of monodromy. Choose a topological space  $X$  with a base point  $x_0$  such that  $\pi_1(X, x_0) \cong G = G(A, \varepsilon)$  and  $\pi_2(X, x_0) = 0$ . To a  $\sigma$ -surface  $S$  associate a homotopy class of maps  $S \rightarrow X$  as follows.  $A$ -dots floating on  $S$  are ignored. Points away from neighbourhoods of  $\sigma$ -circles are mapped to the basepoint  $x_0$ . An interval transverse to a  $\sigma$ -circle is mapped to the loop at  $x_0$  representing element  $\sigma \in \pi_1(X, x_0)$ , using the co-orientation to choose between a map representing  $\sigma$  or  $\sigma^{-1}$ , see Figure 5.14.

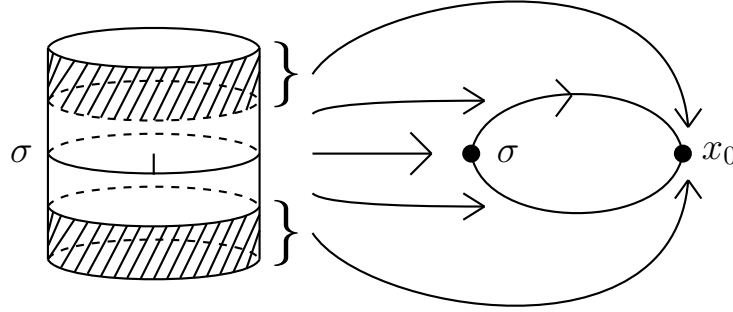


FIGURE 5.14. Map into  $X$  near a seam circle of  $S$ .

In this way, our construction is reminiscent of Turaev’s homotopy TQFTs in dimension two [Tu1, Tu2, MS], Landau-Ginzburg orbifolds [IV, BH, BR, LS, KW] and orbifolded Frobenius algebras [Ka].

Furthermore, consider a circle  $L$  with 3 defect points, co-oriented in the same direction, such that their labels multiply to  $1 \in G$ , see Figure 5.15. In the  $\sigma$ -circles setup, this decorated circle cannot bound a decorated surface, so its space is zero.

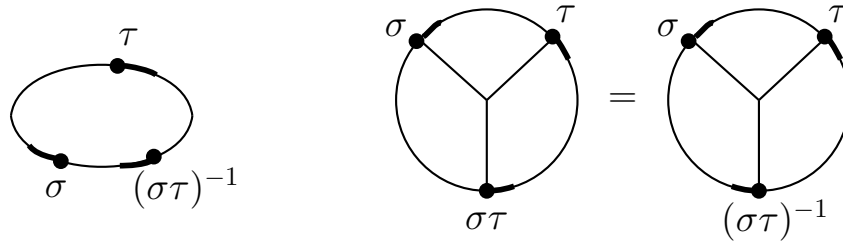


FIGURE 5.15. “Monodromy” along the circle on the left is trivial and motivates the introduction of a trivalent vertex.

However, the “monodromies” along the circle multiply to the trivial element of  $G$ , and it is natural to introduce a trivalent vertex, as shown in Figure 5.15.

Seam lines and trivalent vertices can be arranged into “networks” on a surface  $S$ . It is natural to require that moves shown in Figure 5.16 and Figure 5.17 should preserve the evaluation of the network.

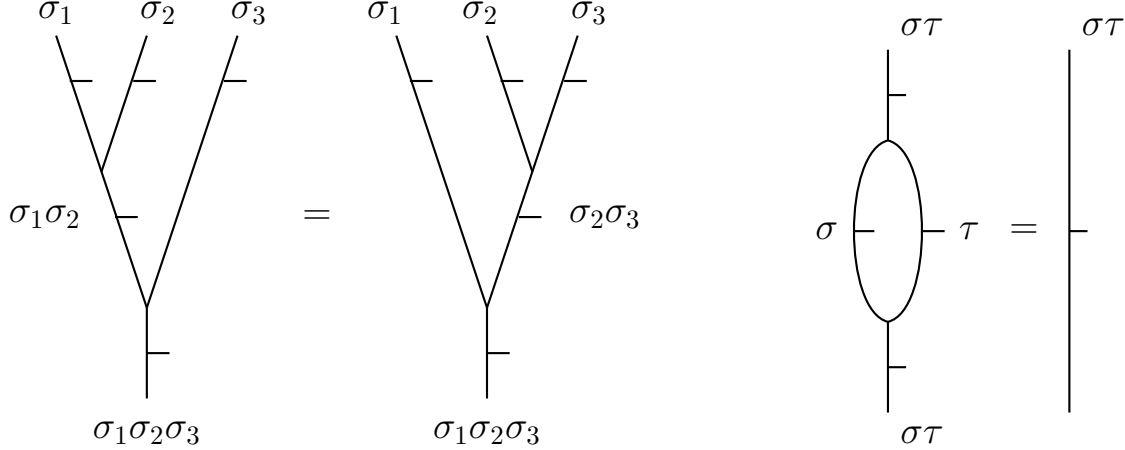


FIGURE 5.16. Associativity and digon simplification moves of  $G$ -labelled networks.

One motivation for these moves is that a representation of  $\pi_1(S)$  into  $G$ , up to conjugation in  $\pi_1(S)$ , gives rise to an equivalence class of networks. Denote the set of equivalence classes by

$$(26) \quad \pi(S, G) := \text{Hom}(\pi_1(S), G) / \pi_1(S), \quad s(\rho)(t) = \rho(s^{-1}ts), \quad s, t \in \pi_1(S), \quad \rho \in \text{Hom}(\pi_1(S), G).$$

To construct a network representing  $\rho : \pi_1(S) \rightarrow G$ , viewed as an element of  $\pi(S, G)$ , decompose a connected surface  $S$  in the usual way as given by gluing a  $4g$ -gon along the sides. The sides represent generators  $a_i, b_i$  of  $\pi_1(S)$ . Draw an interval crossing each the side, place the label  $\rho(a_i), \rho(b_i) \in G$  on it, and suitably coorient the interval as well. Inside the  $4g$ -gon these  $4g$  intervals naturally extend to a connected network, uniquely defined, since the relation

$$(27) \quad \prod_{i=1}^n \rho(a_i) \rho(b_i) \rho(a_i)^{-1} \rho(b_i)^{-1} = 1$$

holds in  $G$ . The network has  $4g - 2$  trivalent vertices and its complement in  $S$  is an open disk (if some edges of the network are labelled  $1 \in G$ , they can then be erased, making the complement not simply connected). An example for  $g = 1$  is shown in Figure 5.21, when necessarily  $\rho(a), \rho(b)$  commute. Since the fundamental group of the two-torus is abelian, there's only one element in the conjugacy class of a homomorphism. Note that we're not conjugating by elements of  $G$ , only by elements of  $\pi_1(S)$  (equivalently, by inner automorphisms of the latter group).

Vice versa, to a  $G$ -network  $w$  on  $S$  we can assign an element of  $\pi(S, G)$ . Choose a  $K(G, 1)$  space  $X$  which is a CW-complex with a single vertex  $v_0$  and 1-cells  $c(g)$  in a bijection with elements of  $G$  such that that the loop along  $c(g)$  represents  $g$  in  $\pi_1(X, v_0) \cong G$ .



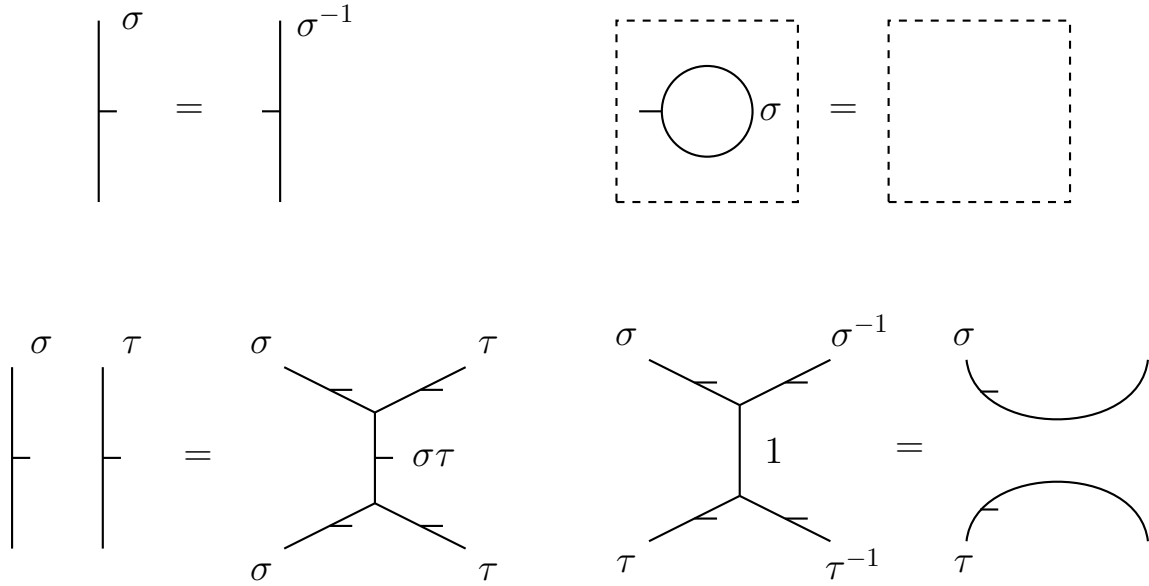


FIGURE 5.17. Some skein relations for  $G$ -networks. Either co-orientation is fine for top right relation. Bottom right relation says that intervals labelled 1 may be erased. This relation can be clarified by removing the interval on the left labelled 1 and keeping the flip points on the two arcs that reverse co-orientation and send  $\sigma$  to  $\sigma^{-1}$ , as in Figure 5.13. Same refinement can be applied to the top left relation. For careful treatment of flip points one should also choose types of allowed triples of coorientations allowed at networks' vertices and add suitable relations, see Figures 5.18, 5.19 and 5.20.

View network  $w$  as a trivalent graph on  $S$ , possibly with loops, and form a standard open neighbourhood  $U$  of  $w$ . Construct a map  $\phi_w : S \rightarrow X$  as follows. All points in  $S \setminus U$  map to the base points  $v_0$  of  $X$ . Neighbourhood  $U$  can be partitioned into a union of intervals, each one intersecting  $w$  at a single point, and triangles, one for each vertex of  $w$ , see Figure 5.22.

Each interval intersecting  $w$  at a point of a line labelled  $\sigma$  is mapped bijectively to the 1-cell  $c(\sigma)$  in the direction of co-orientation. Around each vertex of  $w$  there's a triangle, with its sides mapped to  $c(\sigma), c(\tau), c(\sigma\tau)$ , respectively. There's a unique, up to homotopy, way to map this triangle to  $X$  given the map on its sides.

Thus, to a network  $w$  we assign a map  $\phi_w : S \rightarrow X$ . Fixing a base point  $s_0$  on  $S$  away from  $w$  induces a map  $\pi_1(S, s_0) \rightarrow \pi_1(X, v_0)$ . Network transformations shown in Figure 5.16 and 5.17 away from the basepoint correspond to basepoint-preserving homotopies of maps  $S \rightarrow X$  and induce the same homomorphism of fundamental groups. Moving a base-point across a line labelled  $\sigma$  conjugates the homomorphism by  $\sigma$ .

**Proposition 5.3.** *The above correspondence gives a bijection between elements of  $\pi(S, G)$  and isotopy classes of  $G$ -networks modulo relations in Figures 5.16 and 5.17.*

*Proof.* Proof is left to the reader. □

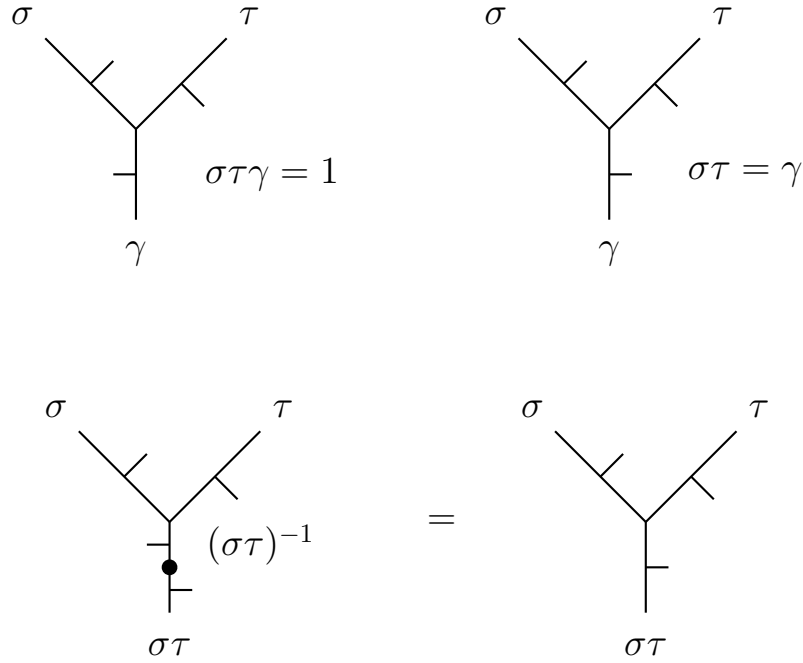


FIGURE 5.18. Two types of co-orientation triples around a vertex of the network are shown on the top. If both types are allowed, it's naturally to add the relation that a vertex can absorb a co-orientation flip point, see bottom equality.

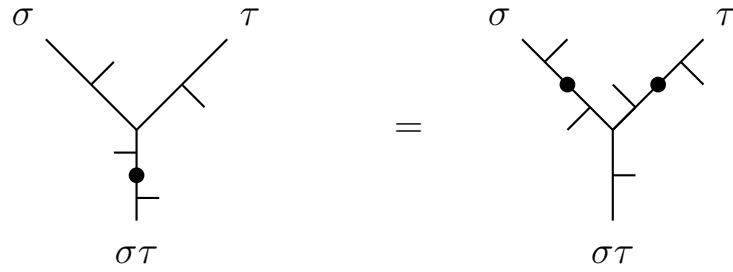


FIGURE 5.19. Moving a flip point through a vertex.

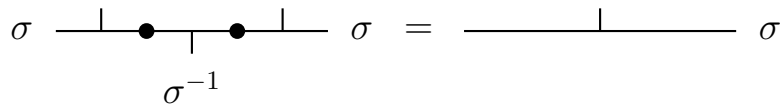


FIGURE 5.20. Canceling a pair of adjacent flip points on a seam.

The description of representations of the fundamental group via networks is Poincare dual to the one commonly used in the literature [Tu2, MS, Ka].

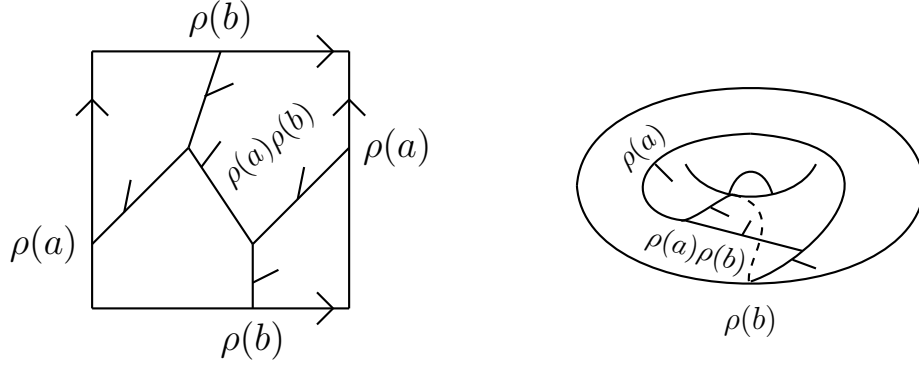


FIGURE 5.21. A network on the torus describing a homomorphism  $\pi_1(T^2) \rightarrow G$ . Commutativity  $\rho(a)\rho(b) = \rho(b)\rho(a)$  is needed for both trivalent vertices to make sense.

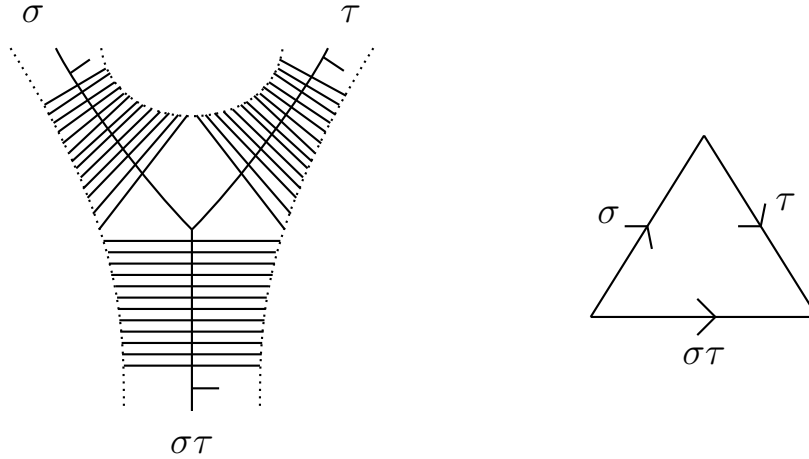


FIGURE 5.22. Left: Decomposing  $U$  near a vertex of  $w$  into a triangle and unions of parallel intervals, one for each leg of the tripod at the vertex. Right: the triangle is mapped to  $X$  in a unique way, up to homotopy, extending the map of its boundary.

We don't expect that  $G$ -valued networks on a surface (equivalently, elements of  $\pi(S, G)$ ) can be evaluated consistently given the data  $(A, \varepsilon)$  of a commutative Frobenius algebra and taking  $G = G(A, \varepsilon)$  the group of trace-respecting automorphisms of  $A$ . Clearly, one needs much more structure to have a natural evaluation.

If  $G$  is fixed, there's the notion of  $G$ -equivariant 2-dimensional TQFT and corresponding  $G$ -equivariant commutative Frobenius algebra, see [Tu1, Tu2, MS, Ka], much more sophisticated than that of a commutative Frobenius algebra. These structures do allow evaluations of surfaces with  $G$ -networks. Additionally, they define tensor functors on the corresponding

categories of two-dimensional  $G$ -cobordisms, thus assigning vector spaces to  $G$ -labelled one-manifold, in a multiplicative way (disjoint union corresponds to tensor product of vector spaces).

Universal theories approach [BHMV, Kh4, KS, KKO, KL] provides a different way to construct a topological theory, given evaluation function on networks on closed surfaces. Fix a group  $G$ . Choose an *evaluation* function, that is, a map of sets

$$(28) \quad \alpha : \pi(S, G) \longrightarrow \mathbf{k}.$$

Given a closed oriented surface  $S$  with a  $G$ -network  $w$ , define  $\alpha(S, w) := \alpha(\rho)$ , where  $\rho$  is the equivalence class of homomorphisms defined by  $w$  (equivalence under *source conjugations*, that is, conjugations in  $\pi_1(S)$ ).

With evaluation  $\alpha$  for closed surfaces with a  $G$ -network at hand, we can define state spaces  $\alpha(L)$  of decorated oriented one-manifolds  $L$  in Section 5.1.3, with  $\alpha$  in place of  $\mathcal{F}$  and  $G$ -networks on  $S$  in place of collections of  $G$ -circles. First interesting question is finding families of evaluations  $\alpha$  such that the state spaces  $\alpha(L)$  are finite-dimensional for all  $L$ , by analogy with a study in [Kh4] and follow-up papers. Such evaluations may be called *rational* or *recognizable*.

The state spaces  $\alpha(L)$  may be zero for some  $G$ -decorated one-manifolds no matter what  $\alpha$  is. For instance if  $\sigma \in G \setminus [G, G]$  is not in the commutator subgroup, the state space of a single circle  $\mathbb{S}^1(\sigma)$  with a mark  $\sigma$  on it is trivial, since such circle cannot bound any  $G$ -network  $w$  on a surface  $S$  with  $\partial(S, w) \cong \mathbb{S}^1(\sigma)$ . We leave studying these state spaces and associated categories (as in [Kh4, KS, KKO]) for another paper.

Following Turaev's homotopy TQFT, one can consider the case of maps of surfaces into a topological space  $X$  with  $\pi_2(X) \neq 0$ . Assume that  $X$  is path-connected. Group  $\pi_1(X, x_0)$  acts linearly on the abelian group  $\pi_2(X, x_0)$ , i.e., see [FF]. Let  $G = \pi_1(X, x_0)$  and  $B = \pi_2(X, x_0)$ . Consider oriented closed surfaces  $S$  decorated by a  $G$ -network together with floating dots labelled by elements of  $B$  and disjoint from the graph of the  $G$ -network. To relations in Figures 5.16, 5.17 we add the rules in Figure 5.23 below.

**Proposition 5.4.** *Homotopy classes of maps of  $S$  into  $X$  are in a bijection with isotopy classes of such diagrams on  $S$  modulo relations in Figures 5.16, 5.17, 5.23.*

Proof is left to the reader.

Universal theories can be further considered for such pairs  $(G, B)$ , and we hope to treat examples elsewhere. When  $G = \{1\}$  is the trivial group, the network with each edge labelled 1 may be erased, and  $S$  is decorated only by dots that are elements of an abelian group  $B$ . Universal theories for this case are discussed in [KKO, Section 8].

One can further assume that  $B$  is an abelian monoid with an action of  $G$  on it rather than an abelian group. The notion of a  $(G, B)$ -decoration of  $S$  modulo Figure 5.16, 5.17, 5.23 relations makes sense, and one can consider universal theories and state spaces for such pairs as well, although there is no underlying topological space  $X$  to interpret equivalence classes of  $(G, B)$ -decorations as homotopy classes of maps into  $X$ .

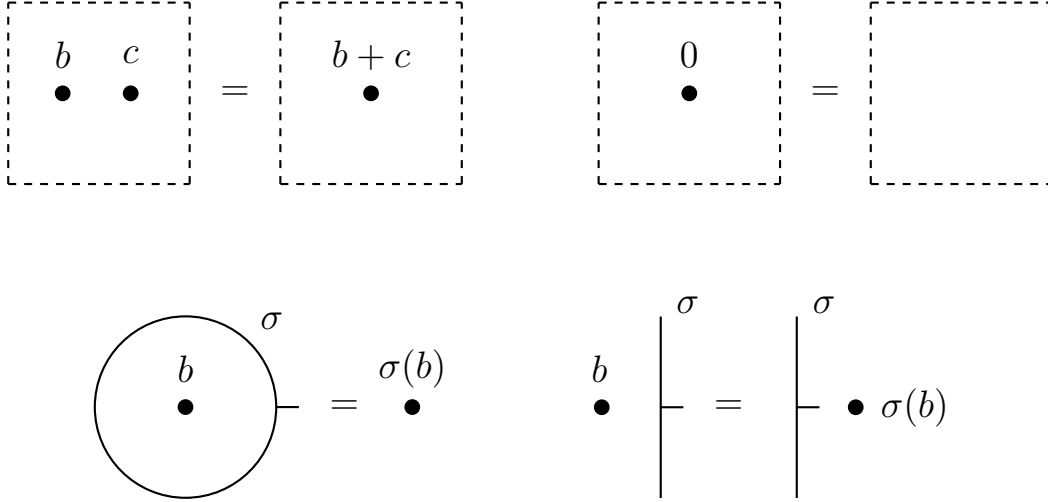


FIGURE 5.23. Top row relations allow to merge dots via addition in  $B$  and to remove a dot labelled  $0 \in B$ . The two relations in the bottom row are easily shown to be equivalent using an isotopy and the relation in Figure 5.5 on the right. The latter relation follows from the relations in the bottom row of Figure 5.17.

Thus, in this subsection we describe the Poincare dual diagrammatics (to the usual diagrammatics) for specifying representations of the fundamental groups of a surface, as well as propose to study universal theories for such representations, which should generalize Turaev's homotopy TQFTs in two dimensions.

**5.1.5. Basic structure of Frobenius automorphisms.** Fix an  $\varepsilon$ -automorphism  $\sigma$  and assume that  $\mathbf{k}$  is algebraically closed (if  $\mathbf{k}$  is not closed, pass to  $\overline{A} := A \otimes_{\mathbf{k}} \overline{\mathbf{k}}$ ). Then  $A$  decomposes into the direct sum of generalized weight spaces for  $\sigma$ ,

$$(29) \quad A = \bigoplus_{\lambda} A_{\lambda}, \quad (\sigma - \lambda)^N|_{A_{\lambda}} = 0, \quad N \gg 0, \quad \lambda \in \mathbf{k}^*.$$

We have  $A_{\lambda}A_{\mu} \subset A_{\lambda\mu}$ , making  $A$  into a graded algebra, and  $\sigma(A_{\lambda}) = A_{\lambda}$ . Note that  $\lambda \neq 0$  for a nonzero weight space  $A_{\lambda}$ , since  $\sigma$  is an automorphism.

Let  $\Lambda = \{\lambda \in \mathbf{k}^* | A_{\lambda} \neq 0\}$  be the subset of weights  $\lambda$  such that  $A_{\lambda} \neq 0$ . Let  $\Lambda^*$  be the subgroup of  $\mathbf{k}^*$  generated by  $\Lambda$ . Algebra  $A$  is naturally graded by the abelian group  $\Lambda^*$ .

Note that, in general,  $\Lambda \neq \Lambda^*$ . As an example, consider a four-dimensional algebra with an automorphism  $\sigma$  given by

$$(30) \quad A = \mathbf{k}[a, b]/(a^2, b^2), \quad \sigma(a) = \lambda a, \quad \sigma(b) = \lambda^{-1}b,$$

where  $\lambda$  is any element of  $\mathbf{k}^*$ , and the trace map

$$(31) \quad \varepsilon(ab) = 1, \quad \varepsilon(1) = \varepsilon(a) = \varepsilon(b) = 0.$$

Then  $\sigma$  is an  $\varepsilon$ -automorphism,  $\Lambda = \{1, \lambda^{\pm 1}\}$ , and  $\Lambda^*$  is the subgroup generated by  $\lambda$ , infinite if  $\lambda$  is not a root of unity in  $\mathbf{k}$ .

**Lemma 5.5.** *The trace map  $\varepsilon$  is zero on  $A_{\lambda}$  for  $\lambda \neq 1$ .*

*Proof.* Let  $v \in A_\lambda$  and assume first  $\sigma(v) = \lambda v$  and  $\varepsilon(v) \neq 0$ . Then  $\varepsilon(\sigma(v)) = \varepsilon(v)$ , forcing  $\lambda = 1$ . By induction on nilpotence degree of  $v$  relative to  $\sigma - \lambda$  we can assume  $\varepsilon(\sigma(v) - \lambda v) = 0$ . Then  $\varepsilon(\sigma(v)) = \lambda \varepsilon(v)$  showing that either  $\lambda = 1$  or  $\varepsilon(\sigma(v)) = \lambda = 0$ . Applying this to  $\sigma^{-1}(v)$  in place of  $v$  and observing that  $A_0 = 0$  completes the proof.  $\square$

**Corollary 1.**  $\varepsilon$  restricts to a nondegenerate pairing  $A_\lambda \otimes A_{\lambda^{-1}} \rightarrow \mathbf{k}$  for each  $\lambda \in \Lambda$ . In particular,  $A_1$  is a commutative Frobenius algebra.

**Example 5.6.** Consider Frobenius algebra  $A$  in (30) with the trace given by (31) but a different  $\sigma$ :

$$(32) \quad \sigma(a) = a + b, \quad \sigma(b) = b,$$

which also requires  $\text{char}(\mathbf{k}) = 2$  to define  $\sigma$ . Then  $A$  is the generalized 1-eigenspace of  $\sigma$  and the action of  $\sigma$  is not semisimple.

The direct sum of eigenspaces  $A'_\lambda \subset A_\lambda$ , over  $\lambda \in \Lambda$ , is a subalgebra of  $A$  which is not necessarily Frobenius (see Example 5.6).

There does not seem to be a substantial literature about Frobenius automorphisms; they are discussed in Wang [Wa] and several other papers.

## 5.2. Field extensions and patched surfaces.

**5.2.1. Traces of field extensions.** Let  $\mathbf{k} \subset F$  be a field extension of finite degree  $n$ . The trace map  $\varepsilon : F \rightarrow \mathbf{k}$ ,  $\varepsilon(x) = \text{tr}_{F/\mathbf{k}}(m_x)$  assigns to  $x \in F$  the trace of multiplication by  $x$  map  $m_x : F \rightarrow F$ ,  $m_x(a) = xa$ , viewed as a  $\mathbf{k}$ -linear endomorphism of vector space  $F$ . A basic result on field extensions says that  $\varepsilon$  is nondegenerate iff the extension is separable, *e.g.*, see [Co].

**Proposition 5.7.** The pair  $(F, \varepsilon)$ , for  $\varepsilon = \text{tr}_{F/\mathbf{k}}$  and a finite separable extension  $F/\mathbf{k}$ , is a commutative Frobenius  $\mathbf{k}$ -algebra. Any element  $\sigma \in \text{Gal}(F/\mathbf{k})$  of the Galois group is an  $\varepsilon$ -automorphism.

Consequently, each extension  $\mathbf{k} \subset F$  as above defines a 2-dimensional TQFT  $\mathcal{F}$  with defect lines and Galois group  $\text{Gal}(F/\mathbf{k})$  being a subgroup of  $G(F, \varepsilon)$ . To  $m$  circles this TQFT associates  $F^{\otimes m}$ , with tensor product taken over  $\mathbf{k}$ . Defect lines in this TQFT are labelled by elements of  $\text{Gal}(F/\mathbf{k})$ .

Closed surfaces with defect lines in  $(\mathbf{k}, F)$  TQFT admit a straightforward computation. A finite extension  $F/\mathbf{k}$  is separable iff the tensor product  $F \otimes_{\mathbf{k}} \overline{\mathbf{k}}$  with the algebraic closure of  $\mathbf{k}$  is a direct product of copies of  $\overline{\mathbf{k}}$ ,

$$(33) \quad F \otimes_{\mathbf{k}} \overline{\mathbf{k}} \cong \overline{\mathbf{k}} \times \overline{\mathbf{k}} \times \cdots \times \overline{\mathbf{k}},$$

(necessarily of  $[F : \mathbf{k}]$  copies). Another equivalent condition is that  $F \otimes_{\mathbf{k}} \overline{\mathbf{k}}$  is a semisimple algebra (equivalently,  $F \otimes_{\mathbf{k}} \overline{\mathbf{k}}$  does not contain nilpotent elements). Trace of  $m_a : F \rightarrow F$  can be computed in the  $\overline{\mathbf{k}}$ -vector space  $F \otimes_{\mathbf{k}} \overline{\mathbf{k}}$ .

Action of  $\text{Gal}(F/\mathbf{k})$  on  $F$  extends to  $F \otimes_{\mathbf{k}} \overline{\mathbf{k}}$  via the trivial action on the second factor. The resulting action is  $\overline{\mathbf{k}}$ -linear.

Writing  $F$  as a simple extension,  $F \cong \mathbf{k}[x]/(f(x))$ , factorization in the algebraic closure

$$(34) \quad f(x) = (x - \lambda_1) \cdots (x - \lambda_n),$$

with distinct  $\lambda_1, \dots, \lambda_n$ , gives minimal idempotents for the direct product decomposition,

$$(35) \quad e_i = \prod_{j \neq i} \frac{x - \lambda_j}{\lambda_i - \lambda_j}.$$

Although we cannot explicitly write down an action of  $\sigma$  on  $x$ , we know that the action permutes minimal idempotents  $e_i$  in the same way  $\sigma$  permutes roots  $\lambda_i$ .

This passage to the algebraic closure results in a 2D TQFT over the ground field  $\bar{\mathbf{k}}$  with the Frobenius algebra  $F \otimes_{\mathbf{k}} \bar{\mathbf{k}}$ , trace map given by

$$(36) \quad \varepsilon(e_i) = 1, \quad i = 1, \dots, n$$

and comultiplication

$$(37) \quad \Delta(e_i) = e_i \otimes e_i, \quad i = 1, \dots, n.$$

Action of  $\sigma \in \text{Gal}(F/\mathbf{k})$  is given by permutation of  $e_1, \dots, e_n$  corresponding to the action of  $\sigma$  on the roots of  $f(x)$ . Consequently, each defect circle map can be computed in the basis of minimal idempotents as their permutation.

The map associated to any surface with defect circles can now be computed explicitly. For instance, consider a one-holed torus with a defect circle  $\sigma$ , see Figure 5.24 left.

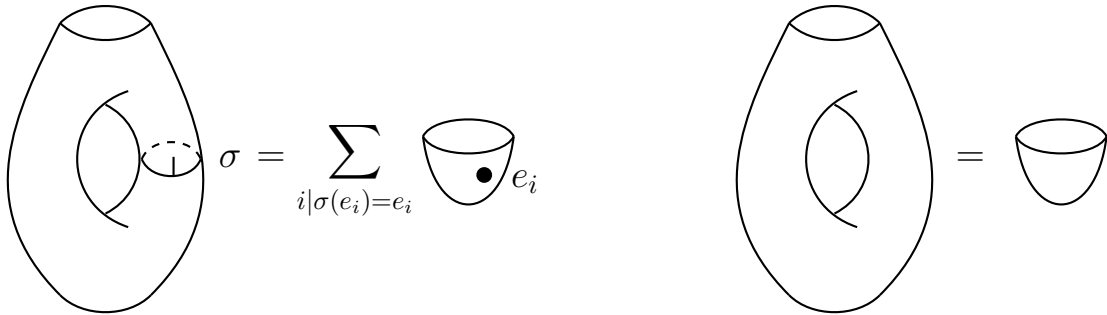


FIGURE 5.24. Left: simplification of a one-holed torus with a defect circle. Right: one-holed torus equals a disk.

We compute the induced map

$$(38) \quad 1 = \sum_i e_i \xrightarrow{\Delta} \sum_i e_i \otimes e_i \xrightarrow{1 \otimes \sigma} \sum_i e_i \otimes \sigma(e_i) \xrightarrow{m} \sum_{i | \sigma(e_i) = e_i} e_i \in F \otimes_{\mathbf{k}} \bar{\mathbf{k}}.$$

In particular, one-holed torus simplifies to a disk, see Figure 5.24 right.

Capping off the boundary by a disk, a 2-torus with an essential  $\sigma$ -defect circle evaluates to  $[F^\sigma : \mathbf{k}]$ , the degree of the fixed field of  $\sigma$  over  $\mathbf{k}$ . An undecorated 2-torus evaluates to  $\dim_{\mathbf{k}}(F) = [F : \mathbf{k}] \in \mathbf{k}$ . Over a field of finite characteristics, these evaluations may be equal to 0.

More complicated cobordisms with circle defects can be computed analogously. For example, Figure 5.25 shows the evaluation of a genus two surface with 3 defect circles labelled  $\sigma_1, \sigma_2, \sigma_3 \in \text{Gal}(F/\mathbf{k})$ .

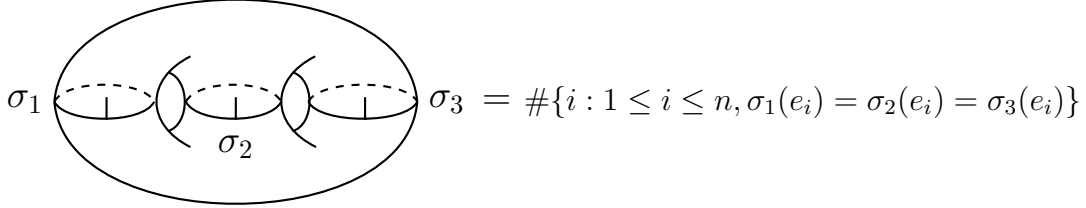


FIGURE 5.25. Evaluating a genus two surface with three circle defects.

Recall also that for a finite Galois extension  $k \subset F$  the trace map is given by

$$(39) \quad \text{tr}_{F/\mathbf{k}}(a) = \sum_{\sigma \in \text{Gal}(F/\mathbf{k})} \sigma(a).$$

5.2.2. *A chain of extensions and evaluation of patched surfaces.* Consider now a chain of finite separable field extensions  $\mathbf{k} \subset F \subset K$  with  $[K : F] = n$ ,  $[F : \mathbf{k}] = m$ . Trace maps

$$\text{tr}_{F/\mathbf{k}} : F \longrightarrow \mathbf{k}, \quad \text{tr}_{K/F} : K \longrightarrow F, \quad \text{tr}_{K/\mathbf{k}} : K \longrightarrow \mathbf{k}$$

are non-degenerate and satisfy

$$(40) \quad \text{tr}_{K/\mathbf{k}} = \text{tr}_{F/\mathbf{k}} \circ \text{tr}_{K/F},$$

see [Ja], and turn  $F$  into a commutative Frobenius  $\mathbf{k}$ -algebra and  $K$  into a commutative Frobenius algebra over  $F$  and over  $\mathbf{k}$ .

Three commutative Frobenius algebras with traces

$$(41) \quad (F, \mathbf{k}, \text{tr}_{F/\mathbf{k}}), \quad (K, F, \text{tr}_{K/F}), \quad (K, \mathbf{k}, \text{tr}_{K/\mathbf{k}})$$

give rise to three 2-dimensional TQFTs that may be denoted

$$(42) \quad \mathcal{F}_F = \mathcal{F}_{F/\mathbf{k}}, \quad \mathcal{F}_K = \mathcal{F}_{K/F}, \quad \mathcal{F}_{K/\mathbf{k}},$$

respectively. Defect lines in these TQFTs are labelled by elements of the corresponding Galois groups

$$\text{Gal}(F/\mathbf{k}), \quad \text{Gal}(K/F), \quad \text{Gal}(K/\mathbf{k}).$$

It's natural to ask whether these three TQFTs can be combined into a single structure, and we now suggest one possible approach, first without the defect lines.

Consider a “patched” or “seamed” closed oriented surface  $S$  which consists of regions labelled  $F$  and  $K$ . Elements of  $F$  and  $K$  may float in the regions labelled by the corresponding field. Seam circles separate regions labelled  $F$  and  $K$ , see Figure 5.26 for an example.

To evaluate such a surface to an element  $\mathcal{F}(S) \in \mathbf{k}$  let us use neck-cutting relations to separate each seam circle from the rest of the diagram. We do surgery on both sides of a seam



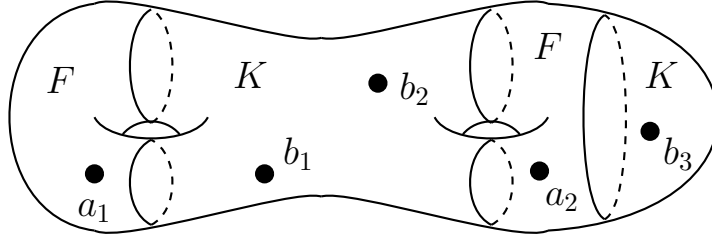


FIGURE 5.26. Seamed surface with facets checkerboard colored by fields  $F, K$ . Elements  $a_i \in F$  and  $b_j \in K$  float in the corresponding regions.

circle using neck-cutting relations in extensions  $F/\mathbf{k}$  and  $K/kk$ , correspondingly. Choose dual bases:

- $\{x_i\}, \{y_i\}, 1 \leq i \leq m$  for the Frobenius pair  $(F, \mathbf{k}, \text{tr}_{F/\mathbf{k}})$ ,
- $\{x'_j\}, \{y'_j\}, 1 \leq j \leq n$  for the Frobenius pair  $(K, F, \text{tr}_{K/F})$ ,
- $\{x''_k\}, \{y''_k\}, 1 \leq k \leq mn$  for the Frobenius pair  $(K, \mathbf{k}, \text{tr}_{K/\mathbf{k}})$ .

Note that we may choose  $\{x_i x'_j\}, \{y_i y'_j\}$  as dual bases for the third extension.

Each seam circle  $C$  bounds one component (facet) labelled  $F$  and one labelled  $K$ . Choose circles parallel to  $C$  in each of these components and apply neck-cutting along these circles as shown in Figure 5.27.

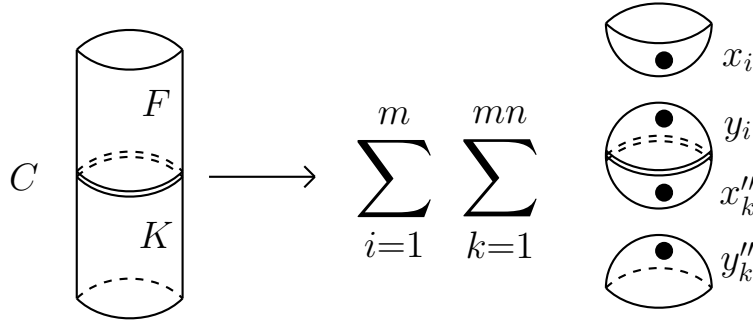


FIGURE 5.27. Surgery on a seam circle. Dotted seamed spheres are then evaluated using trace maps.

Doing this neck-cutting along each seam circle converts  $S$  into a sum of terms which are disjoint unions of connected components of three types:

- closed connected surfaces labelled  $F$  with elements of  $F$  floating on them,
- closed connected surfaces labelled  $K$  with element of  $K$  floating on them,
- spheres with a seam circle and an element of  $F$ , respectively  $K$ , in a disk labelled  $F$ , respectively  $K$ , see Figure 5.28.

Components of the first and second kind are evaluated via TQFTs for  $(F, \mathbf{k}, \text{tr}_{F/\mathbf{k}})$  and  $(K, \mathbf{k}, \text{tr}_{K/\mathbf{k}})$ , respectively, to yield elements of  $\mathbf{k}$ . We propose the following evaluation of the

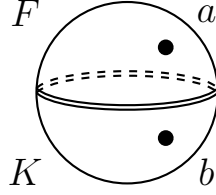


FIGURE 5.28. Seamed 2-sphere, denoted  $\mathbb{S}^2(a, b)$ , with dots  $a \in F$  and  $b \in K$  floating in the  $F$ -disk and  $K$ -disk.

seamed 2-sphere  $\mathbb{S}^2(a, b)$ :

$$(43) \quad \mathcal{F}(\mathbb{S}^2(a, b)) = \text{tr}_{F/\mathbf{k}}(a \text{tr}_{K/F}(b)).$$

We can interpret this evaluation, see Figure 5.29, as first removing the  $K$ -disk with dot  $b$  and inserting dot  $\text{tr}_{K/F}(b) \in F$  in its place, now floating on the 2-sphere labelled  $F$  alongside the original dot  $a$ . Now multiply the two dots and evaluate using  $\varepsilon_F = \text{tr}_{F/\mathbf{k}}$ . Figure 5.29 shows the two steps in this evaluation.

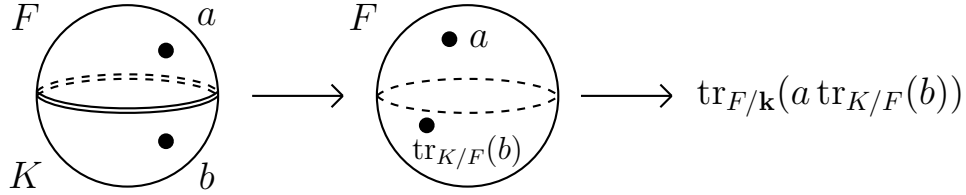


FIGURE 5.29. Evaluation of the seamed sphere  $\mathbb{S}^2(a, b)$ , given by pushing  $b$  via relative trace into the  $F$ -facet and evaluating via  $\text{tr}_{F/\mathbf{k}}$ .

With evaluations for all three types of connected components at hand, we know how to evaluate an arbitrary seamed  $(F, K)$ -surface  $S$  as above. In the sum resulting after neck-cutting, for each term we take the product of evaluations of all connected components and then sum these elements of  $\mathbf{k}$ . Denote this evaluation by  $\mathcal{F}(S)$  or  $\langle S \rangle$ .

It's easy to see that, if a seam circle  $C$  bounds an  $F$ -disk or a  $K$ -disk on one side (or such disks on both side), possibly with some dots in them, then one can skip the neck-cutting procedure on the corresponding side of  $C$  (or on both sides of  $C$ ) without changing the evaluation. This observation implies relations in the top row of Figure 5.30.

Specializing Figure 5.30 relation on top right to  $b \in F$ , the dot on the right hand side has label  $nb$ , since  $\text{tr}_{K/F}(b) = nb$  then, where  $n = [K : F]$ . Consequently, if  $\text{char } \mathbf{k} = p$  and  $p|n$ , the right hand side is 0.

A dot on an  $F$ -component can be pushed across a seam into an adjacent  $K$ -component, since the trace  $\text{tr}_{K/F}$  is  $F$ -linear, see Figure 5.31. If the  $F$ -component were a disk, it can then be removed.

This allows us to move dots away from any  $F$ -component that bounds a seam (otherwise it's a connected component of  $S$ ). Furthermore, Figure 5.32 relation holds. It allows to reduce

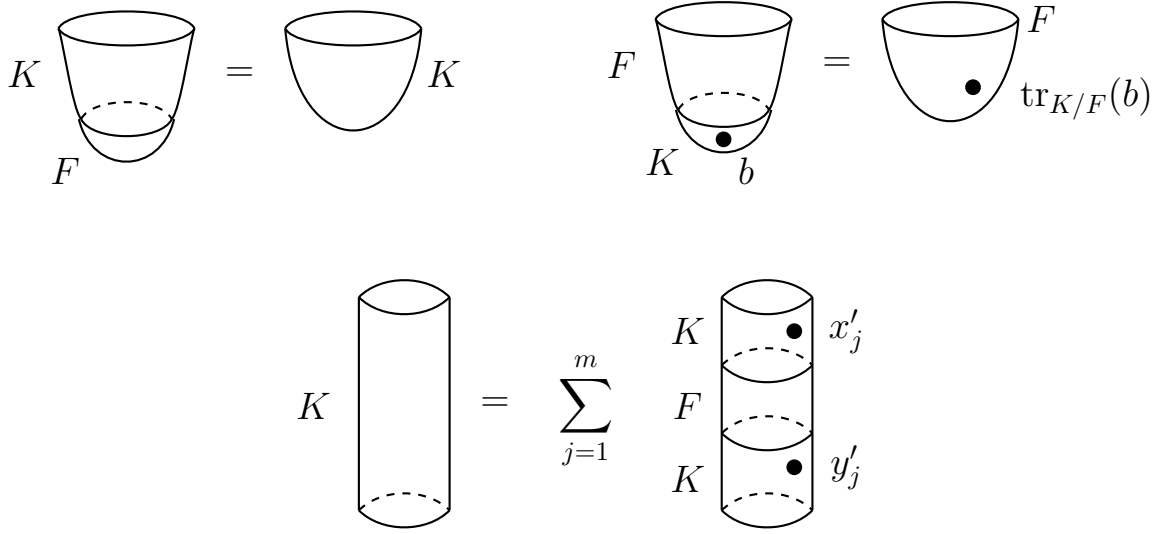


FIGURE 5.30. Some skein relations. Top left: a dotless  $F$ -disk may be removed. Top right: pushing a dot off a  $K$ -disk. Bottom: partial neck-cutting from  $K$  to  $F$ .

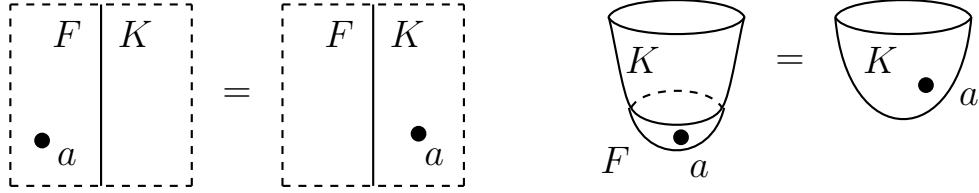


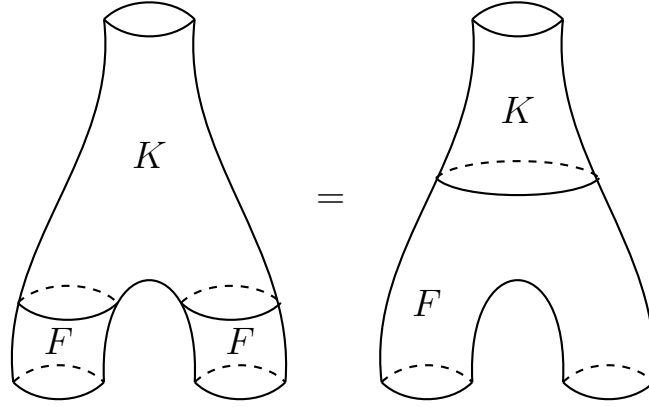
FIGURE 5.31. Left: pushing an  $F$ -dot  $a \in F$  across a seam into a  $K$ -component. Right: removing a dotted  $F$ -disk.

$S$  to a surface where each  $K$ -facet has at most one boundary component. The relation can be checked by doing surgeries on  $F$ -sides of the two circles on the left hand side, then using relations in Figure 5.31.

Similar to the discussion in Section 5.2.1, such patched surfaces can be evaluated by tensoring the fields with the algebraic closure  $\bar{\mathbf{k}}$  and looking at the chain of  $\bar{\mathbf{k}}$ -algebra inclusions and trace maps between them

$$(44) \quad \bar{\mathbf{k}} \subset F \otimes_{\mathbf{k}} \bar{\mathbf{k}} \subset K \otimes_{\mathbf{k}} \bar{\mathbf{k}}.$$

Both rings  $F \otimes_{\mathbf{k}} \bar{\mathbf{k}}$ ,  $K \otimes_{\mathbf{k}} \bar{\mathbf{k}}$  are direct product of fields  $\bar{\mathbf{k}}$ , and under the inclusion  $F \otimes_{\mathbf{k}} \bar{\mathbf{k}} \subset K \otimes_{\mathbf{k}} \bar{\mathbf{k}}$  minimal idempotents in  $K \otimes_{\mathbf{k}} \bar{\mathbf{k}}$  go to sums of distinct minimal idempotents of  $F \otimes_{\mathbf{k}} \bar{\mathbf{k}}$ . Relative traces have a similar simple description. This allows to easily evaluate a patched surface to an element of  $\mathbf{k}$ . In this way, the TQFT reduces to set-theoretic computations with roots of an irreducible polynomial describing the extension  $K/\mathbf{k}$ , together with the Galois group action on the roots, and the partition of roots corresponding to the subfield  $F \subset K$ .

FIGURE 5.32. Different boundary components of a  $K$ -facet can be merged into one.

If one allows elements of  $F$  and  $K$  to float in the corresponding regions of the surface, evaluation requires decomposing these elements in the bases of minimal idempotents of  $F \otimes_{\mathbf{k}} \bar{\mathbf{k}}$  and  $K \otimes_{\mathbf{k}} \bar{\mathbf{k}}$ .

**5.2.3. Defect lines and Galois symmetries.** Here we use notations from the previous subsection, including having a chain of finite separable field extensions  $\mathbf{k} \subset F \subset K$ . We can extend patched surfaces setup in that subsection by adding defect lines for Galois symmetries of extensions  $F/\mathbf{k}$  and  $K/\mathbf{k}$ . Let  $S$  be a patched  $(F, K)$ -surface. Choose a collection of disjoint circles with co-orientations on  $F$ -patches of  $S$  and label each of them by an element  $\sigma \in \text{Gal}(F/\mathbf{k})$  (not necessarily the same one). Likewise, choose a collection of disjoint circles with co-orientations on  $K$ -patches of  $S$  and label each of them by an element  $\tau \in \text{Gal}(K/\mathbf{k})$ . As before, dots labelled by elements of  $F$  and  $K$  may float in  $F$ - and  $K$ -regions of  $S$ , correspondingly. To evaluate such a decorated patched surface  $S$ , one applies neck-cutting around each of three types of seamed circles of  $F$ :

- $(F, K)$ -circles, along which  $K$ - and  $F$ -regions of  $S$  meet,
- $\text{Gal}(F/\mathbf{k})$ -circles in  $F$ -patches,
- $\text{Gal}(K/\mathbf{k})$ -circles in  $K$ -patches.

After that evaluation reduces to the familiar cases that have already been discussed. We can denote the evaluation by  $\mathcal{F}(S)$  or  $\langle S \rangle \in \mathbf{k}$ .

If  $\sigma \in \text{Gal}(K/\mathbf{k})$  preserves the subfield  $F$ , one can allow  $\sigma$ -circles to intersect seam lines separating  $F$ - and  $K$ -regions of  $S$ , see Figure 5.33.

Such a network can be evaluated as before, by tensoring all fields with  $\bar{\mathbf{k}}$ , representing  $K$  as a simple extension, and working with the set of roots of the corresponding irreducible polynomial.

Finally, one can consider arbitrary finite Galois extensions  $\mathbf{k} \subset F$  and patched surfaces with regions labelled by finite extensions  $F_i$ . A seam circle separating regions labelled  $F_i$  and  $F_j$  is assumed to be co-oriented, and an inclusion  $F_i \subset F_j$  is assigned to each such circle, see Figure 5.34 left. Elements of  $F_i$  may float in  $F_i$ -regions. These regions may contain  $\sigma$ -circles, for  $\sigma \in \text{Gal}(F_i/\mathbf{k})$ . Furthermore, these circles can be viewed as a special case of the seam

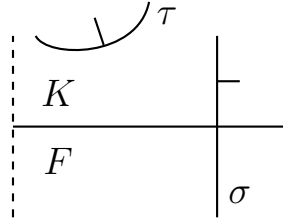


FIGURE 5.33. Caption.

circles of the first type, for the case when fields  $F_i = F_j$  and the inclusion (isomorphism)  $F_i \subset F_j$  is given by  $\sigma$ .

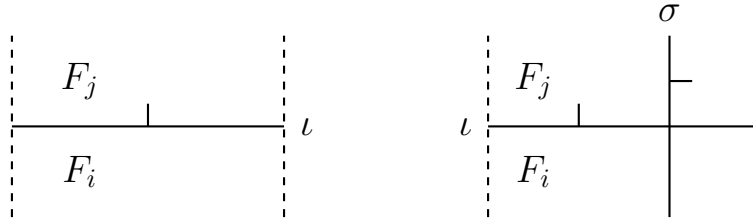


FIGURE 5.34. Left:  $\iota : F_i \hookrightarrow F_j$  is a field inclusion. Right: A seam line that intersect  $(F_i, F_j)$ -line corresponds to an automorphism  $\sigma : F_j \rightarrow F_j$  that preserves the subfield  $F_i$ , that is,  $\sigma(\iota(F_i)) = \iota(F_i)$ .

Seamed circles labelled by Galois group elements may intersect seamed circles of the first type, as long as the Galois symmetry  $\sigma$  preserves the fields  $F_i$  for all regions along the  $\sigma$ -circle, see Figure 5.34.

Such closed networks can then be evaluated by working with a splitting field  $K$  that contains copies of fields  $F_i$ , over all patches of the surface  $S$ , tensoring with the algebraic closure  $\overline{\mathbf{k}}$ , and working with minimal idempotents in  $K \otimes_{\mathbf{k}} \overline{\mathbf{k}}$  to evaluate the network.

With these evaluations at hand, one can then define state spaces for collections of circles that are patched from intervals labelled by various fields  $F_i$  separated by points labelled by inclusions  $F_i \subset F_j$  and Galois symmetries  $\sigma : F_i \rightarrow F_i$ .

The same approach allows to evaluate even more general networks. Namely, beside seam circles for inclusions  $F_i \subset F_j$  one can consider networks with co-oriented edges labelled by inclusions  $F_i \subset F_j$  that may contain trivalent (or even more general) vertices where three regions meet, see Figure 5.35 left.

In the special case when all fields are the same field  $F$  and seam edges are Galois symmetries  $\sigma \in \text{Gal}(F/\mathbf{k})$  these networks are identical to those in Section 5.1.4. One then obtains a special case of Turaev's homotopy 2D TQFTs, where networks describe conjugacy classes of homomorphisms  $\pi_1(S) \rightarrow \text{Gal}(F/\mathbf{k})$ , up to conjugation by elements of  $\pi_1(S)$  or, more generally, homotopy classes of maps  $S \rightarrow X$  for  $X$  as specified in the caption for Figure 5.35.

Suitable state spaces for decorated patched circles for these theories can then be studied.

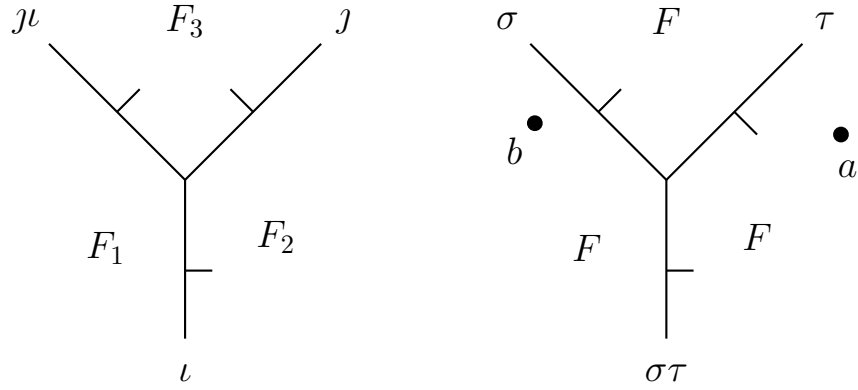


FIGURE 5.35. Left:  $F_1$ ,  $F_2$ , and an  $F_3$ -region meet at a vertex, with the inclusion  $F_1 \subset F_3$  given by the composition  $j \circ \iota$  of inclusions  $\iota : F_1 \hookrightarrow F_2$ ,  $j : F_2 \hookrightarrow F_3$ . Right: as a special case, when all 3 fields are  $F$  and the inclusions are isomorphisms in  $G = \text{Gal}(F/\mathbf{k})$ , the networks match those that appear in homotopy 2D TQFTs with the group  $G$ . Picking an abelian subgroup  $A \subset F$  stable under  $G$  and allowing dots labelled by elements of  $A$  to float in the regions corresponds to working with a space  $X$  with  $\pi_1(X) \cong G$  and  $\pi_2(X) \cong A$  with the matching action of  $G$  on  $A$ .

It is possible to further refine the theory by introducing “orbifold” points with a nontrivial “monodromy” around them. These points may be located on facets of a network, along seam lines, along Galois ( $\sigma$ -defect) lines, and at vertices of the network, see Figures 5.36, 5.37 and 5.38. An orbifold point with a label  $\sigma$  inside a facet (type (1) point, shown in Figure 5.36) can be defined via a connected sum with a torus with a  $\sigma$ -defect circle. In the state sum, only idempotents  $e_i$  with  $\sigma(e_i) = e_i$  placed on that facet will contribute to the evaluation.

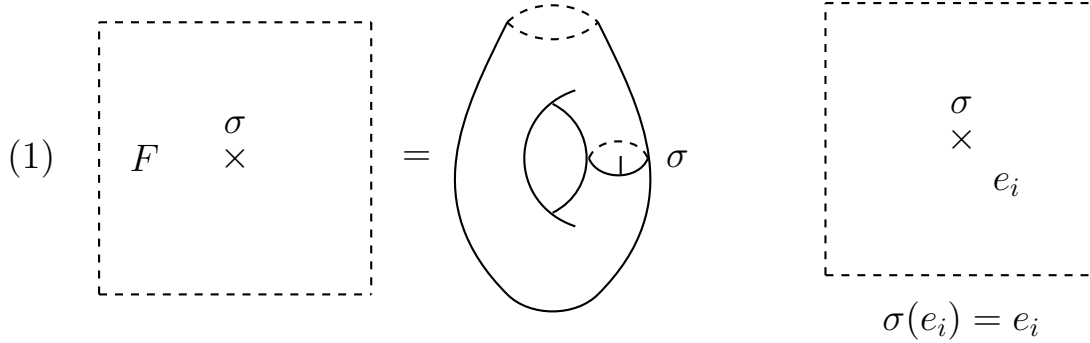


FIGURE 5.36. Type (1) orbifold point, on an  $F$ -patch of surface.

At an orbifold point on a  $\sigma$ -defect circle (type (2a) orbifold point) the automorphism label in  $\text{Gal}(F/\mathbf{k})$  may change from  $\sigma_0$  to  $\sigma_1$ , see Figure 5.37. In the corresponding evaluation, only minimal idempotents  $e_i$  with  $\sigma_0(e_i) = \sigma_1(e_i)$  may contribute.

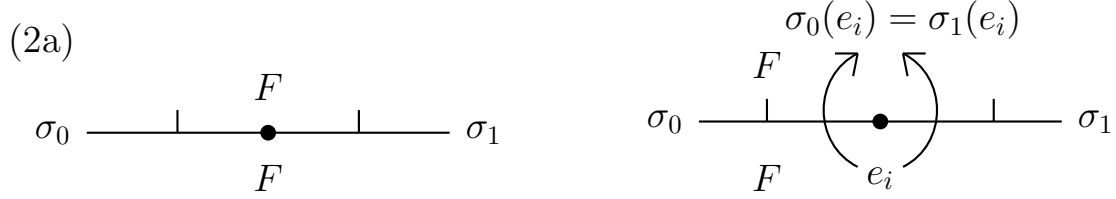


FIGURE 5.37. Type (2a) orbifold point on an  $(F, F)$ -seam of a surface, with field automorphisms different along the seam on the two sides of the point.

At more general type (2) orbifold point on an  $(F, K)$ -seam, an embedding  $\iota_0 : F \hookrightarrow K$  may change to a different embedding  $\iota_1 : F \hookrightarrow K$ , see Figure 5.38 left. At a type (3) orbifold point, at a vertex of the network, the embedding  $j : F_1 \hookrightarrow F_3$  corresponding to the Northwest seam may be different from the composition of embeddings  $j_0 \circ \iota_0$  for the South seam  $\iota_0 : F_0 \hookrightarrow F_1$  and the Northeast seam  $j_0 : F_2 \hookrightarrow F_3$ , see Figure 5.38 right.

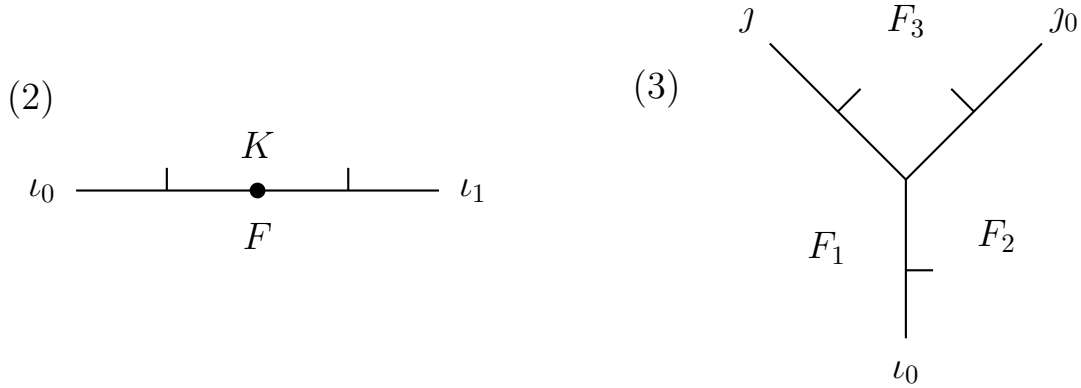


FIGURE 5.38. Left: type (2) orbifold point, with different embeddings  $\iota_0, \iota_1 : F \hookrightarrow K$  on the two sides of the seam. Right: type (3) orbifold point, with  $j \neq j_0 \iota_0$ .

## 6. FOAMS, GALOIS EXTENSIONS, AND SYLVESTER SUMS

**6.1. Base change for  $\mathrm{GL}(N)$  foams and field extensions.** Consider the ring of polynomials

$$(45) \quad R' = \mathbb{Z}[\alpha_1, \dots, \alpha_N]$$

in variables  $\alpha_1, \dots, \alpha_N$ , and its subring of symmetric polynomials

$$\begin{aligned} R &= \mathbb{Z}[\alpha_1, \dots, \alpha_N]^{S_N} \subset R', & R &= \mathbb{Z}[E_1, \dots, E_N], \\ E_i &= \sum_{i_1 < \dots < i_k} \alpha_{i_1} \dots \alpha_{i_k}, \end{aligned}$$

where  $E_i$  is the  $i$ -th elementary symmetric function in  $\alpha_1, \dots, \alpha_N$ .

Most constructions of equivariant  $\mathrm{GL}(N)$  link homology, as an intermediate step, associate a free graded  $R'$ -module  $\langle \Gamma \rangle$  to a planar trivalent graph  $\Gamma$  with oriented edges labelled by weights in  $\{1, 2, \dots, N\}$  subject to the flow constraint that the sum of weights of out edges equals the sum of weights of in edges at each vertex of  $\Gamma$ , see Figure 6.1. There is an extensive literature on  $\mathrm{GL}(N)$  homology. We refer to [KK] for a partial list of references and to [RW2] for a combinatorial way to define  $\langle \Gamma \rangle$ .

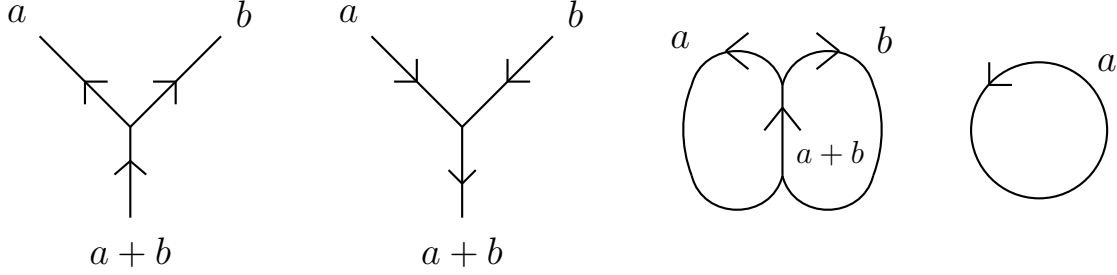


FIGURE 6.1. Left: split and merge vertices of an MOY graph. Right: simplest MOY graphs, the  $(a, b)$ -theta graph and thickness  $a$  circle.

A planar graph as above is called a Murakami-Ohtsuki-Yamada (MOY) graph or a *web*. Graded rank of  $\langle \Gamma \rangle$  equals the quantum  $\mathfrak{gl}(N)$  invariant  $P(\Gamma) \in \mathbb{Z}_+[q, q^{-1}]$ , also known as the Murakami-Ohtsuki-Yamada (MOY) invariant, i.e., see [MOY]. One can refer to  $\langle \Gamma \rangle$  as the *homology* or *state space* of  $\Gamma$ .

Homology groups of a link are obtained as a complex built out of state spaces  $\langle \Gamma \rangle$  for various MOY webs  $\Gamma$  given by taking a planar projection  $D$  of a link and substituting certain elementary subgraphs in place of crossings of  $D$ .

For the empty web  $\emptyset$  the associated module is  $R$ ,  $\langle \emptyset \rangle \cong R$  and the MOY invariant is  $P(\emptyset) = 1$ .

Denote by  $\Gamma_a$  the MOY web which is a circle labelled  $a$ ,  $1 \leq a \leq N$ , see Figure 6.1 right. Then  $\langle \Gamma_a \rangle$  can be canonically identified with the subring

$$(46) \quad R_{a, N-a} = \mathbb{Z}[\alpha_1, \dots, \alpha_N]^{S_a \times S_{N-a}}.$$

Here,  $S_a \times S_{N-a} \subset S_N$  is the parabolic subgroup for the decomposition  $(a, N-a)$ , separately permuting the first  $a$  variables and the last  $N-a$  variables.

Web  $\Gamma_N$ , a circle of thickness  $N$ , has the state space isomorphic to  $R$ , so that  $\langle \Gamma_N \rangle \cong \langle \emptyset \rangle$ . In general, with a minimal amount of effort and little or no loss of information, lines labelled  $N$  can be hidden (erased) from MOY diagrams. This corresponds to passing from  $\mathrm{GL}(N)$  to  $\mathrm{SL}(N)$  link homology. However, it's often convenient to keep these lines.

When  $a = 1$ , we can also identify

$$(47) \quad \langle \Gamma_1 \rangle \cong R[X]/(X^N - E_1 X^{N-1} + \dots + (-1)^N E_N).$$

More generally, choose a sequence  $\underline{a} = (a_1, \dots, a_k)$  of non-negative integers that add up to  $N$ ,  $a_1 + \dots + a_k = N$ , and consider the graph  $\Gamma_{\underline{a}}$  in Figure 6.2 left.



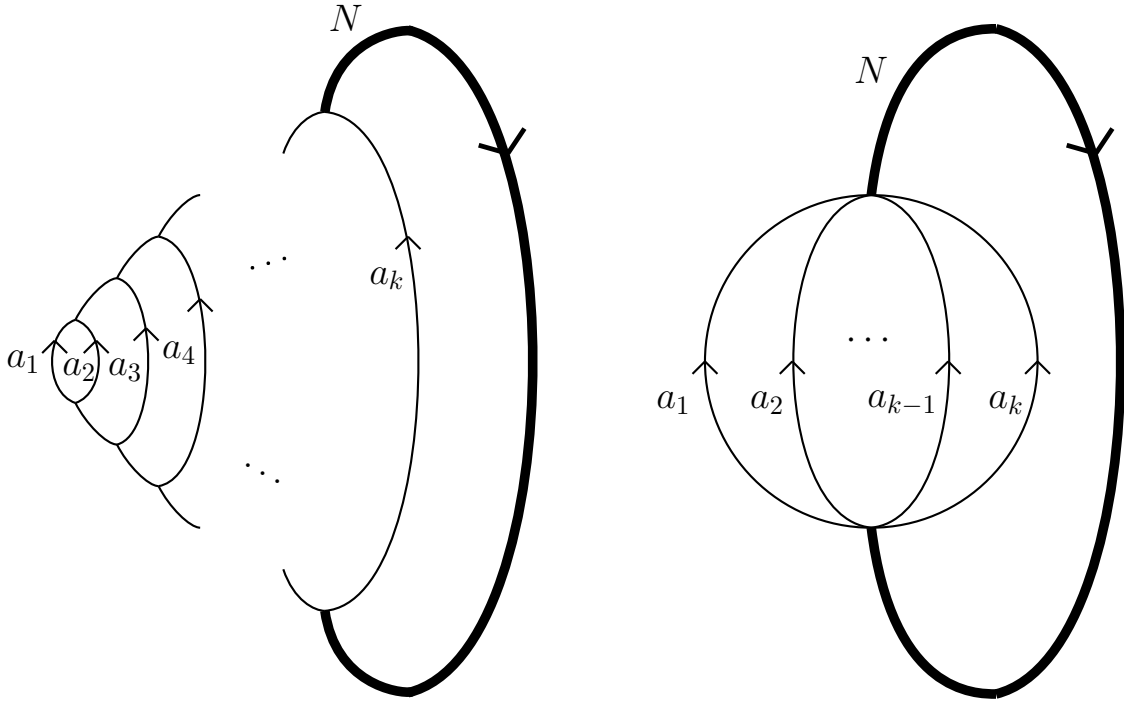


FIGURE 6.2. Left:  $\mathrm{GL}(N)$  web  $\Gamma_{\underline{a}}$ . Lines of thickness  $a_1, \dots, a_k$  merge into a line of thickness  $N$ . Right: a schematic way to depict this web, with  $k$  lines merging at once into the  $N$ -line. Changing the order of merges of lines results in webs with canonically isomorphic state spaces.

In this web lines of weight  $a_1, a_2, \dots, a_k$  merge into thicker and thicker lines, eventually merging into a line of thickness  $N$  that goes around and then splits off into the original lines. The state space  $\langle \Gamma_{\underline{a}} \rangle$  does not depend on the order in which the  $k$  lines merge and the graph can be denoted as in Figure 6.2 right, where the order of merge is not specified. The value of the quantum MOY invariant on the graph  $\Gamma_{\underline{a}}$  is the  $q$ -multinomial coefficient

$$(48) \quad P(\Gamma_{\underline{a}}) = \left[ \begin{matrix} N \\ a_1, \dots, a_k \end{matrix} \right], \quad [m] = \frac{q^m - q^{-m}}{q - q^{-1}},$$

and the state space  $\langle \Gamma_{\underline{a}} \rangle$  is a free  $R$ -module of that graded rank.

When doing quantum  $\mathrm{SL}(N)$  homology or  $\mathrm{SL}(N)$  MOY invariants, lines of thickness  $N$  may be erased and lines of thickness  $N - a$  converted to those of thickness  $a$  with the opposite orientation. This procedure does not change the value of the MOY invariant, and can be made to preserve homology groups. In this case, Figure 6.2 graphs may be reduced by erasing thickness  $N$  interval and sometimes further simplifying, see Figure 6.3 below.

Let  $G = \mathrm{GL}(N, \mathbb{C})$  or its maximal compact subgroup  $G = \mathrm{U}(N)$ , with the standard action on  $\mathbb{C}^N$ . Consider the induced action of  $G$  on the flag variety

$$(49) \quad \mathrm{Fl}(\underline{a}) := \{0 \subset L_1 \subset L_2 \subset \dots \subset L_k \cong \mathbb{C}^N \mid \dim(L_i) - \dim(L_{i-1}) = a_i, \ i = 1, \dots, k\}.$$

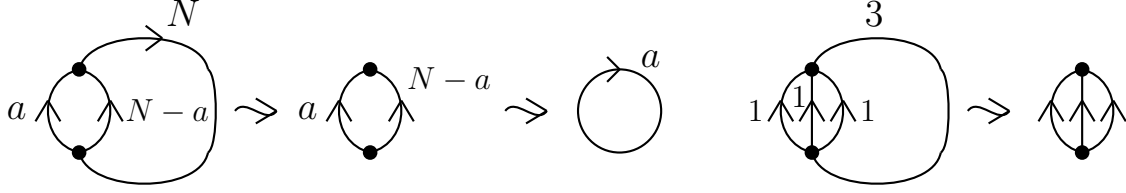


FIGURE 6.3. Left: graph  $\Gamma_{(a,N-a)}$  turns into  $\Gamma_a$  upon reducing from  $\mathrm{GL}(N)$  to  $\mathrm{SL}(N)$  homology. Right: Reducing  $\mathrm{GL}(3)$  graph  $\Gamma_{(1,1,1)}$  to the corresponding  $\mathrm{SL}(3)$  graph, with all edges of the latter labelled 1. In the  $\mathrm{SL}(3)$  case, MOY graphs are equivalent to Kuperberg's  $A_2$  spiders, see [Ku].

Equivariant cohomology  $H_G(\mathrm{Fl}(\underline{a}))$  is naturally a module over equivariant cohomology of a point  $H_G(*) \cong R$ . There's a natural isomorphism of  $R$ -algebras

$$(50) \quad \langle \Gamma_{\underline{a}} \rangle \cong H_G(\mathrm{Fl}(\underline{a})) \cong R_{\underline{a}},$$

where

$$(51) \quad R_{\underline{a}} := \mathbb{Z}[x_1, \dots, x_N]^{S_{\underline{a}}}, \quad S_{\underline{a}} := S_{a_1} \times \dots \times S_{a_k} \subset S_N,$$

is the subring of invariants for the parabolic subgroup  $S_{\underline{a}}$  of  $S_N$  acting on the ring of polynomials in  $N$  variables.

In the special case  $\underline{a} = (1, \dots, 1) = (1^N)$ , the parabolic subgroup is trivial and

$$(52) \quad R_{(1^N)} = \mathbb{Z}[x_1, \dots, x_N] \cong H_G(\mathrm{Fl}((1^N)))$$

is isomorphic to the polynomial ring and to the equivariant cohomology of the full flag variety  $\mathrm{Fl}((1^N))$ , which we can also denote  $\mathrm{FF}(N)$ .

State spaces  $\langle \Gamma \rangle$  are functorial, in a suitable sense. A graph cobordism  $F$ , which is a decorated combinatorial 2-dimensional  $CW$ -complex with prescribed singularities [RW2, KK] and embedded in  $\mathbb{R}^2 \times [0, 1]$ , also called a *foam* or  $\mathrm{GL}(N)$ -*foam*, induces a homomorphism of state spaces

$$(53) \quad \langle F \rangle : \langle \partial_0 F \rangle \longrightarrow \langle \partial_1 F \rangle.$$

Together, these homomorphisms form a functor from the category of  $\mathrm{GL}(N)$ -foams to the category of graded  $R$ -modules, see [RW2, KK] and references therein.

Suppose that a web  $\Gamma$  admits a reflection symmetry about an axis  $\ell$ . Then  $\langle \Gamma \rangle$  is naturally a unital associative Frobenius  $R$ -algebra, due to the presence of unit  $\iota$ , counit  $\varepsilon$  and multiplication  $m$  cobordisms as schematically shown in Figure 6.4 for a so-called  $\Theta$ -web, resembling the letter  $\Theta$  (orientations and weights of edges are omitted for simplicity). Note that a symmetry axis may contain some edges of the web, a simple example is given by a  $\Theta$ -web with edges of thickness  $a, a, 2a$ , in which case there's a symmetry axis through the  $2a$  edge.

A homomorphism of commutative rings

$$(54) \quad \phi : R \longrightarrow S,$$

where  $S$  is not necessarily graded, can be used to define a version  $\langle \Gamma \rangle_S$  of state spaces, a kind of base change from  $R$  to  $S$ , such that  $\langle \Gamma \rangle_S$  is a free  $S$ -module of rank  $P(\Gamma)_{q=1}$  for any MOY

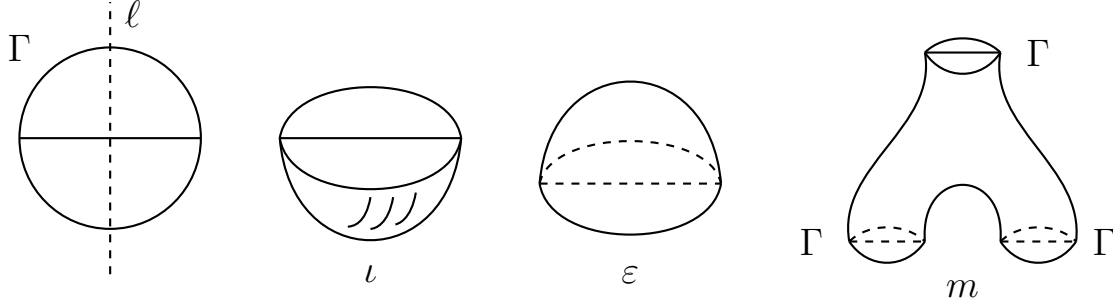


FIGURE 6.4. A web  $\Gamma$  with a symmetry axis  $\ell$  and schematically depicted unit, counit, and multiplication morphisms.

graph  $\Gamma$ . Here  $P(\Gamma)_{q=1}$  is the specialization of the Laurent polynomial  $P(\Gamma) \in \mathbb{Z}_+[q, q^{-1}]$  to its value at  $q = 1$ .

Due to all modules being free, one way to define it is by

$$(55) \quad \langle \Gamma \rangle_S := \langle \Gamma \rangle \otimes_R S.$$

A more intrinsic way to define  $\langle \Gamma \rangle_S$  is via  $S$ -valued closed foam evaluation that uses  $\phi$ , see [KR1, Section 4] for a similar definition in a different case where the state spaces are not known to be free modules over the ground ring.

Consider now a special case when the ground ring  $S = \mathbf{k}$  is a field and we pick a separable polynomial

$$(56) \quad f(x) = x^N + u_{N-1}x^{N-1} + \dots + u_0, \quad u_i \in \mathbf{k}, \quad i = 1, \dots, N-1,$$

irreducible over  $\mathbf{k}$ . Let  $K$  be a splitting field of  $f(x)$  over  $\mathbf{k}$  and  $F$  be the field

$$(57) \quad F := \mathbf{k}[\alpha]/(f(\alpha)).$$

Polynomial  $f(x)$  has  $N$  roots  $\alpha_1, \dots, \alpha_N \in K$ , and each of them defines a homomorphism of  $\mathbf{k}$ -algebras  $F \rightarrow K$ .

Consider the homomorphism

$$(58) \quad \phi : R \rightarrow \mathbf{k}, \quad \phi(E_i) = (-1)^i u_i.$$

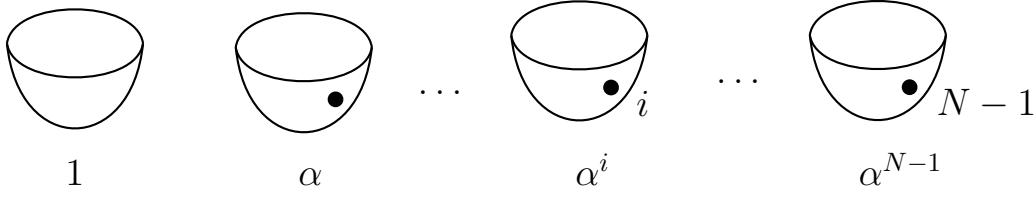
and state spaces  $\langle \Gamma \rangle_\phi$  associated to MOY graphs via the foam construction. The state spaces of the empty graph and the  $N$ -circle are isomorphic to  $\mathbf{k}$ ,

$$(59) \quad \langle \emptyset \rangle_\phi \cong \langle \Gamma_N \rangle \cong \mathbf{k}.$$

The state space of the 1-circle is isomorphic to  $F$ ,

$$(60) \quad \langle \Gamma_1 \rangle \cong F,$$

via a homomorphism that take a one-dotted disk with boundary  $\Gamma_1$  to  $\alpha$  (facets of foam may be labelled by symmetric functions in the number of variables equal to the thickness of the facet). The state space  $\Gamma_1$  is a free  $\mathbf{k}$  module with the basis of disks with  $i$  dots,  $i = 0, \dots, N-1$ , see Figure 6.5. The corresponding basis of  $F$  is that of powers of  $\alpha$ ,  $\{1, \alpha, \dots, \alpha^{N-1}\}$ .

FIGURE 6.5. Basis of powers of a dot (powers of  $\alpha$ ) in  $\langle \Gamma_1 \rangle$ .

There is a surjective homomorphism

$$(61) \quad \phi_1 : R_{(1^N)} \longrightarrow K, \quad \phi_1(x_i) = \alpha_i, i = 1, \dots, N,$$

into the splitting field  $K$  that extends homomorphism  $\phi$ , so the square below commutes

$$\begin{array}{ccc} R_{(1^N)} & \xrightarrow{\phi'} & K \\ \uparrow & & \uparrow \\ R & \xrightarrow[\phi]{} & \mathbf{k}. \end{array}$$

Recall that the source ring of  $\phi_1$  is the state space of  $\Gamma_{(1^N)}$ , which consists of  $N$  weight 1 lines that merge and split into an  $N$ -line.

**Proposition 6.1.**  $\phi_1$  induces a surjective homomorphism of  $\mathbf{k}$ -algebras

$$(62) \quad \tilde{\phi} : \langle \Gamma_{(1^N)} \rangle_{\phi} \longrightarrow K.$$

This map is an isomorphism if and only if the Galois group of the splitting field extension  $K/\mathbf{k}$  is the symmetric group  $S_N$ .

Thus,  $\tilde{\phi}$  is an isomorphism if the splitting field extension  $K/\mathbf{k}$  has the largest possible degree  $N!$  given that  $\deg(f) = N$ .

Recall that extension  $K/\mathbf{k}$  is Galois and there's a bijection between intermediate subfields of  $K/\mathbf{k}$  and subgroups of the Galois group  $\text{Gal}(K/\mathbf{k})$ .

Assuming that the Galois group is the largest possible given that  $f$  has degree  $N$ , we can understand the state spaces of webs  $\langle \Gamma_{\underline{a}} \rangle_{\phi}$  for all decompositions  $\underline{a}$  via a part of the Galois correspondence.

**Proposition 6.2.** Suppose that  $\text{Gal}(K/\mathbf{k}) = S_N$ . Then for each decomposition  $\underline{a}$  of  $N$  there is a ring isomorphism

$$(63) \quad \langle \Gamma_{\underline{a}} \rangle \cong K^{S_{\underline{a}}}$$

between the  $\phi$ -state space of the web  $\Gamma_{\underline{a}}$  and the intermediate subfield  $K^{S_{\underline{a}}}$ .

The proof is straightforward and left to the reader. Inclusions of subfields as well as trace maps between different subfields correspond to foams that merge and split lines in these webs,

corresponding to combining to consecutive parts of  $\underline{a}$  or splitting a part into two parts,

$$(\dots, a_{i-1}, a_i, a_{i+1}, a_{i+2}, \dots) \leftrightarrow (\dots, a_{i-1}, a_i + a_{i+1}, a_{i+2}, \dots).$$

Thus, state spaces for theta-like webs  $\Gamma_{\underline{a}}$  correspond to subfields for the parabolic subgroups  $S_{\underline{a}}$ . In this correspondence we don't encounter all intermediate subfields but only those that come from "flattening" or ordering the set of roots of  $f$  and can be matched to decompositions  $S_{\underline{a}}$ .

For the partition  $(1, N-1)$  the state space

$$\langle \Gamma_{(1, N-1)} \rangle \cong F,$$

also see (60) and Figure 6.3 left for  $a = 1$ .

We encounter the ground field  $\mathbf{k}$ , field  $F$ , the splitting field  $K$  as well as intermediate fields for the parabolic subgroups as  $\phi$ -state spaces of theta-like webs. These webs can be thought of as bubbling off an  $N$ -line or  $N$ -circle, see Figure 6.6.

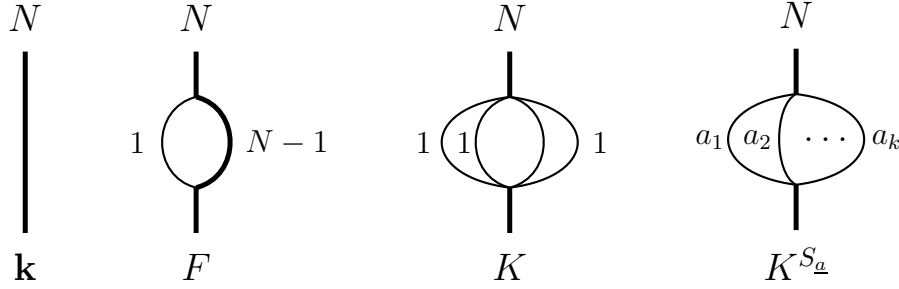


FIGURE 6.6. Basic webs along an  $N$ -line with field extensions of  $\mathbf{k}$  as state spaces. Top label is the thickness of the edge, bottom label is the corresponding field.

When  $[K : \mathbf{k}] < N!$ , the Galois group is a proper subgroup of  $S_N$ . For each permutation  $s$  of  $N$  roots of  $f(x)$  in  $K$  there is a surjective map

$$(64) \quad \phi_s : \mathbf{k}[x_1, \dots, x_N] \longrightarrow K, \quad \phi_s(x_i) = x_{s(i)}, \quad i = 1, \dots, N$$

that lifts homomorphism

$$(65) \quad \phi_S : R \otimes_{\mathbb{Z}} \mathbf{k} \cong \mathbf{k}[E_1, \dots, E_N] \longrightarrow \mathbf{k}, \quad \phi_S(E_i \otimes 1) = (-1)^i u_i,$$

(similar to homomorphism (58)). Map  $\phi_s$  factors through a homomorphism

$$\begin{aligned} \psi_s &: \langle \Gamma_{(1^N)} \rangle_{\phi} \longrightarrow K, \\ \phi_s &: \mathbf{k}[x_1, \dots, x_N] \xrightarrow{\gamma} \langle \Gamma_{(1^N)} \rangle_{\phi} \xrightarrow{\psi_s} K, \end{aligned}$$

where  $\gamma$  is the canonical quotient map, sending  $x_i$  to the unit element cobordism into  $\Gamma_{(1^N)}$  decorated by a dot on the  $i$ -th thin disk.

For two  $s$  that differ by an element of  $\text{Gal}(K/\mathbf{k})$  the two homomorphisms are related by an automorphism of  $K$ . Choose representatives  $s_1, \dots, s_m$  of left cosets of  $\text{Gal}(K/\mathbf{k})$  acting on roots  $\alpha_1, \dots, \alpha_N \in K$  of  $f(x)$ . Here  $m = N!/[K : \mathbf{k}]$  is also the index of  $\text{Gal}(K/\mathbf{k})$  as a

subgroup of  $S_N$  of all permutations of roots of  $f(x)$ . Each of these representatives determines a surjective homomorphism

$$(66) \quad \psi_{s_i} : \langle \Gamma_{(1^N)} \rangle_\phi \longrightarrow K, \quad i = 1, \dots, m.$$

Note that  $\langle \Gamma_{(1^N)} \rangle_\phi$  is a commutative  $\mathbf{k}$ -algebra of dimension  $N!$  and a quotient of  $F \otimes_{\mathbf{k}} F \otimes \dots \otimes F = F^{\otimes N}$ . Consequently, it's a commutative semisimple  $\mathbf{k}$ -algebra and necessarily a direct product of field extensions of  $\mathbf{k}$ . The product of homomorphisms

$$(67) \quad \langle \Gamma_{(1^N)} \rangle_\phi \xrightarrow{(\psi_i)_{i=1}^m} \prod_{i=1}^m K$$

is easily seen to be surjective and then necessarily an isomorphism.

**Proposition 6.3.** *There is an isomorphism of algebras*

$$(68) \quad \langle \Gamma_{(1^N)} \rangle_\phi \cong K^{\times m}, \quad m = N!/[K : \mathbf{k}],$$

given by (67), between  $\phi$ -state space of  $(1^N)$  theta web and the direct product of  $m$  copies of  $K$ , where  $m$  is the index of the Galois group  $\text{Gal}(K/\mathbf{k})$  in  $S_N$ .

It is a reasonable question whether the above observations can be developed into something of interest to number theory or algebraic geometry, with the caveat that the Galois correspondence, that we see above in connection with webs and foams, is about 200 years old. One can ask whether it make sense to assign a commutative ring  $A$  to a line and etale extensions  $B$  of  $A$  to webs  $\Gamma$  that “bubble off” that line, additionally admitting a symmetry axis, so that the state space of web  $\Gamma$  is a ring  $B$ . Can étale cohomology be then connected to some version of foam theory?

The universal extension  $R \subset \mathbb{Z}[x_1, \dots, x_N]$  is used to build equivariant link homology. Specializing  $N = 2$  results in Khovanov homology. Further specializing to a separable degree two characteristic zero field extension  $\mathbf{k} \subset F$  results in Lee homology, i.e., see [Le, KR2]. Lee homology groups depend on linking numbers only, but looking at the degeneration from the universal extension to a field extension allows to pull out the Rasmussen invariant [Ra] of knot concordance and its variations. This pattern extends to  $N > 2$ , see [Go, Wu, Lo, Lw]. Specializing to separable field extensions results in near-trivial theories, from the topological viewpoint, but the way the universal theory degenerates into those leads to a wealth of information about concordance of knots and links. One can wonder whether more advanced structures in Galois theory and number theory may admit such liftings or deformations relating them to non-trivial low-dimensional topology.

**6.2. Overlapping foams and Sylvester double sums.** A straightforward extension of the Robert-Wagner evaluation formula to overlapping foams was proposed in [Kh4, Section 3]. It allows to interpret the Sergeev-Pragacz formula for the supersymmetric Schur functions (hook Schur functions) and the Day formula for Toeplitz determinants of rational functions via overlapping foams, see [Kh4] and references there. The same paper also suggested a relation between overlapping foam evaluation and resultants and speculated on possible relevance of overlapping foams to categorification of quantum groups.

In this section we explain how to interpret Sylvester double sums and relations on them (the Exchange Lemma) as developed in [KSV] and earlier work (see references in [KSV]) via overlapping foams as well. We assume familiarity with Section 3 of [Kh4].

A closed  $\mathrm{GL}(N)$  foam  $F$  is a decorated combinatorial 2-dimensional CW-complex embedded in  $\mathbb{R}^3$ . It consists of oriented *facets* (connected surfaces) each carrying a *thickness* from 1 to  $N$ . Facets are joined along *seams* where facets of thickness  $a$  and  $b$  merge into a facet of thickness  $a + b$ , subject to compatibility of orientations. A foam may contain *vertices*, which are singular points that connect pairs of seams between two different ways of merging three facets of thicknesses  $a, b, c$  into a facet of thickness  $a + b + c$ . A facet of thickness  $k$  of a foam may contain dots labelled by symmetric functions in  $k$  variables. A foam  $F$  evaluates to  $\langle F \rangle$  which is a symmetric polynomial in  $N$  variables. We refer to [RW2, KK] and references in [KK] for details.

It's useful to label the set of variables by  $X$  with  $|X| = N$  and view  $\langle F \rangle$  as a symmetric function in these variables, denoting the corresponding ring of symmetric functions by  $\mathrm{Sym}(X)$ .

When  $F$  is a connected surface (a single facet) of maximal thickness  $N$ , with a dot on it labelled by  $f(X) \in \mathrm{Sym}(X)$ , the evaluation  $\langle F \rangle = f(X)$  does not depend on the genus of the surface, see Figure 6.7. Of course, for most other foams, including surfaces of thickness less than  $N = |X|$ , the evaluation will strongly depend on the genii of components of the foam.

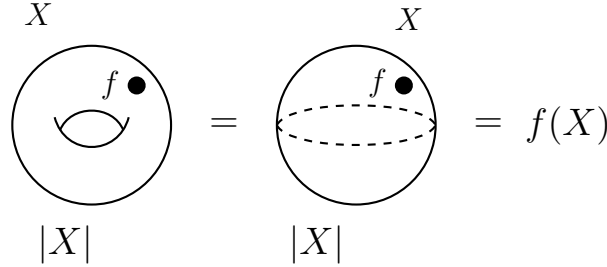


FIGURE 6.7. When  $F$  is a single facet foam, of maximal thickness  $N = |X|$ , it evaluates to the product of symmetric functions over all the dots on  $F$ . In particular, the evaluation does not depend on the genus of the surface  $F$ . The figure shows the case of a single dot and surface  $F$  having genus 1 or 0. Dashed circle on the sphere is there to depict the sphere schematically (it's not a seam circle on a sphere separating its into two facets of complementary thickness). The latter seam lines appear in the next few figures.

In [Kh4, Section 3] an extension of this evaluation is proposed when several foams for disjoint sets of variables overlap in  $\mathbb{R}^3$ . Foam evaluation  $\langle F \rangle$ , which is a sum of evaluations  $\langle F, c \rangle$  over all colorings  $c$ , is modified by scaling  $\langle F, c \rangle$  by  $(x_i - y_j)^{m(i,j,c)}$ , where  $m(i, j, c)$  is the number of circles in the intersection of the union  $F_i(c)$  of facets colored  $i$ ,  $x_i \in X$  and the union  $F_j(c)$  of facets colored  $j$ ,  $y_j \in Y$ . The product of these terms is taken over all pairs  $X, Y$  and  $x_i \in X, y_j \in Y$ . Ordering of each pair of sets  $(X, Y)$  of foam labelings is fixed to have a well-defined term  $x_i - y_j$  versus  $y_j - x_i$ .

For a closely related notion of an  $\mathrm{SL}(N)$  foam and its evaluation, other seam lines are allowed as well, where oriented facets of thickness  $a, b, c$  with  $a + b + c = N$  or  $a + b + c = 2N$  meet along seams. Case  $N = 3$  and foams with  $(a, b, c) = (1, 1, 1)$  seam lines have been treated in details in the literature, but for  $N > 3$  foam evaluation is mostly considered for  $\mathrm{GL}(N)$  foams. See Section 2.3.1 in [RW1] for a brief discussion on modifying evaluation from  $\mathrm{GL}(N)$  to  $\mathrm{SL}(N)$  foams, with the caveat that what call  $\mathrm{GL}(N)$  foams is referred to as  $\mathfrak{sl}_N$  foams in [RW1], and our  $\mathrm{SL}(N)$  foams are called *generalized foams* in [RW1].

Given finite sets of variables  $Y$  and  $Z$ , define

$$(69) \quad \mathcal{R}(Y, Z) = \prod_{y \in Y, z \in Z} (y - z), \quad \mathcal{R}(Y, Z) = 1 \quad \text{if } Y = \emptyset \text{ or } Z = \emptyset.$$

Note that  $\mathcal{R}(Y, Z)$  is a polynomial that's symmetric in variables in  $Y$  and symmetric in 'variables in  $Z$ , thus

$$\mathcal{R}(Y, Z) \in \mathrm{Sym}(Y) \otimes \mathrm{Sym}(Z),$$

where  $\mathrm{Sym}(Y)$  stands for the ring of symmetric polynomials in  $Y$  with coefficients in  $\mathbb{Z}$  or in a field  $\mathbf{k}$ , likewise for  $\mathrm{Sym}(Z)$ . Polynomial  $\mathcal{R}(Y, Z)$  equals the evaluation as in [Kh4, Section 3] of overlapping connected surfaces (foams with one facet) labelled by  $Y$  and  $Z$  and of maximal thickness  $|Y|$  and  $|Z|$ , respectively, see Figure 6.8.

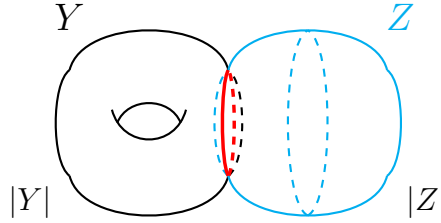


FIGURE 6.8. Overlapped connected surfaces labelled  $Y$  and  $Z$  of maximal thickness  $|Y|$  and  $|Z|$ , respectively, evaluate to  $\mathcal{R}(Y, Z)$ . In the picture, the surfaces are a torus and a sphere.

Given sets of variables  $A = \{\alpha_1, \dots, \alpha_m\}$  and  $B = \{\beta_1, \dots, \beta_n\}$ , the Sylvester double sum [Sy, DHKS, KSV], for  $0 \leq p \leq m$  and  $0 \leq q \leq n$ , is given as follows:

$$(70) \quad \mathrm{Syl}_{p,q}(A, B)(x) := \sum_{\substack{A' \subset A, B' \subset B, \\ |A'|=p, |B'|=q}} \mathcal{R}(A', B') \mathcal{R}(A \setminus A', B \setminus B') \frac{\mathcal{R}(x, A') \mathcal{R}(x, B')}{\mathcal{R}(A', A \setminus A') \mathcal{R}(B', B \setminus B')}.$$

The sum is over all subsets of  $A$  and  $B$  of cardinality  $p$  and  $q$ . We refer the reader to [LP1] and the above papers for applications of Sylvester double sums and their relation to subresultants.

Sylvester double sum is a polynomial in  $x$  of degree at most  $d := p + q$ . When  $p = 0$  or  $q = 0$ , the expression is called a *single sum*. Function  $\mathrm{Syl}_{p,q}(A, B)(x)$  is a polynomial in  $x$  with coefficients in the ring  $\mathrm{Sym}_{m,n} \cong \mathrm{Sym}(A) \otimes \mathrm{Sym}(B)$  which is the tensor product of rings of symmetric functions in the  $m$  variables in  $A$  and  $n$  variables in  $B$ , respectively.



To interpret this sum via foam evaluation, we observe that denominator terms may come from seamed 2-spheres, since in foam evaluation their positive Euler characteristics make the corresponding products go into the denominators. These 2-spheres should have seam circles splitting the 2-spheres into pairs of discs of complementary thickness  $p, m - p$  for the  $A$ -variables sphere and  $q, n - q$  for the  $B$ -sphere. This would produce denominator terms  $\mathcal{R}(A', A \setminus A')$  and  $\mathcal{R}(B', B \setminus B')$  in the sum.

Furthermore, the 2-spheres should intersect, to account for the two other terms in the product that do not contain  $x$ . Finally, to incorporate  $x$ , we introduce a third group of variables  $\{x\}$ , in addition to  $A$  and  $B$ , and a connected surface of thickness one for  $\{x\}$  that intersects the 2-spheres labelled  $A$  and  $B$  in one circle each, to account for the terms in the product that contain  $x$ . These three components of the foam are shown in Figure 6.9.

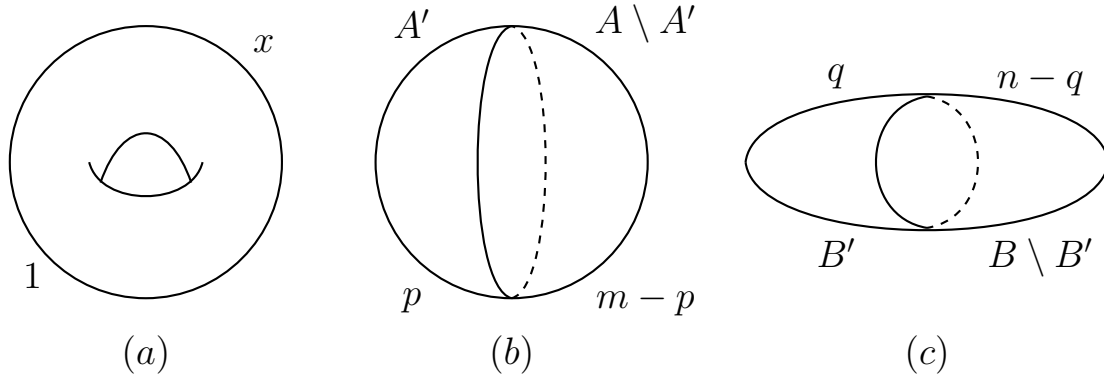


FIGURE 6.9. Three components of the double sum foam in Figure 6.10, from left to right: (a) connected surface (genus is unimportant, chosen to be one) of maximal thickness 1 carrying variable set  $X = \{x\}$ , (b) seamed 2-sphere glued from disks of thickness  $p$  and  $m - p$ , respectively, with the variable set  $A$ , (c) seamed 2-sphere glued from disks of thickness  $q$  and  $n - q$ , respectively, with the variable set  $B$ . Colorings of (b) are in bijections with  $A' \subset A$ ,  $|A'| = p$ , colorings of (c) are in bijections with  $B' \subset B$ ,  $|B'| = q$ .

Figure 6.10 shows how these three foams can overlap in  $\mathbb{R}^3$ , with the resulting evaluation equal to  $\text{Syl}_{p,q}(A, B)(x)$ .

**Remark 6.4.** In our evaluation of 2-spheres with a seam line separating disks with complementary thickness we are tacitly considering SL evaluation. To convert to GL evaluation, 2-spheres should be changed into theta-foams with one disk facet of maximal thickness. The relation is shown in Figure 6.12.

For each of the foam configurations in this section, it's easy to find an embedding into  $\mathbb{R}^3$  that extends to an embedding of the corresponding GL foam, with seamed 2-spheres becoming theta-foams with the new disk facet of maximal thickness, while preserving the evaluation.

Figure 6.11 shows the GL version of the foam that evaluates to the Sylvester double sum.

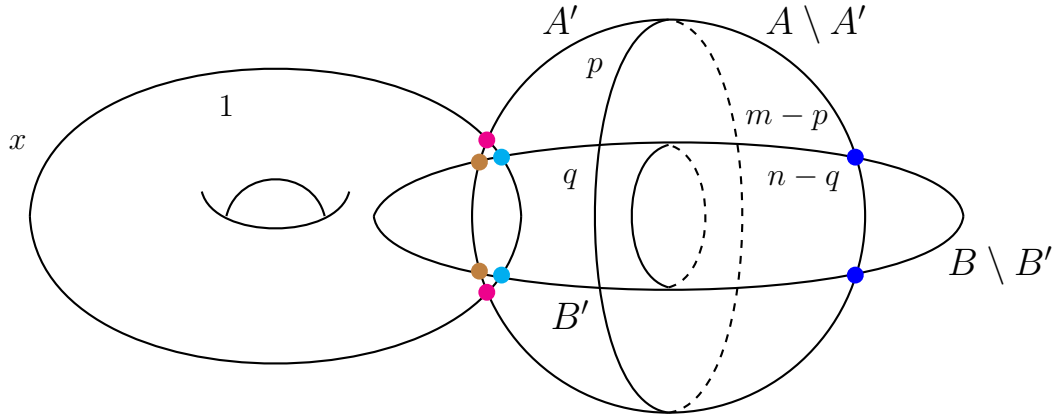


FIGURE 6.10. Foam evaluating to  $\text{Syl}_{p,q}(A, B)(x)$ . Four intersection circles of three components are shown schematically, as pairs of points of four different colors (blue, red, brown, cyan). The two seamed 2-spheres intersect along two circles (indicated as pairs of blue and brown points), and the third surface (shown as a torus, but its genus is irrelevant for the evaluation) intersects each seamed 2-sphere along a circle (indicated as red and cyan pairs of points). A coloring of this foam consist of assigning a subset  $A' \subset A$  of cardinality  $p$  to the left disk of the  $A$  sphere and a subset  $B' \subset B$  of cardinality  $q$  to the left disk of the  $B$  sphere.

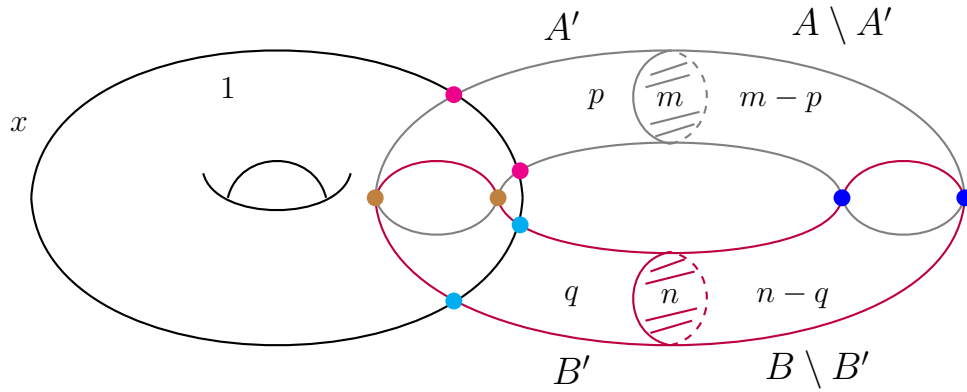


FIGURE 6.11. GL version of the foam in Figure 6.10.  $A$ -foam (shown in grey) and  $B$ -foam (shown in red) are theta-foams, with one disk of maximal thickness in each (shaded disks labelled  $m$  and  $n$ ). Intersection circles are schematically depicted by pairs identically colored points.

Chen and Louck in [CL, Theorem 2.1] give a certain polynomial identity for a finite set of variables  $A = \{\alpha_1, \dots, \alpha_m\}$  and set of variables  $X = \{x_1, \dots, x_{m-d}\}$ . This is an identity in

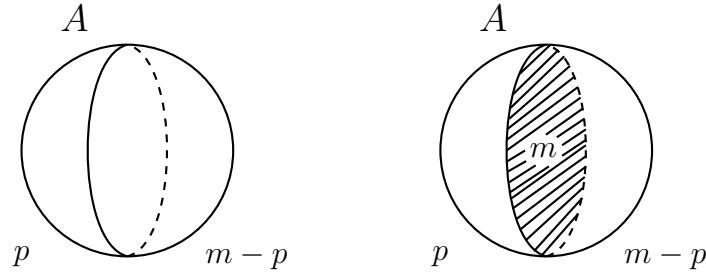


FIGURE 6.12.  $\mathrm{SL}(m)$  vs  $\mathrm{GL}(m)$  foams. Left: An  $\mathrm{SL}(m)$  foam 2-sphere made of two disks with complementary thicknesses  $p$  and  $m-p$ . Right: A  $\mathrm{GL}(m)$  theta-foam obtained by adding a disk of maximal thickness  $m$  to the 2-sphere. There are two ways to orient the seam edge in the foams and the two evaluations differ by  $(-1)^{p(m-p)}$ , see [RW1, KK].

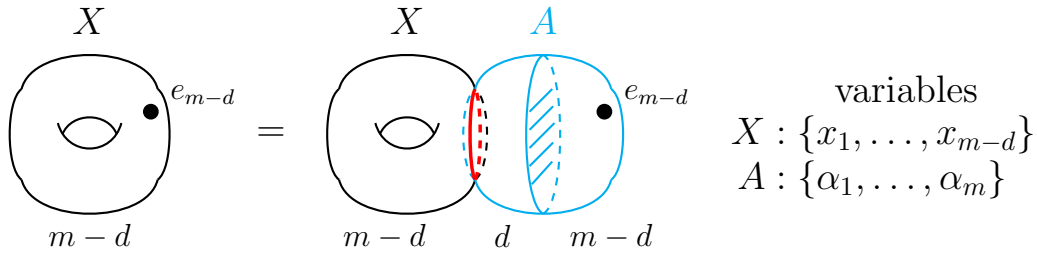


FIGURE 6.13. Foams for the relation (71). The thickness of  $X$  is  $m-d$ . The thickness of the left portion of  $A$  is  $d$ , the thickness of its right portion is  $m-d$ . The two components on the right hand side overlap along a circle.

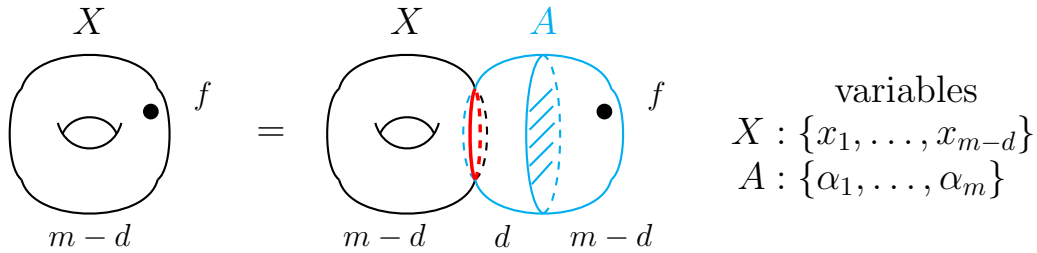


FIGURE 6.14. Foams for the relation (72), a generalization of Figure 6.13 foam. Genus of the  $X$  component is unimportant.

the ring of rational functions  $\mathbb{Q}(\alpha_1, \dots, \alpha_m, x_1, \dots, x_{m-d})$ :

$$(71) \quad x_1 \cdots x_{m-d} = \sum_{A' \subset A, |A'|=d} \left( \prod_{\alpha_j \notin A'} \alpha_j \right) \frac{\prod_{x_j \in X, \alpha_i \in A'} (x_j - \alpha_i)}{\prod_{\alpha_j \notin A', \alpha_i \in A'} (\alpha_j - \alpha_i)}.$$

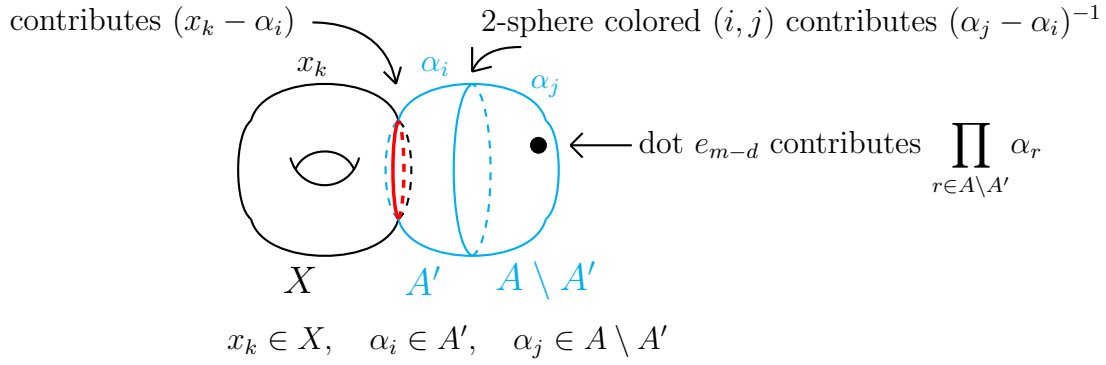


FIGURE 6.15. Foam for the RHS of the identity (71). The 2-torus  $X$  has maximal thickness  $m - d = |X|$  and a unique coloring, by  $X$ . It contributes 1 to the product. Left disk of 2-sphere is colored by  $A' \subset A$ , right disk by its complement  $A' \setminus A$ . The denominator term on the RHS is the product of  $\alpha_j - \alpha_i$ , over  $\alpha_i \in A'$  and  $\alpha_j \in A \setminus A'$ . The intersection circle contributes the product of  $x_k - \alpha_i$ , over all  $k = 1, \dots, m - d$  and  $\alpha_i \in A'$ . Dots on the LHS and RHS are labelled by the elementary symmetric function of the degree equal to the thickness  $m - d$  of the facets and contribute  $x_1 \cdots x_{m-d}$ , respectively product of  $\alpha_j \in A \setminus A'$ , to the terms.

More generally, they have the formula

$$(72) \quad f(X) = \sum_{A' \subset A, |A'|=d} f(A \setminus A') \frac{\prod_{x_j \in X, \alpha_i \in A'} (x_j - \alpha_i)}{\prod_{\alpha_j \notin A', \alpha_i \in A'} (\alpha_j - \alpha_i)}$$

for a symmetric polynomial  $f$  in  $m - d$  variables such that the degree of  $f$  in any of its variables is at most  $d$ . When  $m = d + 1$ , so that  $X = \{x_1\}$ , their formula specializes to the classical Lagrange interpolation formula for a one-variable polynomial of degree at most  $d$ , see [CL].

Foam equivalents of formulas (71) and (72) are depicted in Figures 6.13 and 6.14, correspondingly.  $X$  foams there have maximal thickness  $m - d = |X|$  and a surface of any genus can be chosen in place of a torus for that component. Figure 6.15 shows in detail why the foam in the RHS of Figure 6.13 evaluates to the RHS of formula (71).

An important role in [KSV] and several related papers is played by the *Exchange Lemma*. To state it, following [KSV], take  $A$  and  $B$  to be disjoint sets of cardinalities  $m$  and  $n$ , respectively. Then

$$(73) \quad \sum_{A' \subset A, |A'|=d} \mathcal{R}(A \setminus A', B) \frac{\mathcal{R}(X, A')}{\mathcal{R}(A \setminus A', A')} = \sum_{B' \subset B, |B'|=d} \mathcal{R}(A, B \setminus B') \frac{\mathcal{R}(X, B')}{\mathcal{R}(B', B \setminus B')},$$

Foam interpretation of the both sides of this identity is shown in Figure 6.16.

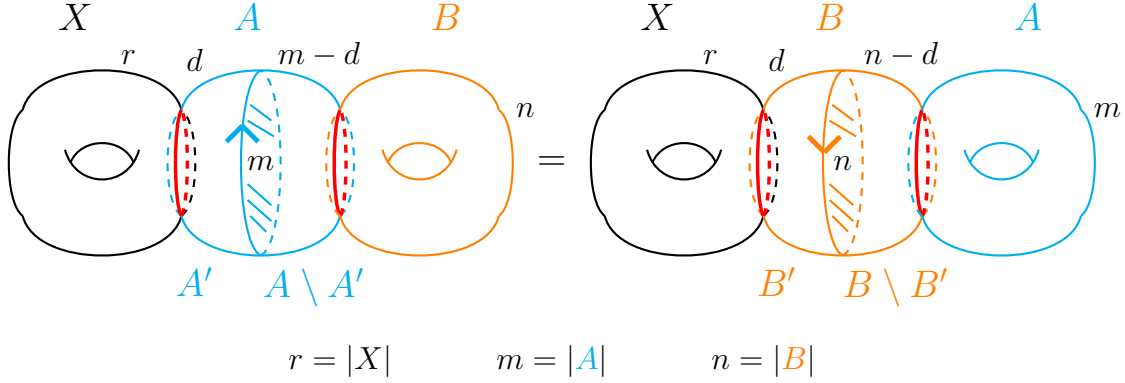


FIGURE 6.16. Exchange Relation written via foam evaluation. Seam circles of blue and orange theta-foams are oriented oppositely, to incorporate implicit sign in formula (73) that appears if in one of the denominators the order of a set and its complement is reversed, see [KSV].  $X$  and  $B$  foams on the LHS and  $X$  and  $A$  foams on the RHS may carry any genus; we chose genus 1 for all four.

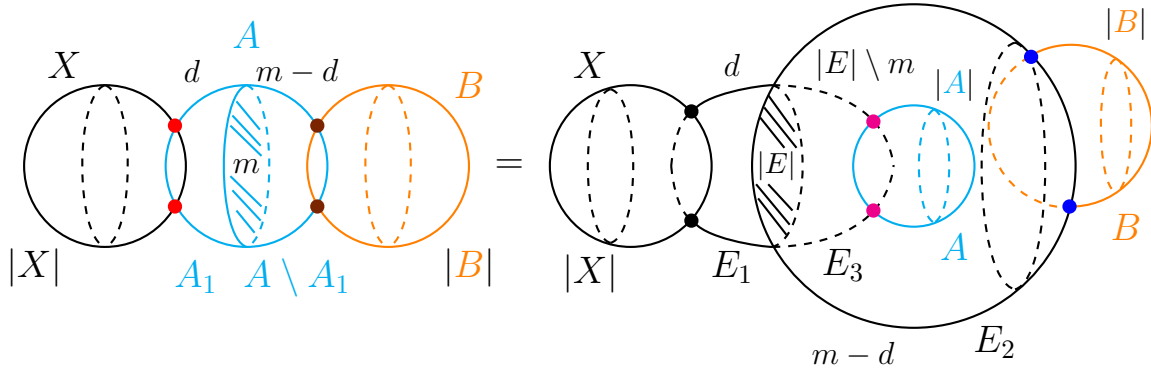


FIGURE 6.17. Foams for the formula (74), also see [DKSV, Proposition 2.1]. On the RHS, generalized theta-foam in the middle for variable set  $E$  consists of a thickness  $|E|$  disk with three adjacent disks of thicknesses  $d$ ,  $m - d$  and  $|E| - m$ , respectively. Each of these three disks intersects one of the spheres for variable sets  $A, B, X$ .

As another example, consider the formula in [DKSV, Proposition 2.1]. To state it, let  $A, B$  be finite sets with  $|A| = m$  and  $|B| = n$ , and choose  $0 \leq d \leq m$ . Let  $X, E$  be finite sets such that

$$|E| \geq \max\{|X| + d, m + n - d, m\}.$$

Then

$$\begin{aligned}
 (74) \quad & \sum_{\substack{A_1 \sqcup A_2 = A \\ |A_1|=d, |A_2|=m-d}} \frac{\mathcal{R}(A_2, B) \mathcal{R}(X, A_1)}{\mathcal{R}(A_1, A_2)} = \\
 & = \sum_{\substack{E_1 \sqcup E_2 \sqcup E_3 = E \\ |E_1|=d, |E_2|=m-d, |E_3|=|E|-m}} \frac{\mathcal{R}(A, E_3) \mathcal{R}(E_2, B) \mathcal{R}(X, E_1)}{\mathcal{R}(E_1, E_2) \mathcal{R}(E_1, E_3) \mathcal{R}(E_2, E_3)}.
 \end{aligned}$$

Foam interpretation of this formula is shown in Figure 6.17. In the evaluation of overlapping foams we assume that variable sets (in this example,  $A, B, X, E$ ) are disjoint, but perhaps this condition can be relaxed (formula (74) holds as well when these sets have non-empty intersections, see [DKSV]).

We leave it to the reader to write a similar foam interpretation of the relation between Sylvester double and single sums, see formula (2) in [DKSV].

From the present examples and those in [Kh4, Section 3] one can make a natural guess that there exists a meaningful theory of overlapping foams, but it is not clear to the authors how to develop it. One possible direction is to use an extension of Sylvester's subresultants to polynomials with multiple roots constructed in [DKS, DKS] to search for the symmetric analogue of the Robert-Wagner foam evaluation [RW1]. Robert-Wagner work and many prior papers (see [KK] for an incomplete survey) deal with *exterior foams* that are used to categorify networks on intertwiners between quantum exterior powers of the fundamental  $U_q(\mathfrak{sl}_N)$  representations. Papers [Ca, QRS, RW2] indicate that a similar theory should exist for *symmetric foams* that would categorify networks of quantum symmetric powers of the fundamental representation, but a definition and evaluation of symmetric foams is unknown as of today.

## 7. APPENDIX (JOINT WITH LEV ROZANSKY): COMPARISON WITH MATRIX FACTORIZATIONS

Each finite degree field extension  $\mathbf{k} \subset F$  is Frobenius. Any nonzero  $\mathbf{k}$ -linear map  $\varepsilon : F \rightarrow \mathbf{k}$  is a non-degenerate trace making  $F$  a commutative Frobenius algebra over  $\mathbf{k}$ . For separable extensions, there's a canonical trace  $\mathrm{tr}_{F/\mathbf{k}}$  used above.

Matrix factorizations deliver a supply of commutative Frobenius algebras and 2-dimensional TQFTs with corners [KRz, CM, DM]. A nondegenerate potential  $w \in \mathbf{k}[x_1, \dots, x_k]$  defines the Jacobi algebra

$$(75) \quad J(w) := \mathbf{k}[x_1, \dots, x_k] / (\partial_1 w, \dots, \partial_k w), \quad \partial_i w := \partial w / \partial x_i$$

(a potential is called nondegenerate when this quotient algebra is finite-dimensional). The Jacobi algebra is commutative Frobenius and carries a canonical trace  $\mathrm{tr}_{\mathrm{Gr}}$ , given by the Grothendieck residue, *i.e.*, see [AGV, GH]. When  $\mathbf{k}$  is a subfield of  $\mathbb{C}$ , the trace may be written as a complex integral

$$(76) \quad \mathrm{tr}_{\mathrm{Gr}}(p(\underline{x})) = \frac{1}{(2\pi i)^k} \int_{|\partial_i w|=R} \frac{p(\underline{x})}{\partial_1 w \cdots \partial_k w} dx_1 \cdots dx_k, \quad p(\underline{x}) \in \mathbf{k}[x_1, \dots, x_k]$$

over a contour that contains all roots of the system of equations  $\partial_1 w = \dots = \partial_k w = 0$ .

Suppose that  $F$  is a subfield of  $\mathbb{C}$  (in particular,  $\text{char}(\mathbf{k}) = 0$ ). Since  $F/\mathbf{k}$  is a simple extension, there is a generating element  $\alpha \in F$ ,  $\mathbf{k}(\alpha) = F$ , and

$$(77) \quad F \cong \mathbf{k}[x]/(f(x)),$$

where  $f$  is the minimal polynomial of  $\alpha$  over  $\mathbf{k}$ ,

$$(78) \quad f(x) = x^n + a_{n-1}x^{n-1} + \dots + a_0, \quad a_i \in \mathbf{k}.$$

We can realize  $F$  as the Jacobi algebra of the singularity with the potential  $w(x)$  in a single variable  $x$  such that  $w'(x) = f(x)$ ,

$$(79) \quad w(x) = \frac{1}{n+1}x^{n+1} + \frac{a_{n-1}}{n}x^n + \dots + a_0x.$$

The polynomial  $f(x)$  is irreducible over  $\mathbf{k}$  and can be fully factored in the algebraic closure  $\overline{\mathbf{k}} \subset \mathbb{C}$ :

$$(80) \quad f(x) = (x - \lambda_1) \cdots (x - \lambda_n), \quad \lambda_i \in \overline{\mathbf{k}}, \quad \lambda_i \neq \lambda_j.$$

The Hessian

$$(81) \quad w''(x) = f'(x) = \sum_{i=1}^n \prod_{j \neq i} (x - \lambda_j),$$

and

$$(82) \quad w''(\lambda_i) = \prod_{j \neq i} (\lambda_i - \lambda_j).$$

For a single variable  $x$  and a potential  $w(x)$  with  $w'(x) = f(x)$  having simple roots only, the Grothendieck trace is given by

$$(83) \quad \text{tr}_{\text{Gr}}(p(x)) = \frac{1}{2\pi i} \int_{|f(x)|=R} \frac{p(x)}{f(x)} dx = \sum_{i=1}^n \frac{p(\lambda_i)}{\prod_{j \neq i} (\lambda_i - \lambda_j)}, \quad p(x) \in \mathbf{k}[x], \quad R \gg 0.$$

To compare the two traces, note that the canonical trace  $\text{tr}_{F/\mathbf{k}}$  in a finite separable field extension can also be characterized as follows. The tensor product  $F \otimes_{\mathbf{k}} \overline{\mathbf{k}}$  of  $F$  with the algebraic closure  $\overline{\mathbf{k}}$  of  $\mathbf{k}$  is isomorphic to the direct product of  $n$  copies of  $\overline{\mathbf{k}}$ , where  $n$  is the degree  $[F : \mathbf{k}]$ ,

$$(84) \quad F \otimes_{\mathbf{k}} \overline{\mathbf{k}} \cong \overline{\mathbf{k}} \times \dots \times \overline{\mathbf{k}}.$$

This algebra contains  $n$  minimal idempotents  $e_1, \dots, e_n$ , one for each term in the product. Trace  $\text{tr}_{F/\mathbf{k}}$  extends  $\overline{\mathbf{k}}$ -linearly to a trace

$$\overline{\text{tr}}_{F/\mathbf{k}} : F \otimes_{\mathbf{k}} \overline{\mathbf{k}} \longrightarrow \overline{\mathbf{k}}$$

that is characterized uniquely by its taking value 1 on each minimal idempotent,  $\overline{\text{tr}}_{F/\mathbf{k}}(e_i) = 1$ .

Any other nondegenerate trace  $\varepsilon : F \longrightarrow \mathbf{k}$  extends likewise to a  $\overline{\mathbf{k}}$ -linear trace

$$\overline{\varepsilon} : F \otimes_{\mathbf{k}} \overline{\mathbf{k}} \longrightarrow \overline{\mathbf{k}}$$

taking a nonzero value on each idempotent  $e_i$ , with at least one of these values different from 1.

Minimal idempotents  $e_k(x) \in \overline{\mathbf{k}}[x]/(f(x))$  are given by

$$(85) \quad e_k(x) = \prod_{j \neq k} \frac{x - \lambda_j}{\lambda_k - \lambda_j}.$$

Indeed,  $e_k(\lambda_i) = \delta_{i,k}$ , so these are delta functions when evaluated on the roots of  $f(x)$ . Evaluating the Grothendieck trace on them gives

$$(86) \quad \mathrm{tr}_{\mathrm{Gr}}(e_k(x)) = \sum_{i=1}^n \frac{e_k(\lambda_i)}{\prod_{j \neq i} (\lambda_i - \lambda_j)} = \frac{1}{\prod_{j \neq k} (\lambda_k - \lambda_j)}.$$

Thus, values of the two traces on minimal idempotents are

$$(87) \quad \overline{\mathrm{tr}}_{F/\mathbf{k}}(e_k) = 1, \quad \mathrm{tr}_{\mathrm{Gr}}(e_k) = \prod_{j \neq k} \frac{1}{(\lambda_k - \lambda_j)}, \quad 1 \leq k \leq n,$$

and the field extension trace can be written as

$$(88) \quad \mathrm{tr}_{\mathrm{Gr}}(p(x)) = \frac{1}{2\pi i} \int_{|f(x)|=R} \frac{w''(x)p(x)}{w'(x)} dx = \sum_{i=1}^n p(\lambda_i), \quad p(x) \in \mathbf{k}[x].$$

Notice that we added the Hessian  $w''(x)$  to the numerator of the integral and kept the denominator. We see that the two traces differ by multiplication by the Hessian,

$$(89) \quad \mathrm{tr}_{F/\mathbf{k}}(p(x)) = \mathrm{tr}_{\mathrm{Gr}}(w''(x)p(x)).$$

The second and first derivatives  $w''(x), w'(x)$  have no common roots, since all roots of  $w'(x) = f(x)$  are simple, and  $w''(x)$  is an invertible element of  $\mathbf{k}[x]/(f(x)) \cong F$  (the latter ring is a field anyway). In the 2D TQFT of the Landau-Ginzburg model for the potential  $w(x)$  the value of a one-holed torus, as an element of the Jacobi algebra (the state space of the circle), is the Hessian  $w''(x)$ , see Figure 7.1.

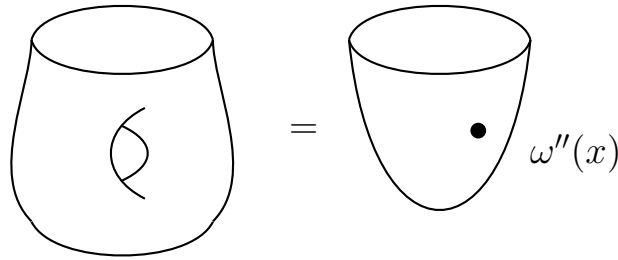


FIGURE 7.1. One-holed torus represents the element  $w''(x)$  in the Jacobi algebra of a one-variable potential.

Consequently, the field extension trace (the map induced by the cap in the TQFT associated to  $(F, \mathbf{k}, \mathrm{tr}_{F/\mathbf{k}})$ ) can be written as the cap with the genus one surface (holed torus) in the Landau-Ginzburg TQFT associated to a given generating element  $\alpha \in F$ , as described earlier, see Figure 7.2.



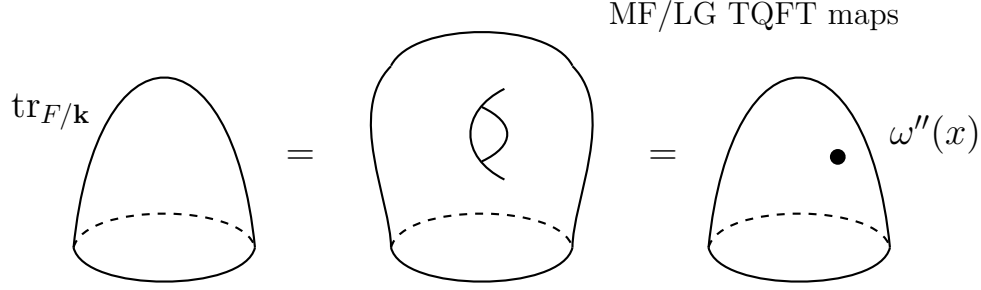


FIGURE 7.2. Cap given by the field extension trace equals the genus one cap trace in the matrix factorization (Landau-Ginzburg) TQFT, for any choice of generator  $x$  and the corresponding potential  $w(x)$ .

Choosing a different generator  $\alpha$  for  $F$  will, in general, change the polynomial  $f(x)$ , potential  $w(x)$  and the value of the trace on idempotents of  $F \otimes_{\mathbf{k}} \overline{\mathbf{k}}$ , while the trace  $\mathrm{tr}_{F/\mathbf{k}}$  is defined canonically. At the same time, it's given by capping off by the holed torus, in any one-variable matrix factorization TQFT realization of  $F$  as the Jacobi algebra.

This amusing relation between matrix factorizations and field extensions may be worth a further exploration. Notice, in particular, that  $F$  may be realized as the Jacobi algebra,  $F \cong J(w)$ , for a multivariable potential  $w(\underline{x}) \in \mathbf{k}[x_1, \dots, x_k]$ . Equivalently,  $F$  is the zero-dimensional complete intersection of hypersurfaces  $\partial_i w = 0$ ,  $i = 1, \dots, k$ . It should be interesting to find nontrivial presentations of that kind for various  $F$  with  $k > 1$  or locate them in the literature.

The Jacobi algebra  $J(w)$  is the endomorphism ring of the canonical matrix factorization

$$(90) \quad K(w) = \bigotimes_{i=1}^k K(x_i - y_i, u_i),$$

a Koszul factorization with the potential  $w_{12} = w(\underline{x}) - w(\underline{y})$  in  $2n$  variables  $x_1, \dots, x_n, y_1, \dots, y_n$ . Here  $u_i$  are any polynomials in  $x$ 's and  $y$ 's such that

$$w_{12} = \sum_{i=1}^k (x_i - y_i) u_i,$$

and  $K(v, u)$  is the factorization

$$\mathbf{k}[\underline{x}, \underline{y}] \xrightarrow{v} \mathbf{k}[\underline{x}, \underline{y}] \xrightarrow{u} \mathbf{k}[\underline{x}, \underline{y}],$$

see [KRz]. Matrix factorization  $K(w)$  represents the identity functor on the triangulated category  $\mathbf{MF}(w)$  of matrix factorizations with potential  $w$  and morphisms being homs of matrix factorizations modulo homotopies [KRz].

Assume that  $F/\mathbf{k}$  is a finite Galois extension in characteristic 0 and consider the Galois group  $G = \mathrm{Gal}(F/\mathbf{k})$ . One can ask to find presentations of  $F$  as the Jacobi algebra  $J(w)$  such that Galois symmetries  $\sigma \in G$  lift to endofunctors of  $\mathbf{MF}(w)$  defining an action of the Galois group on that category. Precisely, for each  $\sigma$  we would like to have a matrix factorization  $M(\sigma) = M_{\underline{x}, \underline{y}}(\sigma)$  (using subindices to specify sets of variables) with the potential  $w(\underline{x}) - w(\underline{y})$

together with isomorphisms in the homotopy category  $\mathbf{MF}(\underline{x} - \underline{z})$  of matrix factorizations with the potential  $w(\underline{x}) - w(\underline{z})$

$$(91) \quad M_{\underline{x}, \underline{y}}(\sigma) \otimes_{\underline{y}} M_{\underline{y}, \underline{z}}(\tau) \cong M_{\underline{x}, \underline{z}}(\sigma\tau), \quad \sigma, \tau \in G,$$

such that  $M_{\underline{x}, \underline{y}}(1) \cong K(w)$ . One can further require that these isomorphisms satisfy compatibility relations so that  $G$  acts on  $\mathbf{MF}(w)$  in a strong sense. Furthermore, factorization  $M(\sigma)$  should induce the symmetry  $\sigma$  on  $J(w) \cong F$  upon taking the trace of the identity endomorphism of  $M(\sigma)$ . Diagrammatically, following notations from [KRz], denote  $M(\sigma) = M_{\underline{x}, \underline{y}}(\sigma)$  by a dot labelled  $\sigma$  on an oriented line with endpoints labelled  $\underline{x}, \underline{y}$ , see Figure 7.3.

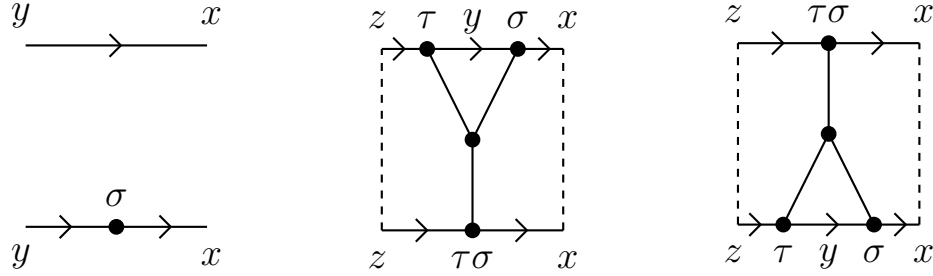


FIGURE 7.3. Top left arc represents the identity factorization  $K(w)$ . Bottom left arc carrying dot  $\sigma$  represents factorization  $M(\sigma)$ . Trivalent vertices on the middle and right pictures show mutually-inverse isomorphisms (91).

The identity map of  $M(\sigma)$  is depicted by a defect interval, shown as a vertical interval in Figure 7.4 left. Taking the trace of the identity map corresponds, on the diagrammatic side, to closing of the square into an annulus with a defect circle on it, see Figure 7.4.

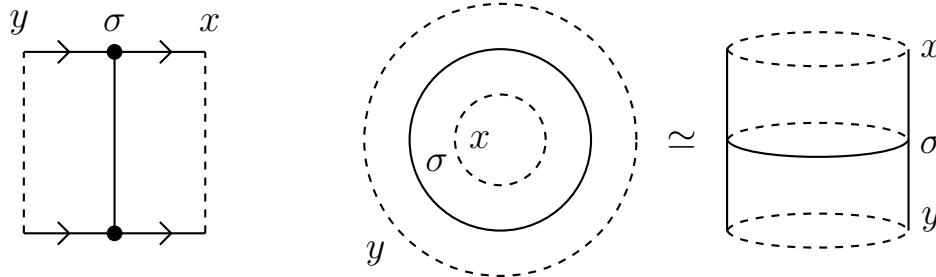


FIGURE 7.4. Left: the identity endomorphism of  $\sigma$ . Middle and right: its trace is a defect circle on an annulus. Boundaries of the annulus correspond to closures of the identity factorization  $K(w)$ , given by equating variables  $\underline{x} = \underline{y}$  in that factorizations and taking cohomology of the resulting 2-periodic complex. Cohomology is precisely the Jacobi algebra  $J(w)$ , and the annulus with the  $\sigma$ -circle defines a linear endomorphism of it.

In general, a defect circle on an annulus would only give a linear endomorphism of the Jacobi algebra, not an algebra homomorphism. For that, we would additionally want the

equality shown in Figure 7.5 left, which may come from a more local relation in Figure 7.5 right.

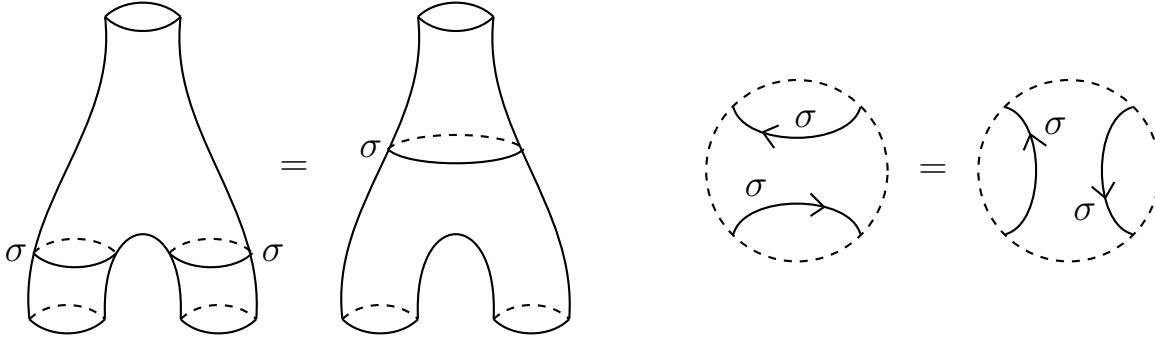


FIGURE 7.5. Left:  $\sigma$ -circle defining an algebra endomorphism of  $J(w)$ . Right: a sufficient local relation for that.

For a general separable finite field extension  $F/\mathbf{k}$ , it seems hard to impossible to pick a potential  $\omega \in \mathbf{k}[x_1, \dots, x_n]$  with the Jacobi algebra  $J(\omega) \cong F$  and invertible factorizations  $M(\sigma), \sigma \in \text{Gal}(F/\mathbf{k})$ , giving an action of the Galois group  $\text{Gal}(F/\mathbf{k})$  on the homotopy category of matrix factorizations  $\text{HMF}_\omega$  with potential  $\omega$  such that the action induces the Galois group action on  $F$ .

Potentially related structures appear in the theory of Landau–Ginzburg orbifolds, where a group  $G$  acts on  $\mathbf{k}[x_1, \dots, x_k]$  preserving the potential  $w$ , leading to the category of  $G$ -equivariant matrix factorizations. In those examples usually  $\mathbf{k} = \mathbb{C}$ , and it’s unclear whether some version of LG orbifold theory may be adapted to relate Galois extensions and matrix factorizations.

## REFERENCES

- [Ab] Lowell Abrams, *Two-dimensional topological quantum field theories and Frobenius algebras*, J. Knot Theory Ramif. **5** (1996), no. 5, 569–587, <http://home.gwu.edu/~labrams/docs/tqft.ps>.
- [AGV] Vladimir I. Arnold, Sabir M. Gusein-Zade and Alexander N. Varchenko, *Singularities of differentiable maps, vol. I*, Monographs in Mathematics **82**, Burkhäuser, Boston, 1985.
- [BH] Per Berglund and Mans Henningson, *Landau–Ginzburg orbifolds, mirror symmetry and the elliptic genus*, Nuclear Physics B **433** (1995), no. 2, 311–332.
- [BHMV] Christian Blanchet, Nathan Habegger, Gregor Masbaum and Pierre Vogel, *Topological quantum field theories derived from the Kauffman bracket*, Topology **34** (1995), no. 4, 883–927.
- [BR] Ilka Brunner and Daniel Roggenkamp, *Defects and bulk perturbations of boundary Landau–Ginzburg orbifolds* Journal of High Energy Physics **2008** (2008), no. 4, 1–34, arXiv:[0712.0188](https://arxiv.org/abs/0712.0188).
- [Ca] S. Cautis, *Remarks on coloured triply graded link invariants*, Algebraic and Geometric Topology **17** (2017), 3811–3836, [arXiv:1611.09924](https://arxiv.org/abs/1611.09924).
- [CL] William Y.C. Chen and James D. Louck, *Interpolation for symmetric functions*, Adv. Math. **117** (1996), no. 4, 147–156.
- [CM] Nils Carqueville and Daniel Murfet, *Adjunctions and defects in Landau–Ginzburg models*, Adv. Math. **289** (2016), 480–566, arXiv:[1208.1481](https://arxiv.org/abs/1208.1481).
- [CST] Tullio Ceccherini-Silberstein, Fabio Scarabotti and Filippo Tolli, *Representation Theory and Harmonic Analysis of Wreath Products of Finite Groups*, Cambridge University Press **410**, London Mathematical Society Lecture Note Series, 2014.

- [Co] Brian Conrad, *Math 154: Algebraic Number Theory. Norm and trace*, <http://virtualmath1.stanford.edu/~conrad/154Page/handouts/normtrace.pdf>, 1–6.
- [DHKS] Carlos D’Andrea, Hoon Hong, Teresa Krick and Agnes Szanto, *Sylvester’s double sums: The general case*, *Journal of Symbolic Computation* **44** (2009), no. 9, 1164–1175.
- [DKS] Carlos D’Andrea, Teresa Krick, Agnes Szanto, *Subresultants in multiple roots*, *Linear Algebra Appl.* **438** no. 5 (2013), 1969–1989.
- [DKSV] Carlos D’Andrea, Teresa Krick, Agnes Szanto and Marcelo Valdetaro, *Closed formula for univariate subresultants in multiple roots*, *Linear Algebra Appl.* **565** (2019), 123–155, arXiv:1612.05160.
- [DM] Tobias Dyckerhoff and Daniel Murfet, *The Kapustin-Li formula revisited*, *Advances in Mathematics* **231** (2012), no. 3–4, 1858–1885, arXiv:1004.0687.
- [FF] Anatoly Fomenko and Dmitry Fuchs, *Homotopical topology*, *Graduate Texts in Mathematics* **273**, Springer, 2016.
- [Go] Bojan Gornik, *Note on Khovanov link cohomology*, arXiv:math/0402266 (2004).
- [GH] Phillip Griffiths and Joseph Harris, *Principles of algebraic geometry*, *Wiley Classics Library*, John Wiley & Sons, Inc., 1994.
- [IO] Mee Seong Im and Can Ozan Oğuz, *Natural transformations between induction and restriction on iterated wreath product of symmetric group of order 2*, arXiv:2106.07776 (2021).
- [IW1] Mee Seong Im and Angela Wu, *Generalized iterated wreath products of cyclic groups and rooted trees correspondence*, *Adv. Math. Sci.* **15** (2018), 15–28, arXiv:1409.0603.
- [IW2] Mee Seong Im and Angela Wu, *Generalized iterated wreath products of symmetric groups and generalized rooted trees correspondence*, *Adv. Math. Sci.* **15** (2018), 29–46, arXiv:1409.0604.
- [IV] Kenneth A. Intriligator and Cumrun Vafa, *Landau-Ginzburg orbifolds*, *Nuclear Physics B* **339** (1990), no. 1, 95–120.
- [Ja] Gerald J. Janusz, *Algebraic number fields*, *Graduate Studies in Mathematics* **7**, American Mathematical Society, 1996.
- [KW] Shamit Kachru and Edward Witten, *Computing the complete massless spectrum of a Landau-Ginzburg orbifold*, *Nuclear Physics B* **407** (1993), no. 3, 637–666, arXiv:hep-th/9307038.
- [Ka] Ralph M. Kaufmann, *Orbifolding Frobenius algebras*, *International Journal of Mathematics* **14** (2003), no. 6, 573–617.
- [Kh1] Mikhail Khovanov, *Functor-valued invariant of tangles*, *Alg. Geom. Topol.* **2** (2002), 665–741 (electronic), arXiv:math/0103190.
- [Kh2] Mikhail Khovanov,  *$\mathfrak{sl}(3)$  link homology*, *Alg. Geom. Top.* **4** (2004), no. 2, 1045–1081, arXiv:math/0304375.
- [Kh3] Mikhail Khovanov, *Heisenberg algebra and a graphical calculus*, *Fund. Math.* **225** (2014), no. 1, 169–210, arXiv:1009.3295.
- [Kh4] Mikhail Khovanov, *Universal construction of topological theories in two dimensions*, arXiv:2007.03361 (2020).
- [KK] Mikhail Khovanov and Nitu Kitchloo, *A deformation of Robert-Wagner foam evaluation and link homology*, arXiv:2004.14197 (2020).
- [KKO] Mikhail Khovanov, Yakov Kononov and Victor Ostrik, *Two-dimensional topological theories, rational functions and their tensor envelopes*, arXiv:2011.14758 (2020).
- [KL] Mikhail Khovanov and Robert Laugwitz, *Planar diagrammatics of self-adjoint functors and recognizable tree series*, arXiv:2104.01417 (2021).
- [KQ] Mikhail Khovanov and You Qi, *Lecture notes on categorification*, <https://www.math.columbia.edu/~khovanov/cat2020/>.
- [KQR] Mikhail Khovanov, You Qi and Lev Rozansky, *Evaluating thin flat surfaces*, arXiv:2009.01384 (2020).
- [KR1] Mikhail Khovanov and Louis-Hadrien Robert, *Foam evaluation and Kronheimer–Mrowka theories*, *Advances in Math.* **376** (2021), 107433, arXiv:1808.09662.
- [KR2] Mikhail Khovanov and Louis-Hadrien Robert, *Link homology and Frobenius extensions II*, arXiv:2005.08048 (2020).
- [KRz] Mikhail Khovanov and Lev Rozansky, *Matrix factorizations and link homology*, *Fundamenta Mathematicae* **199** (2008), no. 1, 1–91, arXiv:math/0401268.
- [KS] Mikhail Khovanov and Radmila Sazdanovic, *Bilinear pairings on two-dimensional cobordisms and generalizations of the Deligne category*, arXiv:2007.11640 (2020).

- [Kc1] Joachim Kock, *Frobenius algebras and 2D topological quantum field theories*, Cambridge University Press **59**, London Mathematical Society Student Texts, Cambridge, 2004.
- [Kc2] Joachim Kock, *Frobenius algebras and 2D topological quantum field theories (short version)*, <http://mat.uab.es/~kock/TQFT/FS.pdf>.
- [KSV] Teresa Krick, Agnes Szanto and Marcelo Valdetaro, *Symmetric interpolation, Exchange Lemma and Sylvester sums*, Communications in Algebra **45** (2017), no. 8, 3231–3250, arXiv:[1503.00607](#).
- [Ku] Greg Kuperberg, *Spiders for rank 2 Lie algebras*, Comm. Math. Phys. **180** (1996), no. 1, 109–151, arXiv:[q-alg/9712003](#).
- [LPr] Alain Lascoux and Piotr Pragacz, *Double Sylvester sums for subresultants and multi-Schur functions*, Journal of Symbolic Computation **35** (2003), no. 6, 689–710.
- [La1] Aaron D. Lauda, *Frobenius algebras and ambidextrous adjunctions*, Theory and Appl. of Categories **16** (2006), no. 4, 84–122, arXiv:[math/0502550](#).
- [La2] Aaron D. Lauda, *An introduction to diagrammatic algebra and categorified quantum  $\mathfrak{sl}_2$* , Bull. Inst. Math. Acad. Sin. (N.S.) **7** (2012), no. 2, 165–270, arXiv:[1106.2128](#).
- [LP] Aaron D. Lauda and Hendryk Pfeiffer, *Open-closed strings: Two-dimensional extended TQFTs and Frobenius algebras*, Topology and its Applications **155** (2008), 623–666, arXiv:[math/0510664](#).
- [Le] Eun Soo Lee, *An endomorphism of the Khovanov invariant*, Adv. Math. **197** (2005), no. 2, 554–586, arXiv:[math/0210213](#).
- [Lw] Lukas Lewark, *Rasmussen’s spectral sequences and the  $\mathfrak{sl}_N$ -concordance invariants*, Advances in Mathematics **260** (2014), 59–83, arXiv:[1310.3100](#).
- [Lo] Andrew Lobb, *A note on Gornik’s perturbation of Khovanov-Rozansky homology*, Algebr. Geom. Topol. **12** (2012), no. 1, 293–305, arXiv:[1012.2802](#).
- [LS] Monika Lynker and Rolf Schimmrigk, *Landau-Ginzburg theories as orbifolds*, Physics Letters B **249** (1990), no. 2, 237–242.
- [MS] Gregory W. Moore and Graeme Segal, *D-branes and K-theory in 2D topological field theory*, arXiv:[hep-th/0609042](#) (2006).
- [MOY] Hitoshi Murakami, Tomotada Ohtsuki and Shuji Yamada, *HOMFLY polynomial via an invariant of colored plane graphs*, Enseign. Math. (2) **44** (1998), no. 3-4, 325–360.
- [OOR] Rosa C. Orellana, Michael E. Orrison and Daniel N. Rockmore, *Rooted trees and iterated wreath products of cyclic groups*, Adv. in Appl. Math. **33** (2004), no. 3, 531–547.
- [QR] Hoel Queffelec and David E. V. Rose, *The  $\mathfrak{sl}(n)$  foam 2-category: a combinatorial formulation of Khovanov-Rozansky homology via categorical skew Howe duality*, Adv. in Math. **302** (2016), 1251–1339, arXiv:[1405.5920](#).
- [QRS] Hoel Queffelec, David E. V. Rose and Antonio Sartori, *Annular evaluation and link homology*, arXiv:[1802.04131](#).
- [Ra] Jacob Rasmussen, *Khovanov homology and the slice genus*, Inventiones Mathematicae **182**, (2010), 419–447, arXiv:[math/0402131](#).
- [RW1] Louis-Hadrien Robert and Emmanuel Wagner, *A closed formula for the evaluation of  $\mathfrak{sl}_N$ -foams*, Quantum Topology **11** (2020), no. 3, 411–487, arXiv:[1702.04140](#).
- [RW2] Louis-Hadrien Robert and Emmanuel Wagner, *Symmetric Khovanov-Rozansky link homologies*, Journal de l’École polytechnique - Mathématiques, Tome **7** (2020), 573–651, arXiv:[1801.02244](#).
- [RWe] David E. V. Rose and Paul Wedrich, *Deformations of colored  $\mathfrak{sl}_N$  link homologies via foams*, Geom. Topol. **20** (2016), no. 6, 3431–3517, arXiv:[1501.02567](#).
- [Sy] James J. Sylvester, *On a theory of syzygetic relations of two rational integral functions, comprising an application to the theory of Sturm’s function and that of the greatest algebraic common measure*, Phi. Trans. R. Soc. London **143** (1853) 407–548 (appears also in Collected Mathematical Papers of James Joseph Sylvester, Chelsea Publishing Co. **1** (1973), 429–586).
- [Tu1] Vladimir Turaev, *Homotopy field theory in dimension 2 and group-algebras*, arXiv:[math/9910010](#) (1999).
- [Tu2] Vladimir Turaev, *Homotopy Quantum Field Theory*, EMS Tracks in Mathematics **10**, European Mathematical Society, 2010.
- [Wa] Kai Wang, *Fixed subalgebra of a Frobenius algebra*, Proceedings AMS **87** (1983), no. 4, 576–578.
- [We] Paul Wedrich, *Exponential growth of colored HOMFLY-PT homology*, Advances in Math. **353** (2019), 471–525, arXiv:[1602.02769](#).

- [Wu] Hao Wu, *On the quantum filtration of the Khovanov-Rozansky cohomology*, Adv. Math. **221** (2009), 54–139, arXiv:[math/0612406](#).

DEPARTMENT OF MATHEMATICS, UNITED STATES NAVAL ACADEMY, ANNAPOLIS, MD 21402, USA  
Email address: [meeseongim@gmail.com](mailto:meeseongim@gmail.com)

DEPARTMENT OF MATHEMATICS, COLUMBIA UNIVERSITY, NEW YORK, NY 10027, USA  
Email address: [khovanov@math.columbia.edu](mailto:khovanov@math.columbia.edu)

DEPARTMENT OF MATHEMATICS, UNIVERSITY OF NORTH CAROLINA, CHAPEL HILL, NC 27599, USA  
Email address: [rozansky@email.unc.edu](mailto:rozansky@email.unc.edu)